SPACE DIVISION

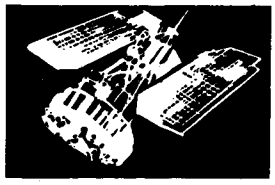
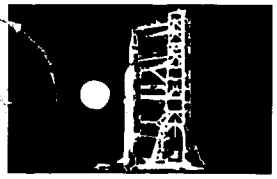
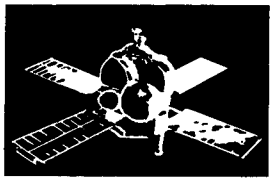

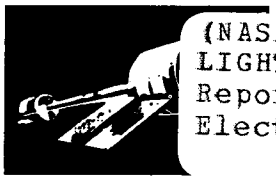
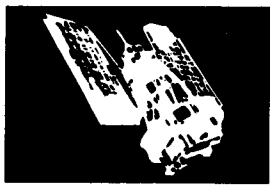
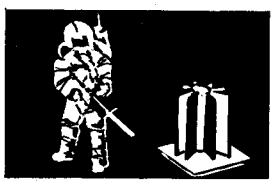
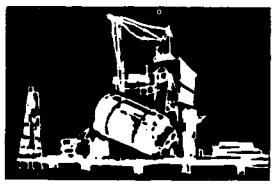

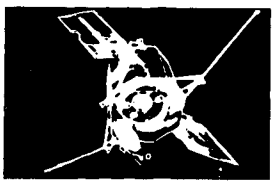

GE Document No. 72SD4233
August 15, 1972

QUARTERLY REPORT NO. 1

FEASIBILITY STUDY OF A 110 WATT PER KILOGRAM LIGHTWEIGHT SOLAR ARRAY SYSTEM

Prepared for:
Jet Propulsion Laboratory

Prepared Under:
Contract 953387

GENERAL ELECTRIC

GE DOCUMENT NO. 72SD4233
AUGUST 15, 1972

QUARTERLY REPORT NO. 1

FEASIBILITY STUDY
OF A
110 WATT PER KILOGRAM
LIGHTWEIGHT SOLAR ARRAY SYSTEM
5 MAY 1972 TO 5 AUGUST 1972

PREPARED FOR

JET PROPULSION LABORATORY
CALIFORNIA INSTITUTE OF TECHNOLOGY
PASADENA, CALIFORNIA

PREPARED UNDER: CONTRACT 953387
CONTRACTING OFFICER: K.L. GLADD
PROJECT MANAGER: E. SEGUEIRA

PREPARED BY: N.F. SHEPARD
A. SCHNEIDER
K.L. HANSON

APPROVED BY: K.L. Hanson
K.L. HANSON
PROJECT MANAGER

THIS WORK WAS PERFORMED FOR THE JET PROPULSION LABORATORY, CALIFORNIA INSTITUTE OF TECHNOLOGY, AS SPONSORED BY THE NATIONAL AERONAUTICS AND SPACE ADMINISTRATION UNDER CONTRACT NAS7-100

GENERAL ELECTRIC
SPACE SYSTEMS ORGANIZATION
Valley Forge Space Center
P. O. Box 8555 • Philadelphia, Penna. 19101

"This report contains information prepared by the General Electric Company, Space Systems Organization, under JPL Subcontract. Its content is not necessarily endorsed by the Jet Propulsion Laboratory, California Institute of Technology, or the National Aeronautics and Space Administration."

ABSTRACT

This report is the first in a series which will describe the technical progress in the investigation of the feasibility of a solar array panel subsystem which will produce 10,000 watts of electrical output at 1 A.U. with an overall beginning-of-life power-to-weight ratio of at least 110 watt/kg. This ultra-lightweight solar array system shall be applied to three generic mission types: (1) interplanetary, (2) geosynchronous, and (3) manned space station. The requirements of each of these missions, as they pertain to the solar array, are presented in this report. A review of existing lightweight solar array system concepts is presented along with conclusions regarding the applicability of this technology to the feasibility of the ultra-lighweight solar array system. Several new system concepts are included for further evaluation. The existing technology base, as it pertains to solar cells, solar cell covers, interconnects and substrates, and deployable booms, is reviewed. A discussion of the attitude control of spacecraft with large flexible solar arrays is also included.

TABLE OF CONTENTS

TABLE OF CONTENTS (Cont'd)

LIST OF ILLUSTRATIONS

LIST OF ILLUSTRATIONS (Cont'd)

LIST OF TABLES

SECTION 1

INTRODUCTION AND SUMMARY

A program to study the feasibility of a 10,000 watt solar array panel system with an overall power-to-weight* ratio of better than 110 watts/kg was initiated on May 5, 1972. This panel system would be one element of a multipanel solar array system on space vehicles for interplanetary, synchronous earth orbit, or manned space station missions. This ultralightweight solar array will require improvements in both the solar cell blanket unit weight and in the elements associated with the deployment and stowage structure. The power-to-weight ratio is interpreted to be the delivered beginning-of-life maximum power output at 1 AU divided by the total system weight which includes all elements of the deployment and support structure and mechanisms, but not the gimbaling or orientation related equipment. Thus, for the specified power output of 10,000 watts at 1 AU, the total panel system weight must be less than 90.9 kg. The design constraints related to each of the three missions will be investigated.

The program has been organized into the following tasks:

Task No.	Task Title
1000	Design Requirements Definition and Analysis
2000	Investigation of Existing Array Technology
3000	Feasibility of Extending Existing Array Concepts to 110 Watts/kg
4000	Definition and Analysis of Improved Configurations
5000	State-of-the-Art Analysis, Projection and Advances

*Throughout this report, the term "weight" is used as a synonym for the term "mass."

In Task 1000 the design requirements for each of the three missions will be investigated. Initially a set of design requirements will be generated to provide guidance to the design and analysis process. The mission design requirements which constrain the designs will be identified and their influence on panel performance determined.

Tasks 2000 and 3000 are an investigation of the use of existing concepts, configuration and technology to meet the design requirements. It is planned to modify and combine the best features of present concepts and configurations into candidate configurations and analyze their performance with respect to the mission requirements.

Task 4000 involves the synthesis of advanced concepts and configurations to meet the system requirements. The distinction between advanced concepts and modification of existing concepts is not distinct and no particular attempt will be made in the study to sharpen the distinction since the categorization is primarily for convenience.

Task 5000 consists of two major parts. One is concerned with the analysis and definition of the state-of-the-art with respect to the design of the candidate configurations. It is a goal of the study to base the design of the system upon component or device performance which has been at least demonstrated in the laboratory. For example, it is planned to base the performance analysis on solar cell performance data, albeit a limited number of samples, rather than on a projection of the state-of-the-art for solar cell performance at some future date. With this approach there is high confidence in achieving predicted system performance. The second part of this task is to assess the relation of the state-of-the-art with the performance objectives, identify needed advances in the state-of-the-art to achieve the performance goals, and assess the performance payoff that results from state-of-the-art advances. Approximately a 5 year program is involved in reaching the point of committing this technology to a flight hardware program. This 5 year time period includes a one year feasibility study, one year for concept development, and one year for engineering design and development testing. The remainder of the time is involved with evaluation and planning periods between these discrete program elements.

The basic requirements for the interplanetary mission are defined in JPL Specification ES506080B which is included as Appendix A of this report. The requirements for the other two missions were derived and are presented in Section 2.1 of this report. In general, the solar array system designs required for the interplanetary and geosynchronous missions will be very similar, if not identical. However, the manned space station mission application places requirements on the solar array system which are considerably different from the other two missions. For example, maneuver and docking loads may require greater solar array rigidity. For this mission, the requirement for complete or partial in-orbit retraction capability must be inferred from the overall mission requirements.

The effort during the first quarter of this contract has been concentrated in the definition of the design requirements for the three mission types, the evaluation of existing lightweight solar array system concepts, the detailed review of the component technology base, and the parametric analyses of the solar cell blanket and bus strip distribution network. A discussion of the selection of a minimum natural frequency of 0.04 Hz for the deployed panel with respect to the integration of a large lightweight solar array into a spacecraft is included.

SECTION 2

TECHNICAL DISCUSSION

2.1 DESIGN REQUIREMENTS

2.1.1 GENERAL

The basic design requirements for the 110 Watt per kilogram Solar Array Feasibility Study are given in JPL Specification ES506080 Revision B which is included as Appendix A of this report. The specification pertains to the interplanetary mission application. The requirements for the other two mission types, viz, geosynchronous and manned space station, are to be derived as a task under this contract. Table 1 lists the assumed orbital parameters for each of these mission types.

Table 1. Mission Orbital Parameters

Mission Type	Orbit Attitude (km)	Orbit Inclination (deg)
Interplanetary	------	--
Geosynchronous	35,700	0
Manned Space Station	500	55

In the following paragraphs, the requirements for each mission type, as they pertain to the solar array system, are presented. These requirements are not intended to place undue restrictions on the solar array system design, but only to act as a guide in the formulation of a design approach for each mission application. Where any design requirement is found to restrict a potentially attractive design approach, this requirement will be reviewed to determine its impact on the ability to achieve the 110 watt/kg goal. For example, in the case of the manned space station mission, if the specified deployed loads are found to impose structural weight penalties on the solar array system which make the 110 watt/kg goal unachieveable, then these loads will be treated as a parameter in determining the affect on total system power-to-weight ratio. The intent is to develop high performance design

concepts which are viable candidates for future missions of the three types being investigated. The design requirements will be representative rather than specific as a detailed design optimization cycle would be a part of any flight hardware application.

2.1.2 INTERPLANETARY MISSION

The significant requirements for this mission, as reflected by JPL Specification ES506080 Revision B, have been summarized in Table 2. During the course of review of these design requirements, sections of the JPL specification which need change or further clarification have been identified. These are listed and discussed below.

The solar panel lifetime, as stated in Section 3.2.3 of the specification, is three years with no greater than a 20 percent loss of power over this period. The effect of this requirement on the solar cell blanket was investigated and is reported in Section 2.5 of this report. The general conclusion regarding this 20 percent maximum degradation restriction is that it imposes shielding requirements which result in a total blanket weight which is too high in relationship to the total system power-to-weight ratio goal. For a nominal 125 μm thick, 10 ohm-cm solar cell, a blanket weight of approximately 66.6 kg (73 percent of the total system weight goal) is required to provide the necessary shielding. For similar 2 ohm-cm cells, the necessary shielding is increased so that a total blanket weight of approximately 71.7 kg (79 percent of the total system weight goal) is required to limit the solar cell radiation degradation to 20 percent.

Thus, unless it is necessary to restrict the allowable maximum power degradation, it would be advantageous from a weight standpoint to allow a greater percentage loss over the 3-year mission duration. The parametric analysis of the solar cell blanket, contained in Section 2.5, shows that an allowable maximum power degradation, due to particle radiation damage to the solar cells, of about 28 percent will allow the use of either 100 or 125 μm thick, 10 ohm-cm solar cells with a minimum front and back shield of 0.008 gm/cm^2. The total blanket weight under these conditions is 48.2 and 50.2 kg for 100 and 125 μm solar cell thicknesses, respectively. These blanket weights represent 53 and 55 percent of the total system weight goal, respectively. Thus, a total degradation of 30 percent will permit an

Table 2. Summary of Design Requirements for the Interplanetary Mission from JPL Specification ES506080B

<table>
<tr><th>Specification Paragraph Number</th><th>Title</th><th>Definition of Requirement</th></tr>
<tr><td>3.2.2</td><td>Power requirement</td><td>• 10 kW at spacecraft interface at 1 AU and at the predicted solar array temperature</td></tr>
<tr><td>3.2.3</td><td>Lifetime</td><td>• 3 years with no greater than a 20-percent loss of power</td></tr>
<tr><td>3.2.4</td><td>Solar panel operating temperature</td><td>• Maintain cell temperature between 50 and 70°C at 1 AU</td></tr>
<tr><td>3.2.5</td><td>Solar panel weight</td><td>• Power-to-weight ratio > 110 watt/kg at 1 AU
• Weight not to include panel gimbaling mechanisms</td></tr>
<tr><td>3.2.6</td><td>Packaging volume envelope</td><td>• Maximize adaptability to various spacecraft configurations
• Assume Titan-Centaur launch vehicle with 907 kg spacecraft which uses two 10 kW solar panels</td></tr>
<tr><td>3.2.7</td><td>Structural interfaces</td><td>• Ease of gimbaling is important
• Consider requirements imposed on spacecraft structure</td></tr>
<tr><td>3.2.8</td><td>Structural rigidity</td><td>• Deployed natural frequency ≥ 0.04 Hz</td></tr>
<tr><td>3.2.9</td><td>Mass center location</td><td>• Minimize displacement of vehicle mass center and center of solar pressure caused by thermal gradients and solar panel temperatures</td></tr>
<tr><td>3.2.10</td><td>Flatness</td><td>• Maximum out-of-plane deflection ± 10 degrees including that caused by thermal gradients when operating from 0.5 to 5.0 AU</td></tr>
<tr><td>3.3.2</td><td>Launch environment</td><td></td></tr>
<tr><td>3.3.2.1</td><td>Sinusoidal vibration</td><td> 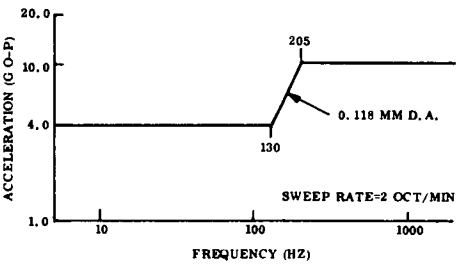
</td></tr>
<tr><td>3.3.2.2</td><td>Acoustic</td><td>• At interface between solar panel assembly and the spacecraft in each of three axes
<table>
<tr><th>1/3 Octave Band Center Frequency (Hz)</th><th>Sound Pressure Level in 1/3 Octave Bands (db ref 2 x 10^{-4} dynes/cm^2)</th></tr>
<tr><td>80</td><td>132.5</td></tr>
<tr><td>100</td><td>136.0</td></tr>
<tr><td>125</td><td>138.0</td></tr>
<tr><td>160</td><td>140.0</td></tr>
<tr><td>200</td><td>142.0</td></tr>
<tr><td>250</td><td>142.5</td></tr>
<tr><td>315</td><td>143.0</td></tr>
<tr><td>400</td><td>142.5</td></tr>
<tr><td>500</td><td>141.5</td></tr>
<tr><td>630</td><td>140.0</td></tr>
<tr><td>800</td><td>138.0</td></tr>
<tr><td>1000</td><td>136.0</td></tr>
<tr><td>1250</td><td>135.0</td></tr>
<tr><td>1600</td><td>133.0</td></tr>
<tr><td>2000</td><td>132.0</td></tr>
<tr><td>2500</td><td>130.0</td></tr>
<tr><td>3150</td><td>128.5</td></tr>
<tr><td>4000</td><td>127.0</td></tr>
<tr><td>5000</td><td>125.5</td></tr>
<tr><td>6300</td><td>124.0</td></tr>
<tr><td>8000</td><td>122.5</td></tr>
<tr><td>10,000</td><td>120.0</td></tr>
</table></td></tr>
</table>

Table 2. Summary of Design Requirements for the Interplanetary Mission from JPL Specification ES506080B (Cont'd)

<table>
<tr><th>Specification Paragraph Number</th><th>Title</th><th>Definition of Requirement</th></tr>
<tr><td>3.3.2.3</td><td>Shock</td><td> 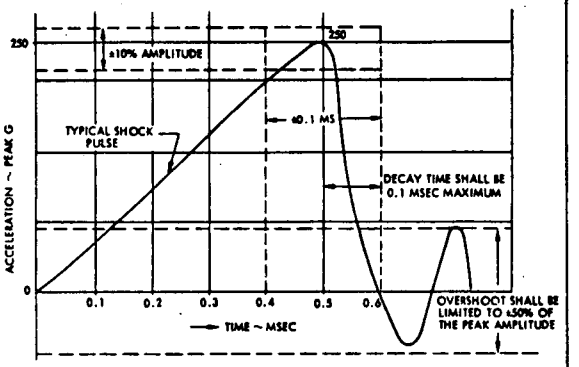
</td></tr>
<tr><td>3.3.2.4</td><td>Static acceleration</td><td>• 9 g's at mass center in three mutually perpendicular axes</td></tr>
<tr><td>3.3.2.5</td><td>Launch pressure profile</td><td>• Maximum rate of change at pressure = 116 ± 8 torr/sec</td></tr>
<tr><td>3.3.2.6</td><td>Aerodynamic heating</td><td>• +30°C/minutes for 200 seconds</td></tr>
<tr><td>3.3.3</td><td>Space flight environment</td><td></td></tr>
<tr><td>3.3.3.1</td><td>Steady state thermal/vacuum</td><td>• -130 to +140°C at 10^{-5} torr or less</td></tr>
<tr><td>3.3.3.2</td><td>Thermal shock</td><td>• -190 to +140°C at 10^{-5} torr or less
• Natural cooling and heating rates
• 1000 cycles</td></tr>
<tr><td>3.3.3.3</td><td>Solar flare proton radiation</td><td><table><tr><th>Proton Energy-E (MeV)</th><th>Total Fluence ϕ>E (p/cm^2)</th></tr><tr><td>1</td><td>2.0×10^{12}</td></tr><tr><td>10</td><td>4.0×10^{10}</td></tr><tr><td>30</td><td>9.0×10^{9}</td></tr><tr><td>100</td><td>1.0×10^{9}</td></tr></table></td></tr>
<tr><td>3.3.3.4</td><td>Pyrotechnic shock</td><td>• Withstand shock environment from firing any pyrotechnic device on the assembly</td></tr>
</table>

additional 3 percent allowance for other degradation sources such as ultraviolet and particle radiation damage to the coverglass material and thermal cycling induced damage. A lighter weight 10,000 watt array could be achieved by the use of higher efficiency 2 ohm-cm cells, but the degradation would be increased to about 37 percent for the same 0.008 gm/cm^2 of front and back shielding.

Another philosophy which might be used in place of the specified beginning-of-life power and allowable degradation constraints is a specified end-of-mission power output with no restrictions on beginning-of-life power.

Section 3.3.3 specifies that the space flight environments are applicable for both the stowed and deployed configurations. However, it may not be realistic to expect the stowed solar array to withstand the specified thermal shock environment.

2.1.3 GEOSYNCHRONOUS MISSION

2.1.3.1 Power Output Requirement

The solar panel shall have a beginning-of-life output power of 10,000 watts, measured at the panel interface, when corrected for normal solar incidence at the nominal intensity of 135.3 mw/cm^2. Figure 1 shows the variation in earth-sun distance, apparent solar declination and eclipse duration for a geosynchronous orbit. It will be assumed that the solar array is oriented by rotation about an axis parallel to the earth's N-S axis. Therefore, the declination of the sun is reflected as an angle of incidence on the solar array surface. This angle reaches a maximum of about 23.5 degrees at the solstice times of year. If the solar array drive axis is not parallel to the earth's N-S axis by some pointing error, this angular error must be added to the angle of incidence due to the solar declination.

2.1.3.2 Mission Lifetime

The solar panel shall be designed to perform over a period of five years with no failures which would prevent the panel from performing successfully in both mechanical and electrical modes. The degradation in solar array maximum power output shall not exceed 32 percent over this period.

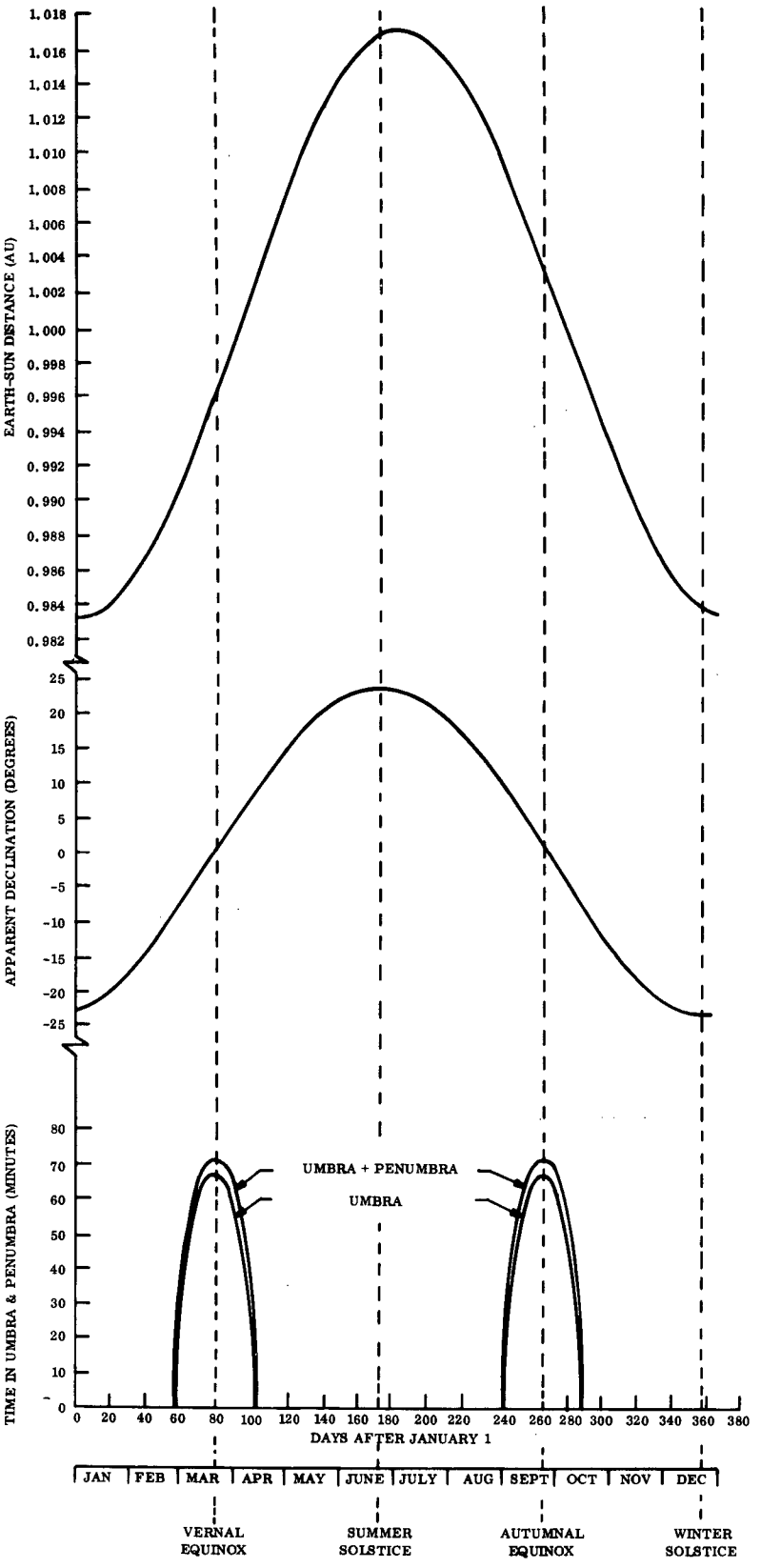

Figure 1. Variation in Earth-Sun Distance, Apparent Solar Declination and Eclipse Duration for a Geosynchronous Orbit

2.1.3.3 Thermal Shock Environment

The thermal shock environment is essentially the same as specified in Appendix A for the interplanetary mission except that the upper temperature limit of $+140^{o}C$ is higher than required for this application. An upper limit of $+70^{o}C$ might be more reasonable as a test extreme in this application.

2.1.3.4 Quasi-Static Loads

Based on ATS F/G data, it is expected that the station keeping thrusters will produce vehicle accelerations of 10^{-4} g. The attitude control thrusters could produce vehicle angular accelerations of about 0.0143 deg/sec^2.

2.1.3.5 Particle Radiation Environment

The particle radiation environment in geosynchronous orbit is similar to interplanetary space except for the addition of trapped electron and proton radiation. The interplanetary space components consist of galactic cosmic radiation, solar wind, and solar flare particle events. Galactic cosmic radiation consists of low intensity, extremely high-energy charged particles which are about 85 percent protons, 13 percent alphas, and the remainder heavier nuclei. These particles have energies from 10^{8} to 10^{19} electron volts (eV) per particle and an intensity of 0.2 to 0.4 particles per cm^2 per steradian per sec outside the influence of the earth's magnetic field (Reference 1). The solar wind consists of very low energy protons and electrons that are continually emitted by the sun. The mean velocity of the solar wind at a distance of approximately 1.0 AU is 450 to 500 km/sec. The solar particle events are the emission of charged particles from distributed regions on the sun during solar flares. These events are composed of energetic protons and alpha particles that occur sporadically and last for several days.

The solar flare proton energy spectra for the five-year duration geosynchronous mission is assumed to be the same as that specified for the three-year duration interplanetary mission. This energy spectra is given in JPL Specification ES506080B and is shown graphically in Figure 2. In comparison with this solar flare proton spectra, the other constituents of the interplanetary particle environment have only a negligible effect on solar cell bulk damage.

The time-averaged trapped electron environment from Reference 2 is shown graphically in Figure 3. The trapped proton environment, shown in Figure 4, is derived from Reference 3 which is extrapolated from the AP5 model.

The radiation environment during the transfer orbit is assumed to have a negligible effect on solar cell degradation.

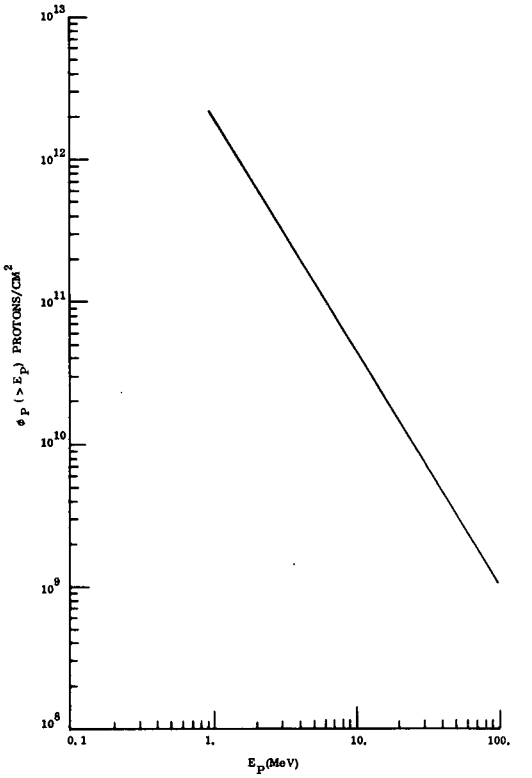

Figure 2. Solar Flare Omnidirectional Proton Integral Energy Spectra for Interplanetary and Geosynchronous Missions

2.1.4 MANNED SPACE STATION MISSION

2.1.4.1 Power Output Requirement

The solar panel shall have a beginning-of-life output power of 10,000 watts, measured at the panel interface, under conditions of normal incidence at the nominal intensity (135.3 mW/cm^2), and at the subsolar point with a β angle of zero degrees (where β is defined as the smallest angle between the orbit plane and the sun line).

2.1.4.2 Mission Lifetime

The solar panel shall be designed to perform over a period of 10 years with no failures which would prevent the panel from performing successfully in both mechanical and electrical modes. The degradation in maximum power over this period shall not exceed 20 percent. The solar array shall be designed to permit the in-orbit replacement of the complete panel.

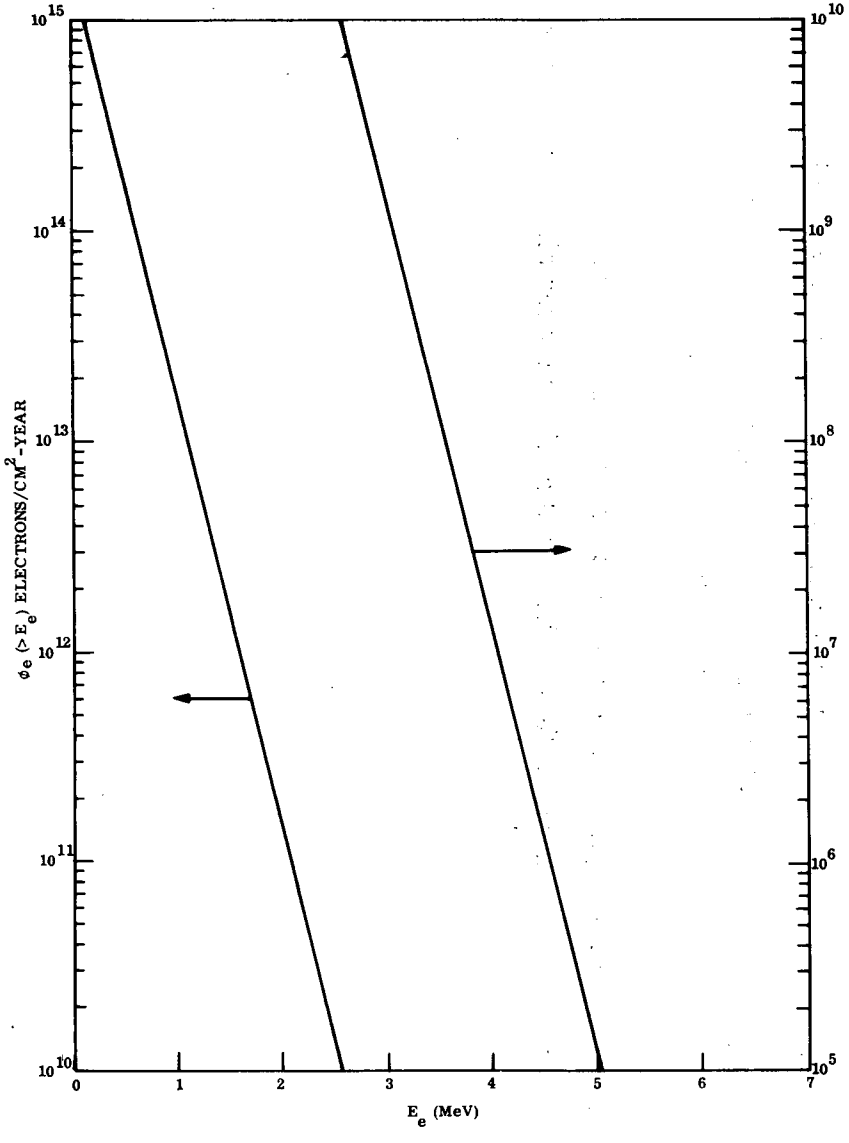

Figure 3. Omnidirectional Trapped Electron Integral Energy Spectra for Geosynchronous Orbit

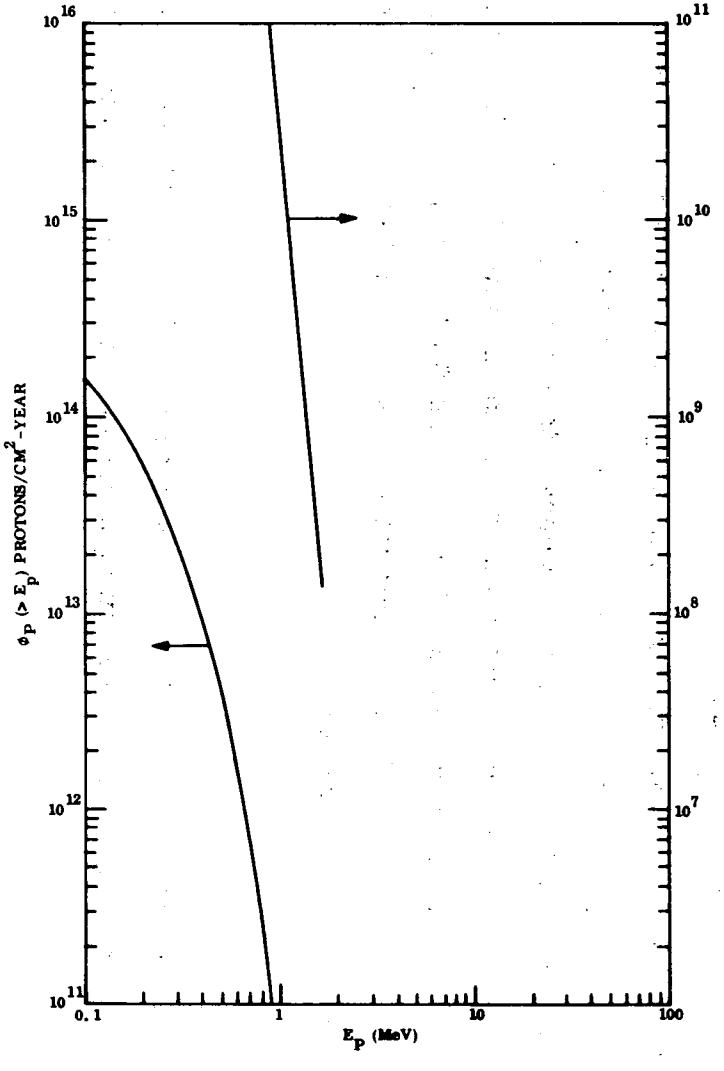

Figure 4. Omnidirectional Trapped Proton Integral Energy Spectra for Geosynchronous Orbit

2.1.4.3 Thermal Shock Environment

The thermal shock temperature extremes on the deployed solar array shall be considered to be $-91^{o}C$ to $+80^{o}C$ at a pressure of 10^{-5} torr or less. The temperature time rates of change during thermal shock shall be at the natural cooling rate of the solar panel in a simulated passage through the earth's shadow, and at the natural heating rate of the solar panel in a normally incident solar flux environment. The heat rates for this mission are given in Figure 5 for the $\beta = 0$ orbit case. The total thermal shock environment shall consist of 60,000 complete cooling and heating cycles.

2.1.4.4 Quasi-static Loads

During the loads analyses, consideration shall be given to loads induced by the solar panel's elastic and rigid body response to the following excitations which were obtained from References 4 and 5:

Due to docking: 0.035 g's for 0.3 seconds in any of three perpendicular axes.

Due to manuevers: 7×10^{-4} g's for 3 seconds in any of three perpendicular axes.

Due to array orientation: 0.137 deg/sec^2 for 2 seconds about each solar array orientation drive axes.

The aerodynamic drag force on a 100 m^2 surface area which is normal to the velocity vector is shown in Figure 6. The effects of this uniformity distributed force should be checked by analysis.

The solar array shall not be required to sustain loading due to an artificial G mode of operation. In the stowed configuration, the static acceleration environment shall be 5 g's at the approximate center of mass of the solar panel. This environment shall be considered equal for each of three mutually perpendicular axes.

2.1.4.5 Packaging Volume Envelope

The volume and shape of the shuttle cargo compartment available to the solar array panels (2 required) is a cylinder 4.27 m in diameter by 11.6 m long.

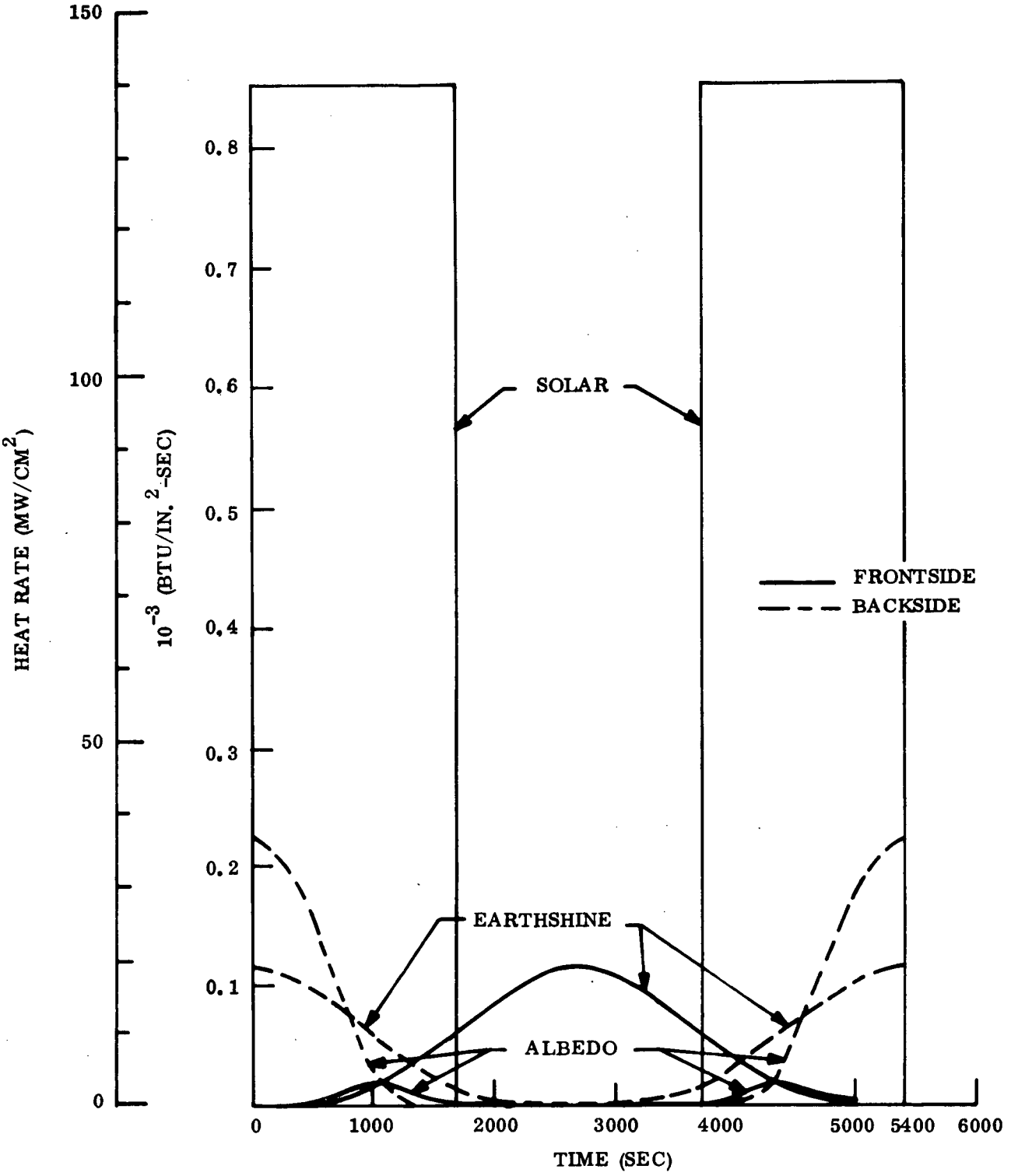

Figure 5. Transient Heat Rates for $\beta=0^{o}$ Orbit
(from Reference 4)

2.1.4.6 Particle Radiation Environment

The trapped proton environment is of primary importance for this mission. Figure 7 shows the trapped proton omnidirectional integral energy spectra for an orbit which is conservatively close to the one of interest. These spectra are based on environment models developed by Vette and his collaborators and reported in References 6, 7 and 8. These models which cover the proton energy (E_p) ranges of interest are:

AP5 ($0.4 < E_p < 4$ MeV)

AP6 ($4 < E_p < 30$ MeV)

AP7 ($E_p > 50$ MeV)

Figure 8 shows the omnidirectional integral energy spectra for the trapped electrons in this same orbit based on data from Reference 9 for the projected 1968 electron environment.

The solar flare proton environment in the 500 km, 55 degree inclination orbit is shown in Figure 9 based on data from Reference 10. This environment represents an integration of all particle events observed over the six peak years of the 19th solar cycle. It has been reduced from the free space spectra to account for the shielding of the geomagnetic field. For the mission duration of 10 years, it is assumed that this spectra, based on solar cycle 19, is applicable with no further modification and can be combined with the corresponding quantities for the trapped radiation environment to arrive at the worst case particle environment.

2.1.5 COMPARISON OF REQUIREMENTS

Table 3 summarizes the significant design requirements for the three mission applications. These requirements on the solar array system design are similar for the interplanetary and geosynchronous missions, but a vast difference exists with the manned space station mission. Generally speaking, the manned space station mission imposes more severe requirements on the solar array design. The deployed array loads induced by maneuvers and dockings are much greater than the loads which occur due to thruster firings on the other two missions. The other significant difference is in the thermal shock requirement. Both the interplanetary

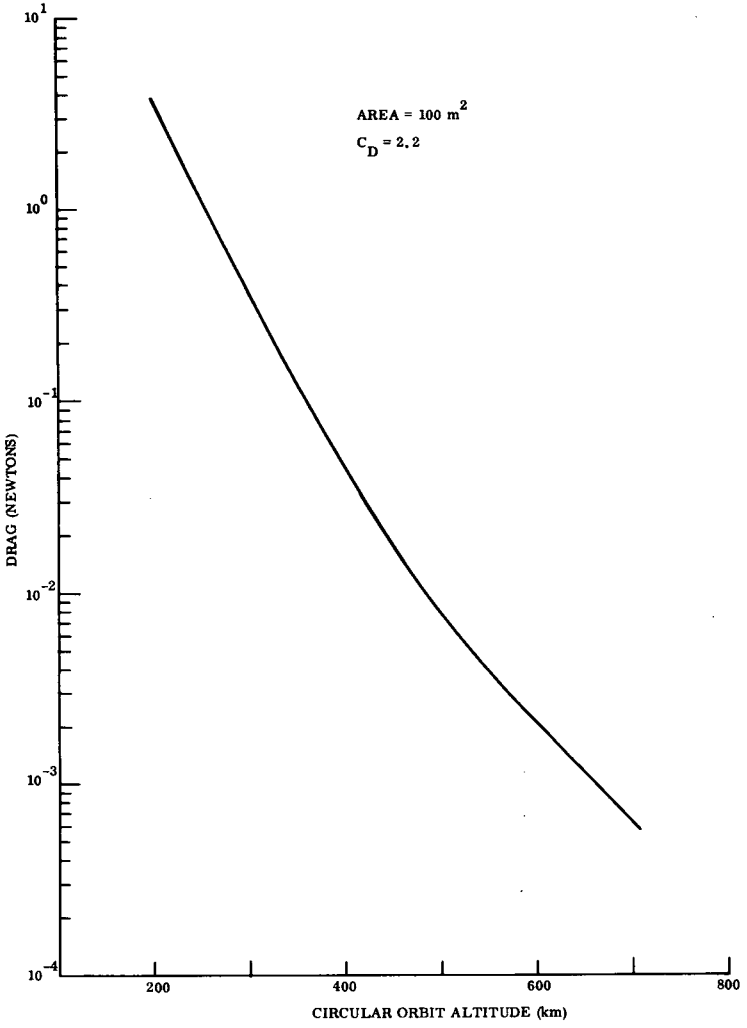

Figure 6. Drag Force with Normal Incidence on 100 m^2 Surface Area

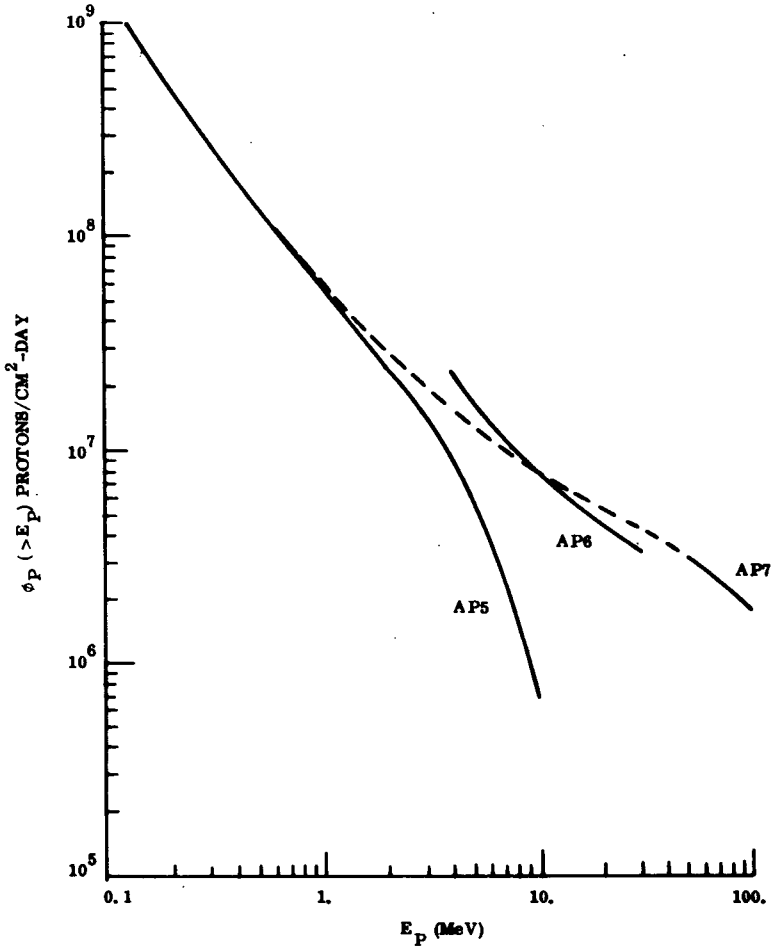

Figure 7. Omnidirectional Trapped Proton Integral Energy Spectra for 555 km, i=60° Orbit

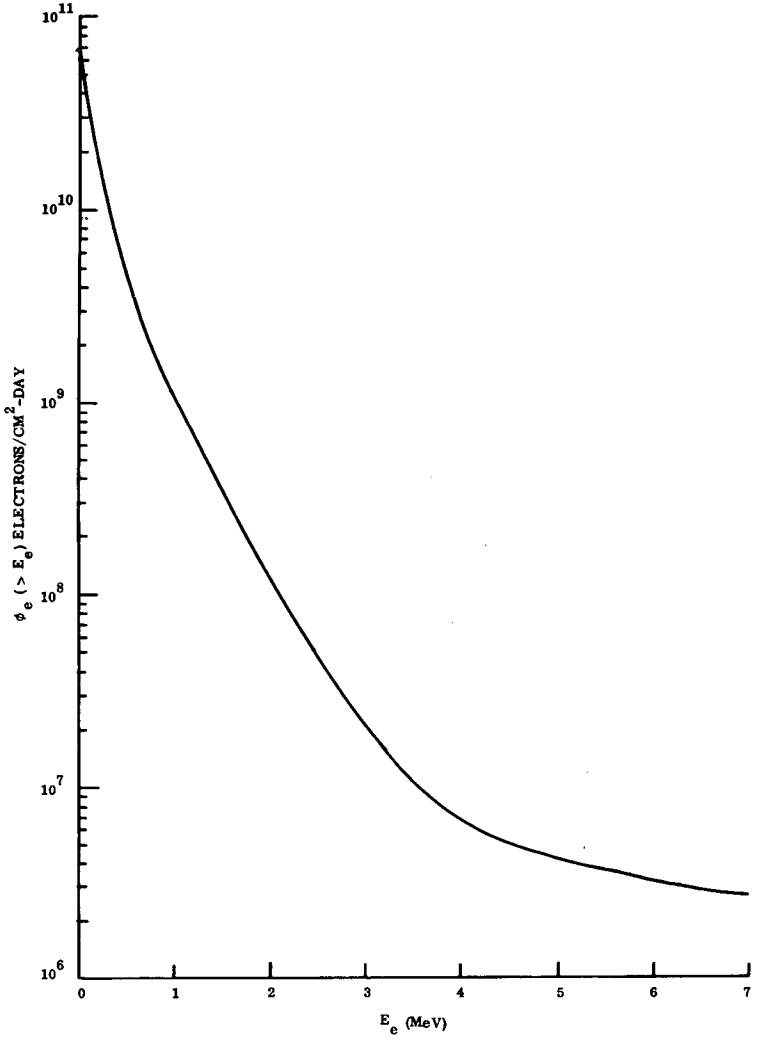

Figure 8. Omnidirectional Trapped Electron Integral Energy Spectra for 555 km, i=60^{o} Orbit

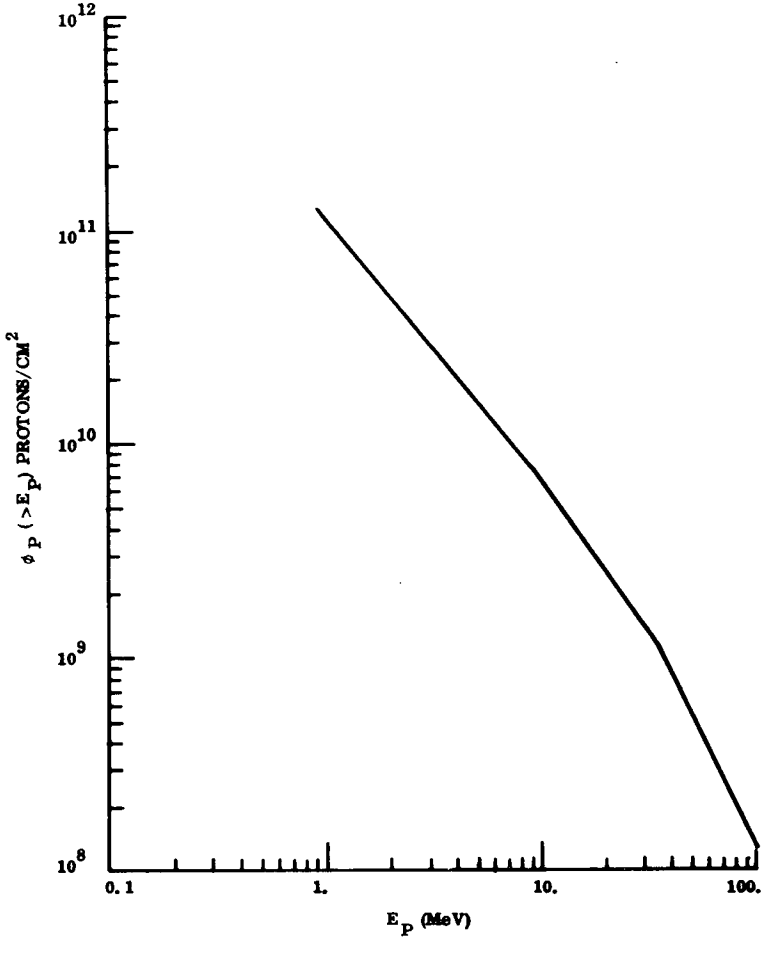

Figure 9. Solar Flare Omnidirectional Proton Integral Energy Spectra for 500 km, i=55^{o} Orbit

Table 3. Comparison of Key Design Requirements

Design Requirement	Definition of Requirement		
	Interplanetary Mission	Geosynchronous Mission	Manned Space Station Mission
Power Output	10 kW at beginning-of-life and at 1 AU		
Lifetime	3 years with loss of power ≦ 20%*	5 years with loss of power ≦ 32%	10 years with loss of power ≦ 20%
Particle Radiation Environment	Solar flare protons per Figure 2	Solar flare protons per Figure 2. Trapped electrons per Figure 3. Trapped protons per Figure 4.	Solar flare protons per Figure 9. Trapped electrons per Figure 8. Trapped protons per Figure 7.
Quasi-Static Load (Deployed configuration)	Not specified	10^4 g's 0.0143 deg/sec^2	0.035 g's for 0.3 sec 7×10^{-4} g's for 3 sec 0.137 deg/sec^2 for 2 sec
Launch Dynamic Loads (stowed configuration)	As specified in JPL Specification ES506080B Assumed to be the same for all mission applications		
Static Launch Acceleration (stowed configuration)	9 g's	9 g's	5 g's
Thermal Vacuum/Thermal Shock Environment	-190 to +140°C 1000 cycles	-190 to +70°C 1000 cycles	-91°C to +80°C 60,000 cycles
Structural Rigidity (deployed configuration)	$f_n \geqq 0.04$ Hz	$f_n \geqq 0.04$ Hz	$f_n \geqq 0.04$ Hz or as determined by deployed loads.

* Analysis has shown that this value should be increased to about 30 percent to allow the use of lightly shielded 10 ohm-cm cells (see Section 2.5)

and geosynchronous missions require a relatively few number of cycles over a wide temperature range while the low orbiting manned space station application, with its 10-year duration, requires approximately 60,000 cycles over a lesser temperature range.

The detailed requirements for the solar array interface with the spacecraft are not specified. Such details are impossible to define for a general feasibility study of this type. However, it is necessary to establish a set of constraints which will determine the philosophy to be used in the definition of the structure required to support the solar array system in the stowed configuration. These constraints, as defined below, will be applied to all mission applications:

1. The solar array system shall be adaptable to a gimballing system which will provide solar orientation.

2. In the stowed configuration, the solar array system will be attached to the spacecraft at a relatively few hardpoint locations rather than by a distributed load attachment.

3. The primary load path for the stowed system will be at the center of the solar array. This will also be the only attachment to the gimballing system in the deployed configuration.

4. The hardpoints of the mounting surface will be assumed to be in a common plane as shown in Figure 10.

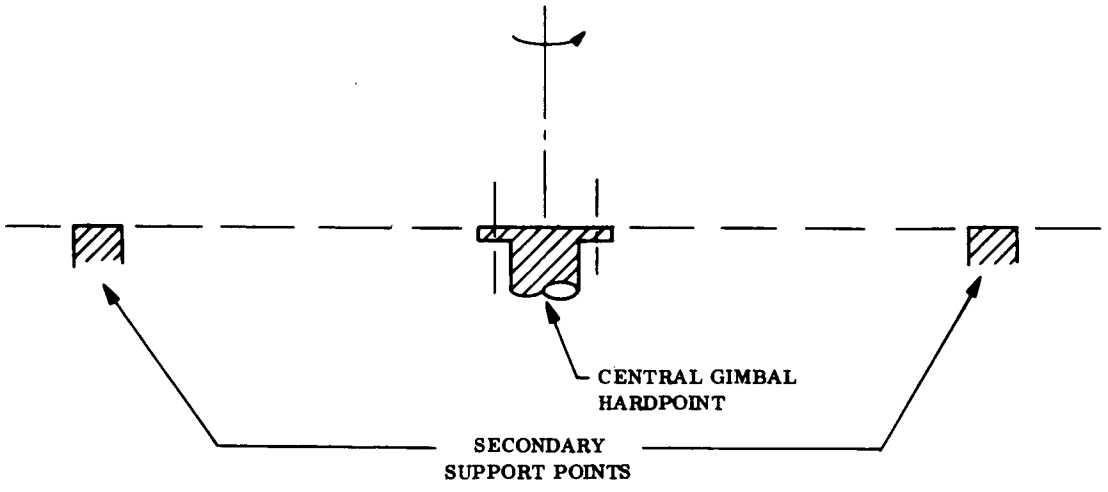

Figure 10. Assumed Spacecraft/Solar Array Interface for All Mission Applications

2.2 EXISTING SOLAR ARRAY SYSTEM CONCEPTS

2.2.1 GENERAL

A number of lightweight solar array system concepts have been developed to the extent that working models have been built and subjected to environmental and functional performance testing. One such system has been flown as an experiment. In this section, each of these systems will be described. No attempt is made to describe all previously proposed lightweight solar array systems since some configurations are similar to existing developed concepts and do not offer any particular advantage from a power-to-weight ratio standpoint.

In general, these existing concepts can be categorized as shown in Table 4.

Table 4. Existing Lightweight Solar Array Types

Solar Array Type	Existing Solar Array Concepts
1. Roll-up	
a. Single boom, two blanket	GE/JPL 30 watt/lb
b. Two boom, single blanket	Hughes/AF
2. Flat-pack	RAE
	CTS
	Lockheed Space Station
3. "Rigid" Folding Panel	Boeing/JPL
	EOS Hollowcore

2.2.2 GE/JPL 30 WATT/LB ROLL-UP SOLAR ARRAY

This roll-up solar array, shown in Figure 11, and referred to as the RA250, was designed, fabricated and tested by the General Electric Company under contract to JPL (Contract Nos. 951970 and 952314). This array provides 23.2 m^2 of deployed solar cell module area which is stored on cylindrical drums during launch (see Reference 11). These storage drums are

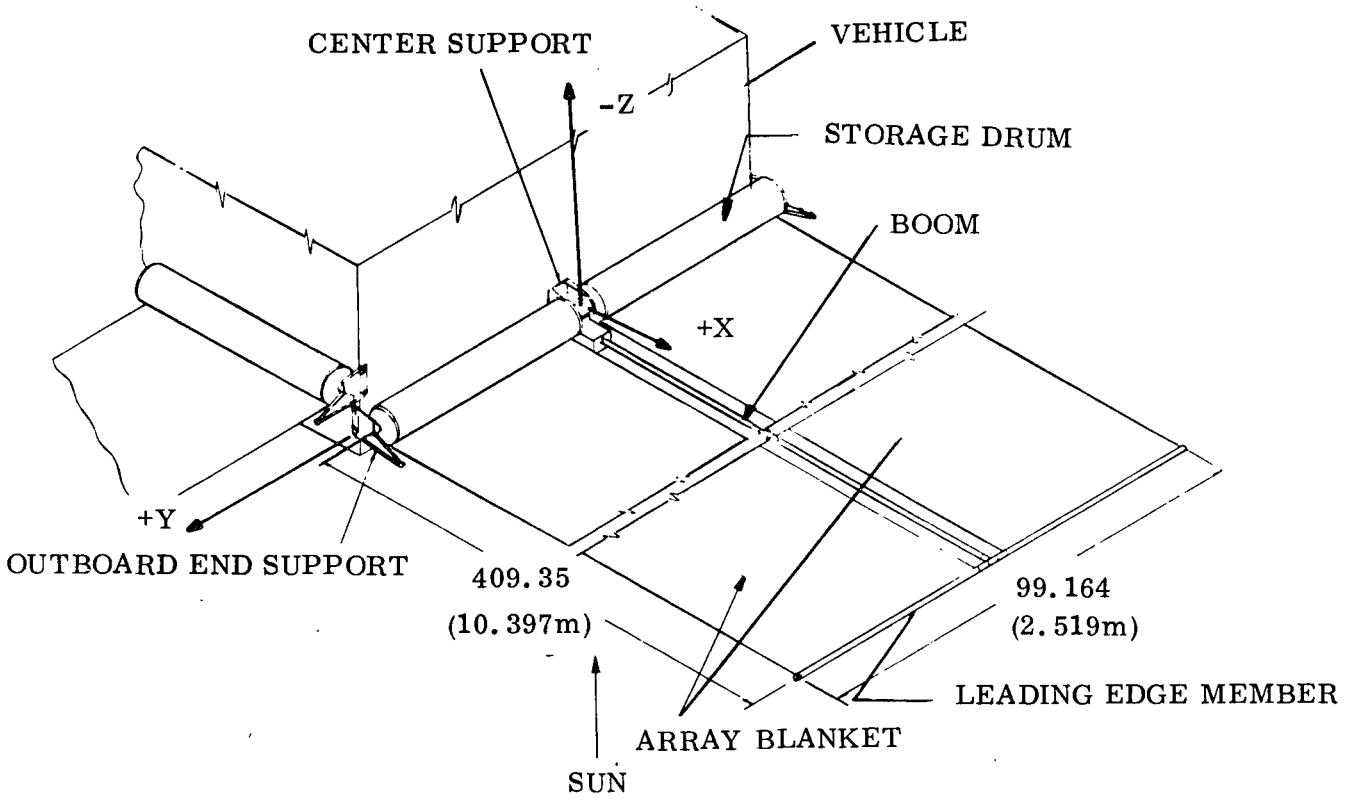

Figure 11. GE/JPL 30 Watt/lb Roll-up Solar Array

mounted on a center support structure. Each drum has a bearing system, a slip ring assembly for the transfer of power and signals, and a Negator spring motor that provides a constant tension in the solar array blanket. A BI-STEM deployable boom is mounted on the center support and is attached to a leading edge member. The solar array blankets consist of an interconnected assembly of 55,176, 180 μm thick, 2 x 2 cm solar cells mounted on a flexible Kapton-H film substrate. A blanket is rolled onto each drum, with the outboard edge attached to the leading edge member. The system is deployed by extending the boom. The deployed boom and the leading edge member comprise the primary structure. Each blanket is under tension from the Negator springs. Outboard end supports are provided in the launch configuration and are pryotechnically released before deployment. The total system weight, including all the structural weight associated with stowage and deployment, is 37.4 kg. Using a specified unit electrical output of 107.6 watt/m^2, the system power-to-weight ratio is 66.8 watt/kg. The total blanket weight-to-area ratio is 0.91 kg/m^2 of module area.

2.2.3 HUGHES/AF ROLL-UP SOLAR ARRAY

The roll-up array developed by Hughes Aircraft Company under Air Force Contract F33615-68-C-1676, is shown in Figure 12. This system was launched as a flight experiment on October 17, 1971, and the array itself has performed satisfactorily in-orbit since that time (References 12 and 13). This system uses two solar cell blankets which are rolled-up on a single storage drum. An embrossed 50 μm thick Kapton cushion protects the solar cells in the launch stowed configuration. During extension, this cushion is rolled-up on an auxiliary take-up roller. The two flexible substrates, which are a laminate of Kapton-H film and fiberglass, are mounted with a total of 34,500 180 μm thick, 2 x 2 cm, 2 ohm-cm cells which are covered with 150 μm thick Microsheet. The solar cell blankets are deployed from the common drum by a pair of extendible boom actuator units. Each unit houses two 2.18 cm diameter BI-STEM booms. The total solar array system weight is given as 32.0 kg with 15.8 kg of this associated with the flexible blankets.

2.2.4 RAE FLAT-PACK SOLAR ARRAY

This lightweight solar array concept, shown in Figure 13, is presently under development at the Royal Aircraft Establishment (see References 14 and 15). This design employs flexible

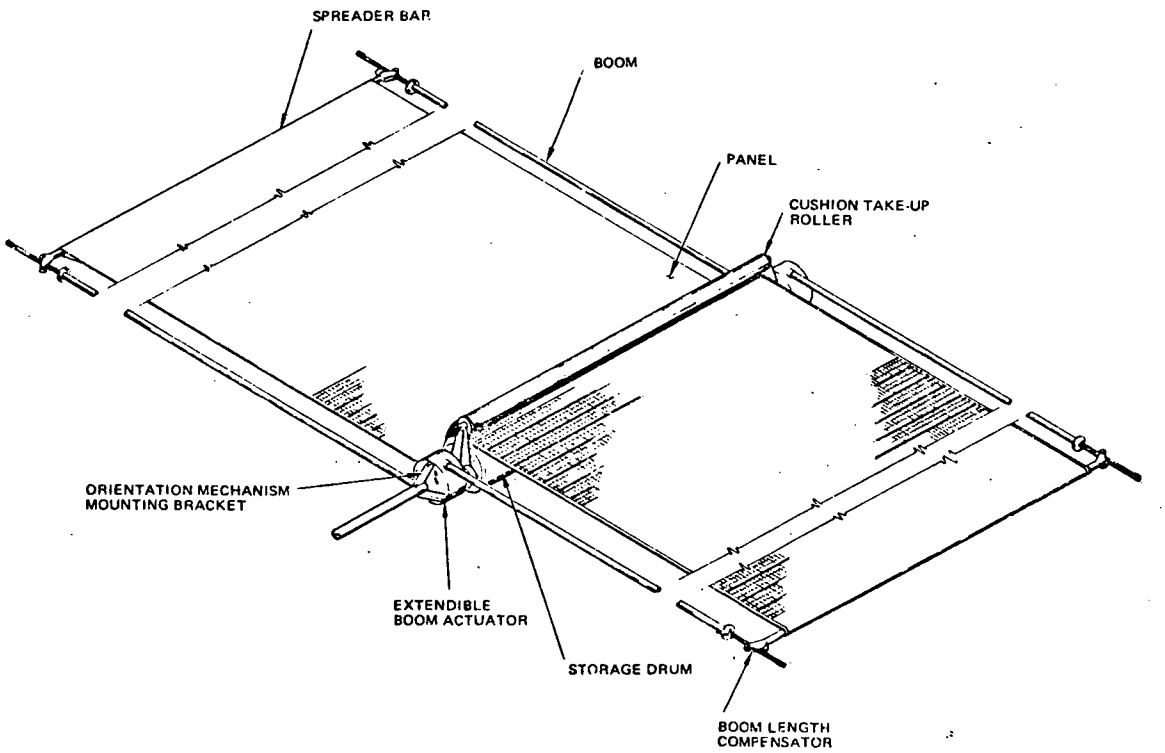

Figure 12. Hughes/AF Roll-up Solar Array

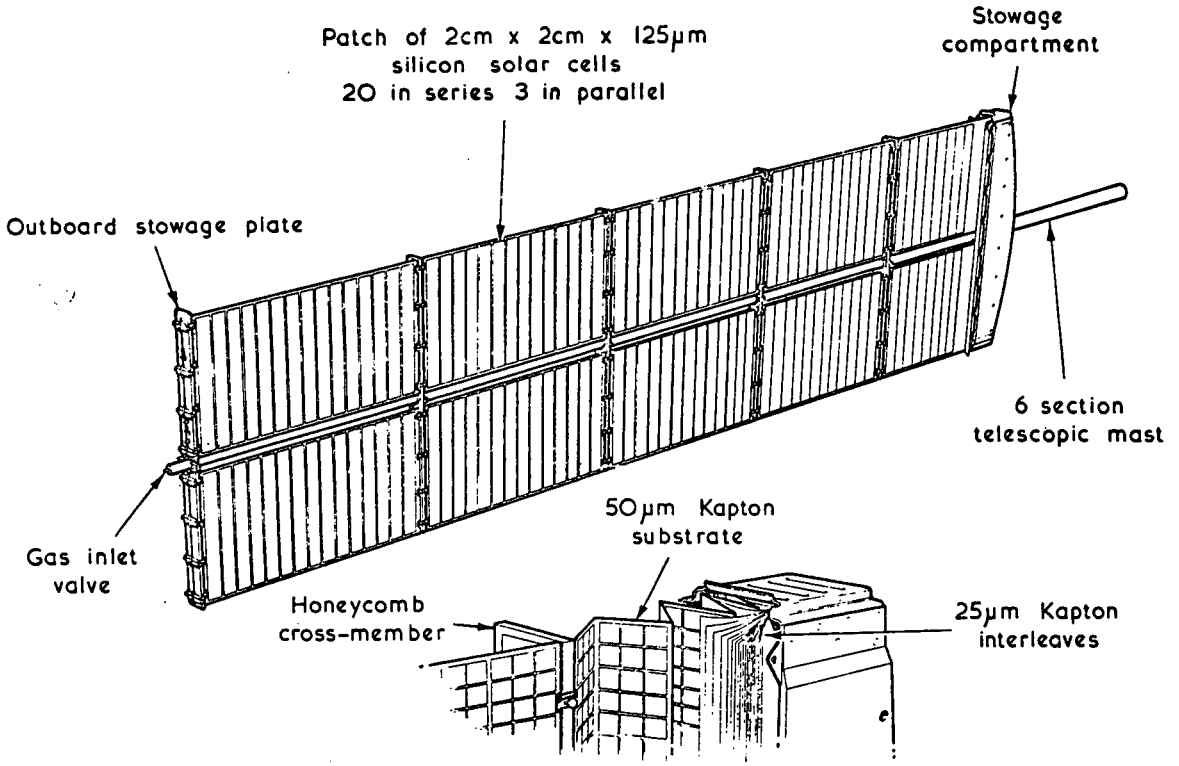

Figure 13. RAE Flat-pack Solar Array

substrates which are folded, accordion fashion, for stowage during launch. The Kapton-H film substrates are mounted with a total of 7440, 125 μm thick, 2 x 2 cm, 10 ohm-cm, bottom wrap-around contact Ferranti cells which are covered with PPE, 100 μm thick, ceria stabilized glass. The solar array is deployed pneumatically through a six section, aluminum telescopic mast. Each section is mechanically latched when fully deployed. Aluminum honeycomb cross members are attached to the tube sections to function as support for the array blanket segments. The total system weight for this model is 5.35 kg. The beginning-of-life power-to-weight ratio is 280/5.35 = 52.4 watt/kg. The solar cell blankets weighed a total of 2.28 kg which yields a unit blanket weight of 0.634 kg/m^2 of total blanket area.

2.2.5 LOCKHEED SPACE STATION SOLAR ARRAY

A solar array system for manned space station application is being developed by Lockheed under contract to MSC (Contract No. NAS9-11039). This system, shown in Figure 14, consists of two array wings per station (Reference 4). A total of 470,000 solar cells are mounted on ten strip

assemblies per wing. Each strip consists of 42 modules each with 1,120 solar cells. These cells are 2 x 4 cm, bottom wraparound contact configuration with a base resistivity of 2 ohm-cm and a thickness of 300 μm. The cells are covered with 300 μm thick fused silica with no blue-reflecting filter. The solar cell copper interconnectors are integral with the substrate and are sandwiched between layers of Kapton-H film with FEP-Teflon used as an adhesive. The solar array strips on a wing are deployed by a single articulated lattice boom which is manufactured by Astro Research Corporation. Each of these strips is stowed by folding it on itself, in flat-pack fashion, within a container which is mounted on the inboard support assembly as shown in Figure 14.

The structural capability of this system is based on an artificial "g" requirement which imposes severe quasi-static loads on the deployed array structure. This requirement has a major influence on the total system weight which is 1341 kg for one wing.

2.2.6 CTS FLAT-PACK SOLAR ARRAY

A flat-pack solar array is presently under development for the Communications Technology Satellite (CTS). This solar array, shown in Figure 15, consists of a single blanket which is deployed by a single 3.5 cm diameter BI-STEM boom (Reference 16). The boom is located behind and on the shadowed side of the blanket. Each blanket is 6.2 m long by 1.295 m wide and is mounted with 13,125 200 μm thick, 2 ohm-cm, 2 x 2 cm cells which are covered with 100 μm thick ceria-stabilized coverglass. A welded interconnection system is utilized and the solar cell modules are mounted on a Kapton-H film substrate. Each blanket is subdivided into 27 active and 3 blank panels which are folded accordion fashion in the packaged configuration. The total system weight is given as 25.29 kg for one of the solar panels. This weight includes the slip rings and orientation drive mechanism associated with one of the panels. The weight of the BI-STEM boom and deployer is 4.08 kg and the weight of each flexible blanket is 6.80 kg.

2.2.7 BOEING/JPL FOLDING PANEL SOLAR ARRAY

The lightweight folding panel solar array shown in Figure 16 was developed by the Boeing Company under contract to JPL (Contract Nos. 951653 and 951934). This solar array panel

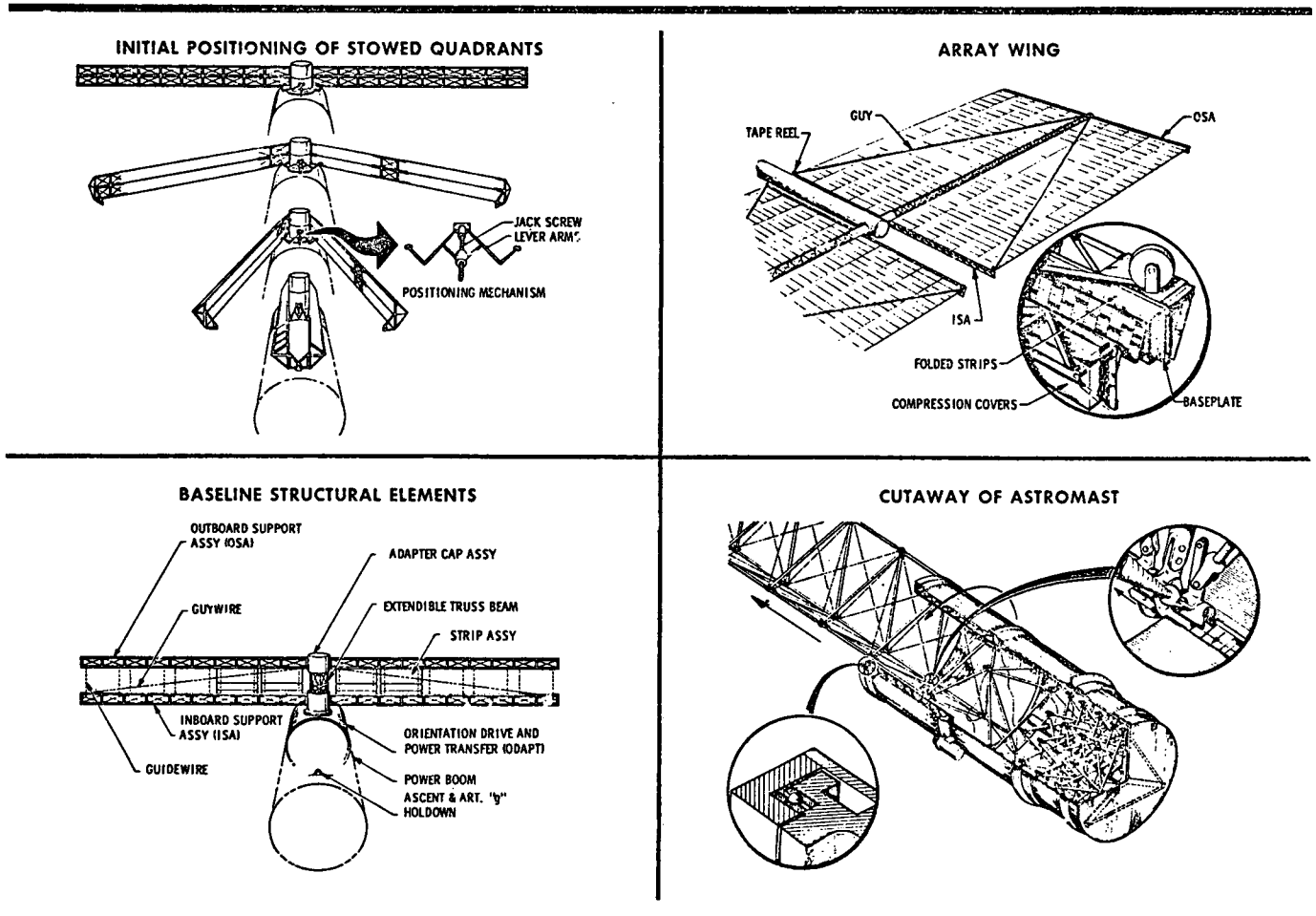

Figure 14. Lockheed Space Station Solar Array

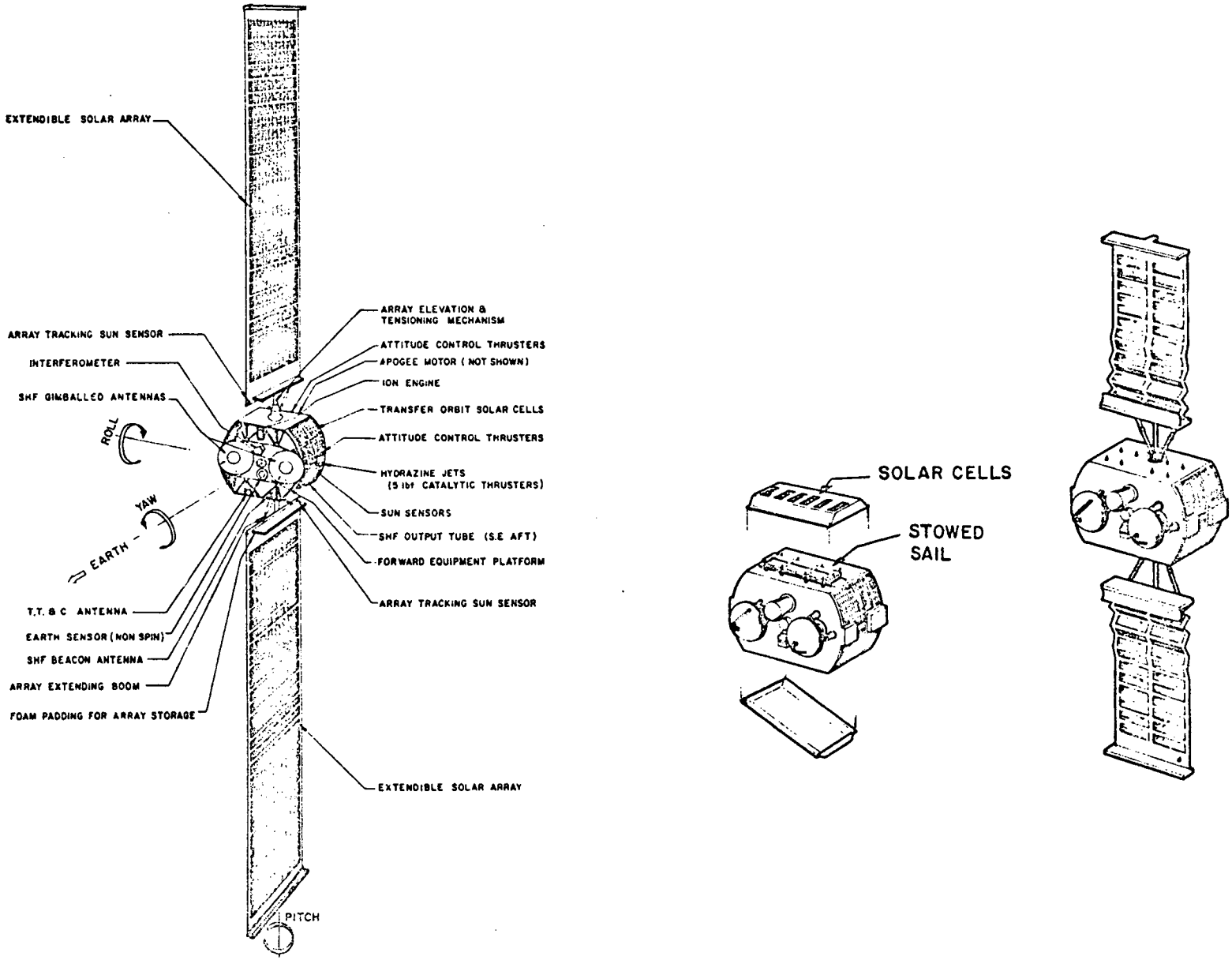

Figure 15. CTS Flat-pack Solar Array

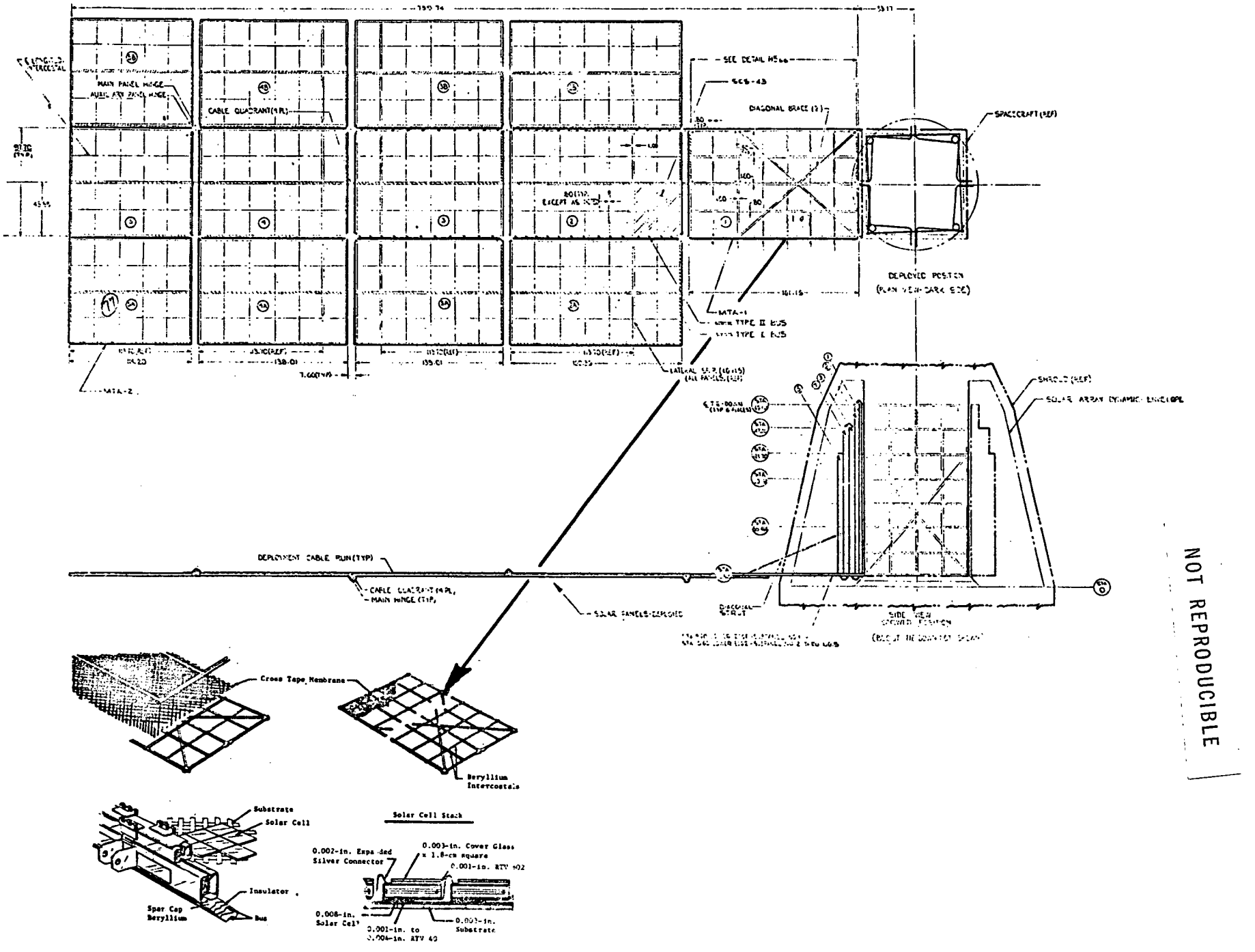

Figure 16. Boeing/JPL Fold-out Solar Array

consists of 13 panels connected by hinges and locked in a common plane when fully deployed (Reference 17). Each subpanel consists of a pretensioned fiberglass tape substrate which is sandwiched between beryllium frames. The solar cell modules, which utilize 180 μm thick, 2 ohm-cm, 2 x 2 cm cells with 75 μm thick Microsheet coverglass, are mounted directly to the stretched fiberglass tape substrate. A total of 256,592 cells are mounted on each panel. The total weight of the panel is 244 kg.

2.2.8 EOS HOLLOWCORE FOLDING PANEL SOLAR ARRAY

This lightweight "rigid" panel concept, shown in Figure 17, was developed by Electro-Optical Systems (EOS) under NASA Contract NAS7-428 (Reference 18). This design employs an electroformed biconvex aluminum hollowcore substrate which is supported in a tubular beryllium frame. The substrate is formed into the surface of a spherical segment with a radius of 414.66 cm. A total of 5040, 100 μm thick, 2 x 2 cm solar cells with 25 μm integral covers are bonded to an intermediate layer of 25 μm thick Kapton-H film. The total panel weight is given as 2.330 kg with 1.435 kg of this associated with the solar cell stack and supporting substrate.

2.2.9 COMPARISON OF EXISTING CONCEPTS

A comparison of these existing lightweight solar array concepts is presented in Table 5. For each system, the total solar cell area per panel is given in Column 4 of the table. This area is computed by multiplying the total number of solar cells by 4×10^{-4} m^2 for 2 x 2 cm cells (or 8×10^{-4} m^2 for 2 x 4 cm cells). A range of over two orders of magnitude in size is reflected by areas which range from the RAE flat-pack at 2.98 m^2 to the Lockheed Space Station at 376.3 m^2. The lowest deployed natural frequency of the solar array system is given in Column 5. For a given system area, a reduction in the deployed natural frequency requirement will result in lower total system weight. The total system weight is given in Column 6. Note that, for the CTS array, the weight includes the orientation drive which can not be separated out to yield the weight of the solar array. The weight of the EOS Hollowcore concept does not include the weight required for stowage and deployment of a multiple panel system. Column 7 of the table gives the total weight per unit area of the system. These total weight-to-area ratios range from 1.279 kg/m^2 for the large RAE flat-pack to 3.570 kg/m^2 for the Lockheed

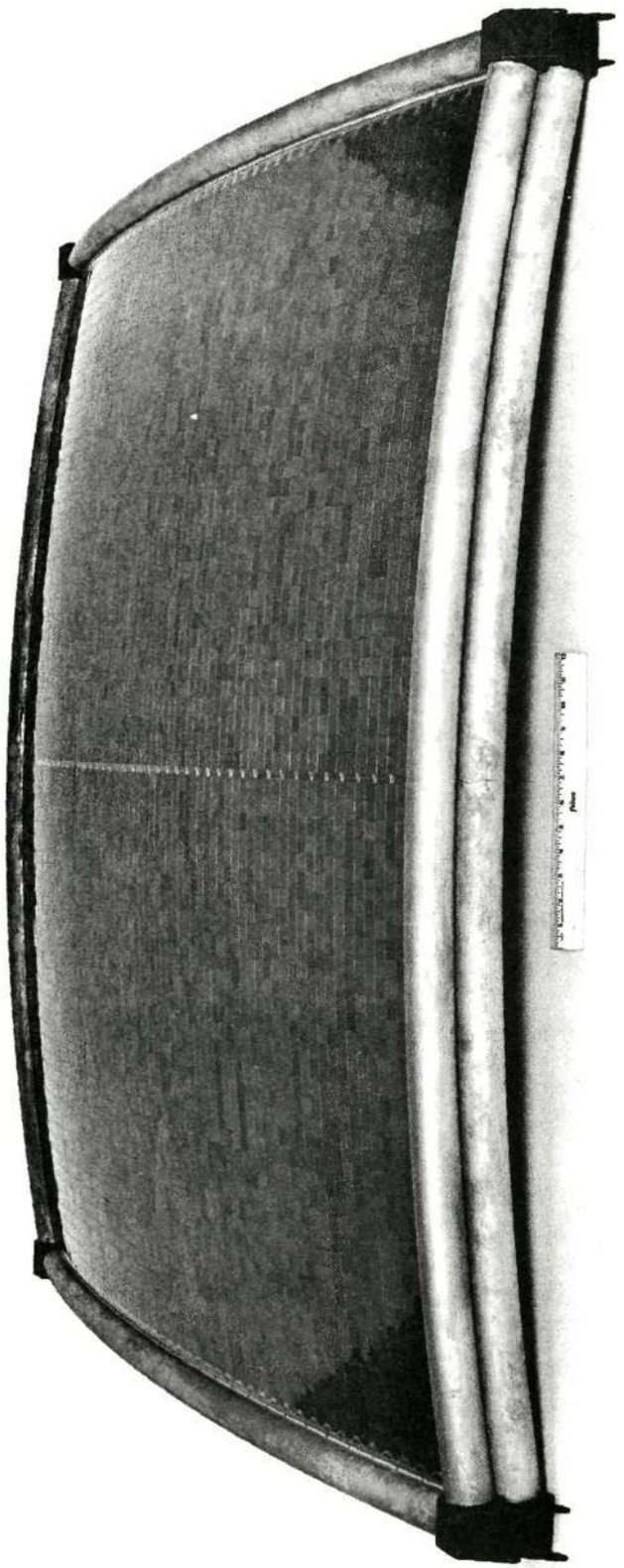

Figure 17. EOS Hollowcore Folding Solar Array (Phase II Demonstration Panels)

Table 5. Comparison of Existing Lightweight Solar Array Designs

No.	Solar Array Configuration Identification	Illustration Figure No.	Total Solar Cell Area Per Panel (m^2)	Lowest Deployed Natural Frequency (Hz)	Total System Weight (kg)	Weight-to-Area Ratio (kg/m^2)					Reference
						Total System	Blanket (or substrate)	Total Structure	Deployment Structure and Mechanisms	Stowage Structure and Mechanisms	
1	GE/JPL 30 Watt/lb Roll-up	1	22.07	0.07	37.4	1.696	0.958	0.738	0.258	0.480	11
2	Hughes/AF Roll-up	2	13.8	0.25	32.0	2.320	1.141	1.179	0.632	0.547	12
3	RAE Flat-pack	3	2.98	0.78	5.35	1.797	0.766	1.031	0.518	0.513	15
		3	13.5	(1)	17.25	1.279	0.718	0.561	0.262	0.299	14
4	Lockheed Space Station	4	376.3	0.062	1341.	3.570	2.258	1.312	(1)	(1)	4
5	CTS	5	5.25	(1)	25.29(2)	4.817(2)	1.295	3.522(2)	0.777	(1)	16, 19
6	Boeing/JPL Fold-out	6	102.6	0.068	244.	2.380	0.894	1.486	(3)	(3)	17
7	EOS Hollowcore	7	2.016	(1)	2.33(4)	1.156(4)	0.712	0.444(4)	(3)	(3)	18

NOTES:

(1) Information not available in the references
(2) Includes solar array orientation drive weight
(3) No attempt was made to separate stowage and deployment structural weight for the folding panel configurations
(4) Does not include weight required to stow and deploy a multiple panel system

space station solar array. Note that the CTS array and the EOS Hollowcore have been disregarded because of the uncertainties associated with the weight numbers. In the remaining weight-to-area ratio columns, the total system weight has been broken down into the contribution due to the flexible blankets and the structure. Where possible, this structural weight has been further divided into the weight associated with: (1) deployment and deployed array support structure and mechanisms, and (2) stowage structure and mechanisms. For example, with the GE/JPL 30 watt/lb roll-up solar array, the total system weight-to-area ratio is 1.696 kg/m^2 which is further divided into 0.958 kg/m^2 for the flexible blankets and 0.738 kg/m^2 for all associated structure. This total structural weight can be further broken down into 0.258 kg/m^2 for deployment and deployed array support structures and mechanisms and 0.480 kg/m^2 for structure associated with stowage. The BI-STEM boom and actuator along with the leading edge member are considered as deployment related structures while the storage drums, center support and outboard end supports are considered part of the stowage related structure. This division of structural weight applies fairly well for the flexible substrate solar arrays, but cannot be applied to the "rigid" folding panel configurations since it is difficult to allocate structural weight between stowage and deployment functions.

2.3 ADVANCED SOLAR ARRAY SYSTEM CONCEPTS

2.3.1 GENERAL

Two advanced solar array system concepts have been identified as potentially attractive from a power-to-weight ratio standpoint. In general, these concepts are based on previously reported, but undeveloped, structural concepts which show promise in the quest for lighter weight systems.

2.3.2 SCHEEL CIRCULAR SOLAR ARRAY

The first of these advanced concepts is the circular array reported by Scheel in Reference 20. This concept, shown pictorially in Figure 18, uses a novel method of packaging a circular sheet around the outer surface of a cylindrical body. Elastic rims, which are attached to the main folds of the array and wrapped up with the blanket in the stowed configuration, must be provided to support the deployed array on a non-spinning spacecraft. These supporting ribs are significantly shorter than the supporting boom(s) of a rectangular flexible array of the same area.

For a given area and minimum deployed natural frequency requirement, the circular array may allow a reduced structural weight when compared to a rectangular configuration flexible array.

2.3.3 WIRE STIFFENED BOOM SOLAR ARRAY

This solar array concept is based on a method for stiffening self-erecting booms which was developed by D. Lee and J. Schwartz of the General Electric Company in 1967. A demonstration model of this wire stiffened boom (Space Lee Girder) is shown in Figure 19. The Space Lee Girder consists of four longitudinal wires, two orthogonal sets of compression rods, and interconnecting guy wires. The four longitudinal wires are parallel to the boom and equally spaced around it. These wires are separated in pairs by two orthogonal sets of compression rods which are axially constrained to the boom at their mid-points, but which can move longitudinally along the boom. The ends of the rods are interconnected by guy wires to form a truss.

Prior to deployment, the wire lengths are preset and the compression rods are stacked alternately in a crisscross pattern. As the boom is erected, the rods are lifted one by one by the wires. When fully deployed, the wires are tensioned by the boom to provide added stiffness.

This stiffened boom concept can be adapted to a solar array as shown in Figure 20. In this proposed configuration, the solar cell blankets eliminate the need for two of the longitudinal wires. One set of compressions rods are in the plane of the blanket and physically part of it. The second set of rods are in the plane of the blanket when stowed and rotate normal to the blanket during deployment.

The remaining longitudinal wires and one-half of the guy wires have preset lengths; the other guy wires are slack during stowage to allow one set of compression rods to rotate into the plane of the blanket. Two slack wires are fastened to the supporting structure at one end, run through a pulley at the intersection of the boom and leading edge member, and then run through pulleys at the ends of the rotatable rods. As the boom is deployed, the length of the slack cable is shortened, causing the compression rods to rotate into position. By selecting a proper ratio of rod spacing (dimension a) a blanket half-width (dimension w), it is possible to have the rods

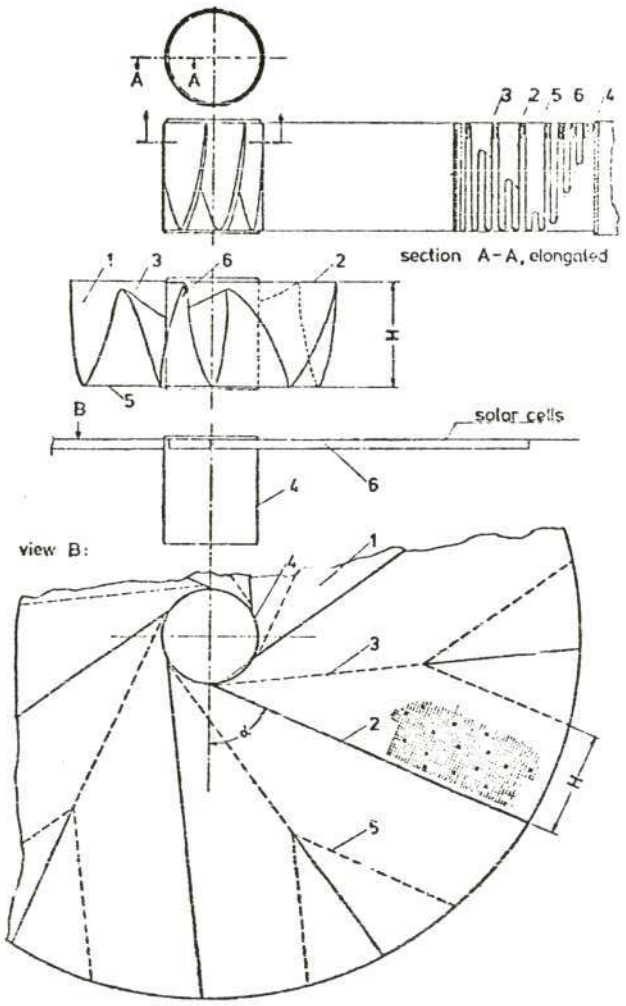

Figure 18. Scheel Circular Solar Array Concept

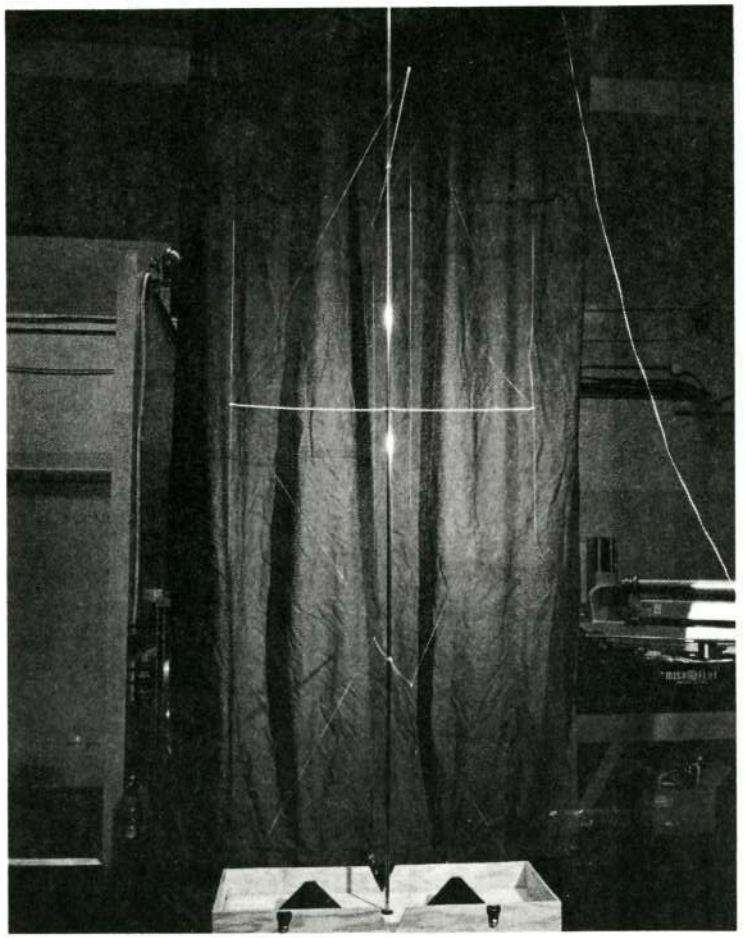

Figure 19. Space Lee Girder Demonstration Model (A67-30D)

rotate into precise position as the boom erects. For example, when a = 101.6 cm and w = 180.34 cm, this precise positioning is achieved. In order to allow for tolerances and to provide tension, the boom is extended slightly further than nominally required. When stowed, the blankets could be folded in flat-pack accordion fashion with the boom extended far enough to engage all rods.

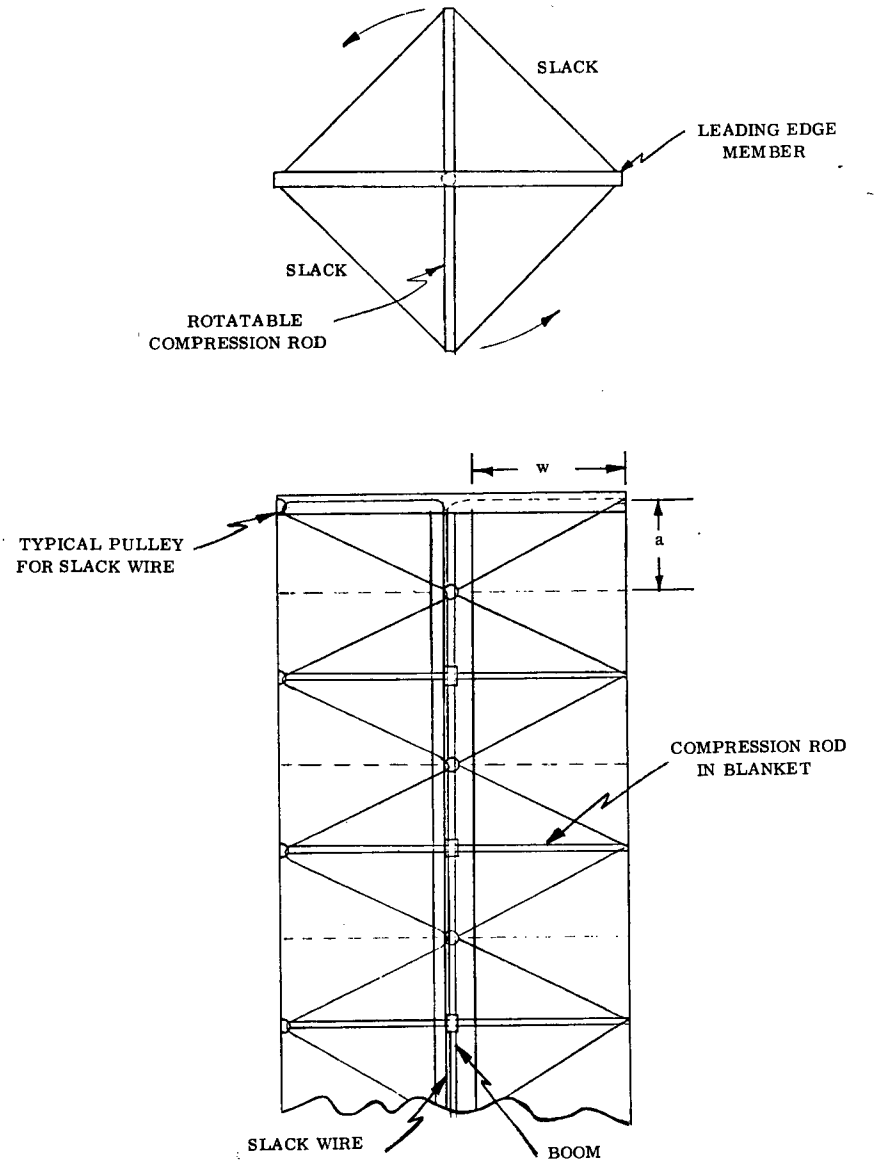

Figure 20. Wire Stiffened Boom Supported Solar Array Concept

2.4 EXISTING COMPONENT TECHNOLOGY BASE

2.4.1 GENERAL

A review of the existing technology base in the areas of solar cells, solar cell covers, interconnects and substrates, and deployable booms was performed during this reporting period in order to have an early assessment of the present state-of-the-art. This section discusses each of these areas with particular emphasis on the applicability to this study.

2.4.2 SOLAR CELLS

This feasibility study will be based on the use of N on P silicon solar cells. This is not intended to rule out the potential offered by future developments in solar cell technology. For example, the recent announcement by IBM regarding an 18-percent efficient gallium arsenide solar cell (Reference 21) will be considered as a potential for improving the solar array system power-to-weight ratio beyond the minimum 110 watt/kg goal. In other words, the feasibility of the 110 watt/kg goal will not be linked to projected improvements in solar cell technology.

Nominal solar cell thickness from 200 to 100 μm were considered as having possible application on this program. Two nominal base resistivities, 2 and 10 ohm-cm, were also considered. In addition to thickness and base resistivity, the solar cells were considered to be of the basic 2 x 2 cm size with a bottom wraparound contact configuration. The bottom wraparound contact configuration, shown in Figure 21, was selected because of the improved reliability for lightweight solar arrays which results from reduced interconnector stresses. This was a conclusion reported by Heliotek, in Reference 22, after performing an extensive study of the stress in conventional Z tab configuration interconnectors. In the bottom wraparound contact configuration shown in Figure 21, the N contact is wrapped around the edge for the full width of the cell.

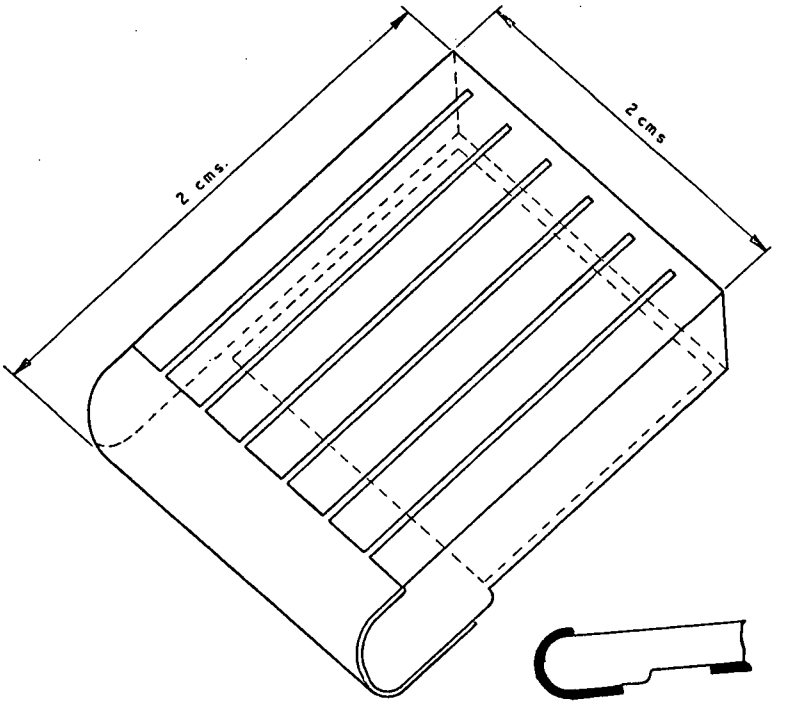

Figure 21. Bottom Wraparound Contact Configuration
(from Reference 23)

The width of the N contact on the front is about 100 μm so that increased active area is available. With this contact geometry, it is possible to make both cell connections with a flat interconnector instead of the out-of-plane Z tab. This leads to the integration of the interconnector pattern with the substrate to provide a weight effective, low stress module configuration.

A cell anti-reflective coating of TiO_x was selected over the commonly used SiO because of the demonstrated improvement in covered cell output. The use of a titanium oxide (TiO_x) anti-reflective coating has demonstrated gains of up to 4 percent in short-circuit current of covered cells when compared to similarly covered cells with SiO anti-reflective coating (Reference 24). Some of this potential output power improvement is offset by a slight increase in the solar absorptance of the covered TiO_x cells which results in an increased in-space operating temperature when compared to covered SiO cells. The net result is a worthwhile improvement in covered cell output with the TiO_x anti-reflective coating.

The electrical performance of solar cells of this type is shown in Figure 22 expressed in terms of unirradiated covered cell maximum power output as a function of nominal cell thickness. This baseline performance is intended to reflect the best obtainable minimum lot average output with an economical yield using 1972 production technology. The maximum lot average cell weight associated with the nominal thickness is shown on the abscissa of the curve. The basis for these curves is data from References 14, 15, 23, 25 and 26 for a 125 μm thick, 10 ohm-cm cell manufactured by Ferranti, Ltd. The design characteristics of this cell are summarized in Table 6. Figure 23 is the I-V characteristic which represents the minimum lot average performance of this cell at two operating temperatures, 25 and 55^{o}C. Based on this one performance data point, the curves on Figure 22 were constructed using normalized data from Reference 27.

Table 6. Design Characteristics of Ferranti 125 μm Thick Solar Cells (Ferranti Cell Type MS36)

Feature	Description
Thickness	125 $\pm$ 25 μm
Size	20 $\pm$ 0.15 x 20 $\pm$ 0.15 mm
Resistivity	7 to 12 ohm-cm Float zone silicon
Contact Configuration	Bottom wrap-around 24 finger grid geometry
Contact Material	Plated - nickel, copper, nickel, gold
Anti-reflective Coating	TiO_x
Minimum Lot Average Electrical Performance (covered)	123 ma at 0.445 volts (equivalent AMO, 1 A.U. illumination at 25 $\pm$ 2^{o}C)
Maximum Lot Average Cell Weight	0.129 gm/cell

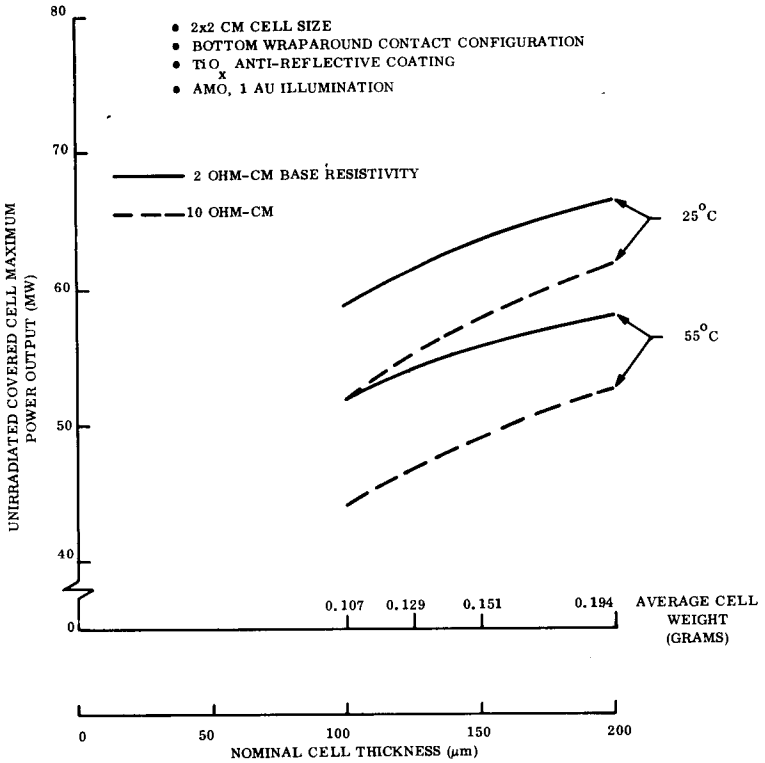

Figure 22. Baseline Solar Cell Electrical Performance

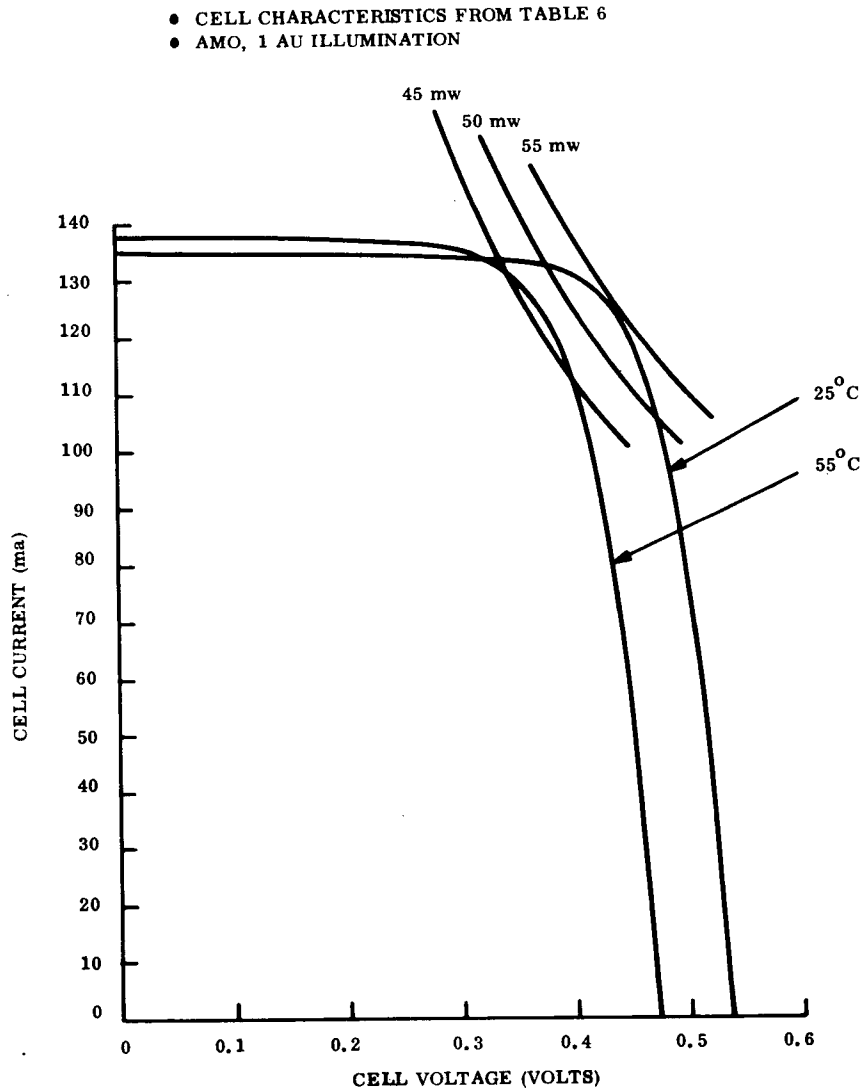

Figure 23. I-V Characteristic for 125 μm Thick, 10 ohm-cm Covered Ferranti Cell

2.4.3 SOLAR CELL COVERS

The conventional method of protecting the active solar cell surface from the damaging effects of particle irradiation entails the application of discrete coverglass (either fused silica or Microsheet) by bonding with a silicone adhesive. Discrete coverglass thicknesses from 75 to 500 μm have been used. A weight of 0.23 kg/m^2 of cell area is associated with the application of 75 μm thick Microsheet with a 25 μm adhesive bond line. This represents approximately 24 percent of the allowable total system weight and is prohibitively high for this application. Two promising approaches are available to provide the coverglass function at significantly reduced weight. The first of these is the integral glass cover which entails the direct deposition of glass onto the cell surface. The second method consists of the direct heat-sealing of FEP-Teflon film to the cell surface.

2.4.3.1 Integral Coverglass

The deposition of glass onto the active surface of a silicon solar cell without the use of an intermediate layer of bonding adhesive has been investigated by a number of workers as reported in References 28 through 34. The following methods for deposition of solar cell integral covers are represented by this work:

1. High Vacuum Ion Beam Sputtering (HVIBS)
2. Electron beam evaporation
3. Radio frequency sputtering
4. Fusion.

The following is a brief discussion of each of these processes with comments concerning the applicability to the 110 watt/kg solar array feasibility study.

2.4.3.1.1 High Vacuum Ion Beam Sputtering (HVIBS)

This method is a proprietary process developed by Ion Physics Corporation, Burlington, Massachusetts. The development of integral covers using this technique was performed under contract to Goddard Space Flight Center and is reported in References 30 and 32.

This process utilizes a focused ion beam propagating through a high vacuum region to sputter from a target onto substrates located in a line-of-sight position relative to the target. The Ion Physics HVIBS facility consists of a 20 kV, 250 ma argon ion beam impacting upon a target area of roughly 260 cm^2. The deposition rate with this facility is 1.2 μm/hr. Table 7 lists the integral cover materials which were evaluated on this program. Corning 7940 fused silica, deposited by HVIBS, produces a cover with excellent physical and performance characteristics. The only drawback is the high intrinsic stress condition which is sufficient to cause cell fragility when coating thickness exceeds 50 μm. Figure 24 shows this stress expressed in terms of cover/cell bow as a function of coating thickness. The SiO_2/Si_3N_4 oxynitride material yielded extreme stress levels which resulted in incidence of cover delamination. The deposited integral cover was brown in color and exhibited strong optical absorption. Corning 7740 and 7070 borosilicate glasses, best known as Pyrex, were selected for their good expansion coefficient match to that of silicon, as shown in Table 8. Corning 0211 Microsheet was investigated because of its known performance characteristics as a conventional cover material. The radiation darkening characteristics of 7740 and 0211 are only marginally acceptable, but this property can be improved through the introduction of CeO_2.

Table 7. Summary of Integral Cover Materials Deposited by HVIBS (From Reference 32)

Material	Deposited Stress	Integral Coating Physical Quality	Integral Coating Optical Quality
7940 fused silica	high	excellent	excellent
SiO_2/Si_3N_4	very high	poor	poor
7740	moderate	excellent	excellent
7740 + CeO2 doping	low	excellent	good
0211 + CeO2 doping	very low	excellent	good
7070	low	initially fair/ improved to excellent	excellent

Table 8. Comparison of Integral Cover Materials
(From Reference 32)

Material	Thermal Expansion Coefficient ($^{o}C^{-1}$)	Annealing Point (^{o}C)	Relative Radiation Resistance	Constituents (weight percent)	
7070	32×10^{-7}	495	good	SiO_2	70.0
				B_2O_3	28.0
				Li_2O	1.2
				Al_2O_3	1.1
				K_2O	0.5
				MgO	0.2
				CaO	0.1
7740	33×10^{-7}	565	fair	SiO_2	80.5
				B_2O_3	12.9
				Na_2O	3.8
				Al_2O_3	2.2
				K_2O	0.4
0211	72×10^{-7}	539	fair	SiO_2	65.5
				B_2O_3	10.0
				Na_2O	7.1
				K_2O	7.1
				ZnO	5.1
				TiO_2	2.7
				Al_2O_3	2.3
Silicon	$10\text{-}30 \times 10^{-7}$				

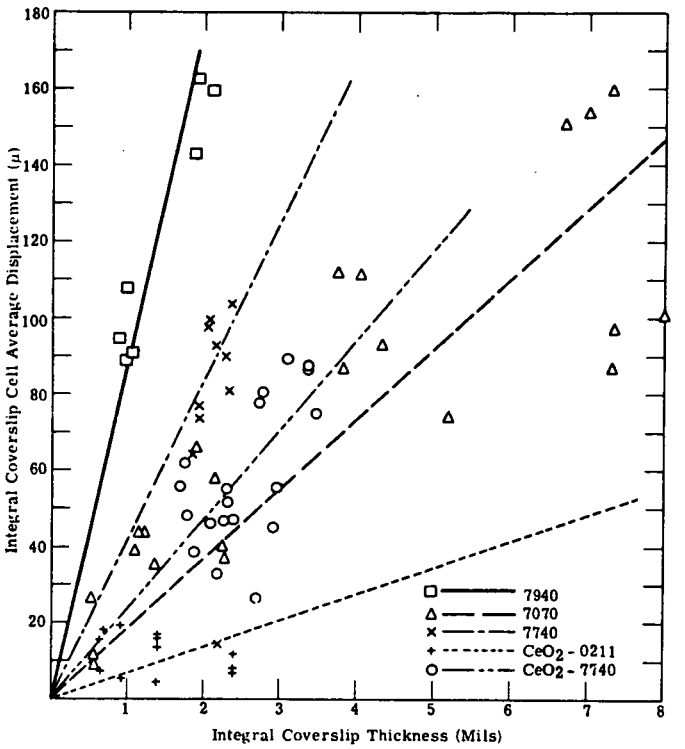

Figure 24. Integral Coverslip Cell Bow Versus Integral Coverslip Thickness (from Reference 32)

In order to evaluate darkening under electron irradiation, 150 μm thick, unfiltered slides of 7070, 7740, 0211, 7940, and 1723 glasses were subjected to 1-MeV electron fluences of 2.5×10^{14} and then 5×10^{15} electrons/cm^2 with the results shown in Figures 25 and 26. It is evident from these results that severe darkening occurred in the 0211, 7740, and 1723 glasses while much smaller losses resulted in 7070 glass and virtually no loss was incurred in the 7940 fused silica.

Solar cell samples which were covered with 50 μm or less of 7940 fused silica have been subjected to 400 keV proton irradiation without evidence of degradation except when solderless contact bars or unprotected gaps were left exposed during irradiation. The results of irradiation with 1-MeV protons are tabulated in Table 9. No integrally covered cell has been observed to have sustained damage due to proton irradiation at an energy which is insufficient to penetrate the coverglass.

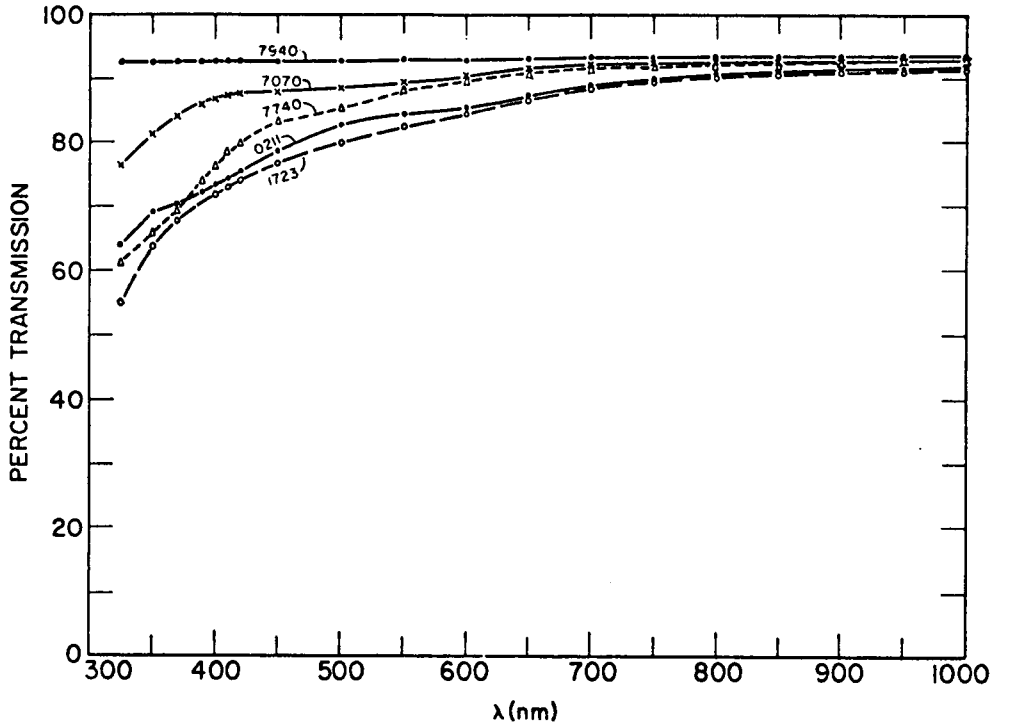

Figure 25. Transmission of 150 μm Slides After 2.5×10^{14} 1 MeV Electrons/cm^2 (from Reference 32)

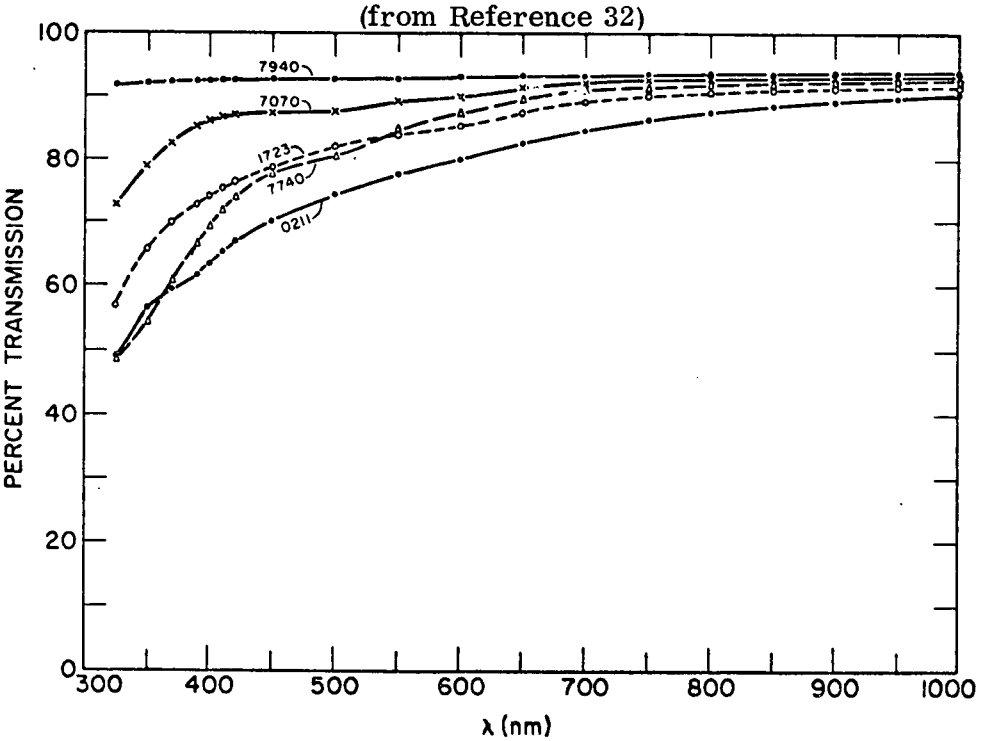

Figure 26. Transmission of 150 μm Slides After 5×10^{15} 1-MeV Electrons/cm^2 (from Reference 32)

Table 9. 1-MeV Proton Irradiation Data
(from Reference 32)

Cell	Integral Cover Material	Nominal Thickness (mils)	Initial Performance			Change After 10^{14} 1 MeV p/cm^2		
			I_{sc} mA	$I_{0.43}$ mA	V_{oc} V	I_{sc} mA	$I_{0.43}$ mA	V_{oc} V
FS155	7070	2	135	128	0.552	0	0	0
478-21	7070	2	139	133	0.560	0	0	0
478-24	7070	2	138	134	0.563	0	0	+0.005
478-22	7070	2	137	131	0.560	-1	+1	+0.005
D4	7070	2	137	133	0.562	+3	+2	0
G45	7070	2	140	135	0.562	0	0	0
G16	7070	6	139	132	0.547	+3	-2	-0.010
G27	7070	6	137	132	0.561	+3	+4	+0.005
B-12*	7940	2	140	134	0.556	-32*	-134*	-0.240
TA90	7940	1	144	138	0.570	-1	0	0
P29	7740	2	139	135	0.566	+3	0	-0.020
P9	7740	2	143	134	0.538	+1	0	0
CD10	CeO_2 doped 0211	2	132	127	0.552	+2	+3	+0.010
CD30	CeO_2 doped 0211	2	138	132	0.560	0	+1	+0.005
CD31	CeO_2 doped 7740	2	140	132	0.560	+1	0	-0.010
CD33	CeO_2 doped 7740	2	142	136	0.556	0	+1	+0.010
ET13	None	-	137	124	0.562	-101	-124	-0.200

*Solderless contact bar mask lost during test with resulting irradiation of bar area.

Additional environmental testing, which included thermal cycling, U.V. radiation, and temperature-humidity storage, has indicated good performance with HVIBS integral covers.

Based on these results, it was concluded that Corning type 7070 glass represented an optimum choice for relatively thick, low stress integral covers which exhibit excellent radiation resistance.

2.4.3.1.2 Electron Beam Evaporation

Work in the area of electron beam evaporation of integral coverglass on silicon solar cells has been performed by Heliotek, Division of Textron, Inc., under contract to the Air Force Materials Laboratory, Wright-Patterson Air Force Base and is reported in References 29 and 33. The system which evolved from this investigation consists of a TiO_x cell anti-reflective coating and an electron beam evaporated integral coverglass. The parent glass was Corning type 1720, but the deposited glass was found to consist principally of SiO_2 (96 percent) with the remainder being alkali oxides. Stress levels in the deposited films can be kept to levels below 4×10^8 dynes/cm^2 (4×10^7 N/m^2). Under these stress conditions, a 300 μm thick, 2 x 2 cm cell with a 50 μm thick integral cover will exhibit a radius of curvature of approximately 157 cm. Integral cover samples were subjected to both 1-MeV electron and ultra-violet irradiation. A coverglass darkening of 2 to 3 percent was observed following a total 1-MeV electron fluence of 10^{15} electrons/cm^2. Ultraviolet exposure of 120 equivalent sun hours produced a coverglass transmission degradation of 1.4 percent.

2.4.3.1.3 Radio Frequency Sputtering

Work in the area of radio frequency (RF) sputtering of integral solar cell coverglass is presently being performed by the Electrical Research Association (ERA), Leatherhead, Surrey, England, under sponsorship from the European Space Research Organization (ESTEC, Noordwijk). This deposition method consists of the sputtering of glass targets in an argon atmosphere with RF power of several kilowatts at a frequency of approximately 13.6 MHz and a peak-to-peak potential of two to three kilovolts. The solar cell substrate is maintained at approximately 25^{o}C during deposition. The experimental equipment at ERA is capable of coating 70 2 x 2 cm cells with Corning 7070 glass at a sustained rate of 2.6 μm

per hour, with ± 10 percent thickness uniformity. Prototype production equipment, with a capacity of 316 2 x 2 cm cells per loading, has been designed and built for operational use in the fall of 1972 (Reference 28).

During the course of this program at the ERA, RF sputtered covers of borosilicate glasses, notably Corning 7740 and 7070, and Schott 8330, as well as Corning 7940 fused silica have been investigated. The borosilicate glass films were found to have significantly lower stress than fused silica. In particular, the type 7070 glass showed very low values of stress as revealed in Figure 27. Films of 7070 glass have been deposited with an intrinsic stress below 3 x 10^7 dynes/cm^2 (3 x 10^6 N/m^2) which is the lower limit of the ERA measurement technique. Unsupported films of 7070 glass remain essentially flat. With this glass, it is possible to cover 125 μm thick cells with scarcely any bowing of the coated cell. In addition, the 7070 glass shows superior optical and radiation resistance properties.

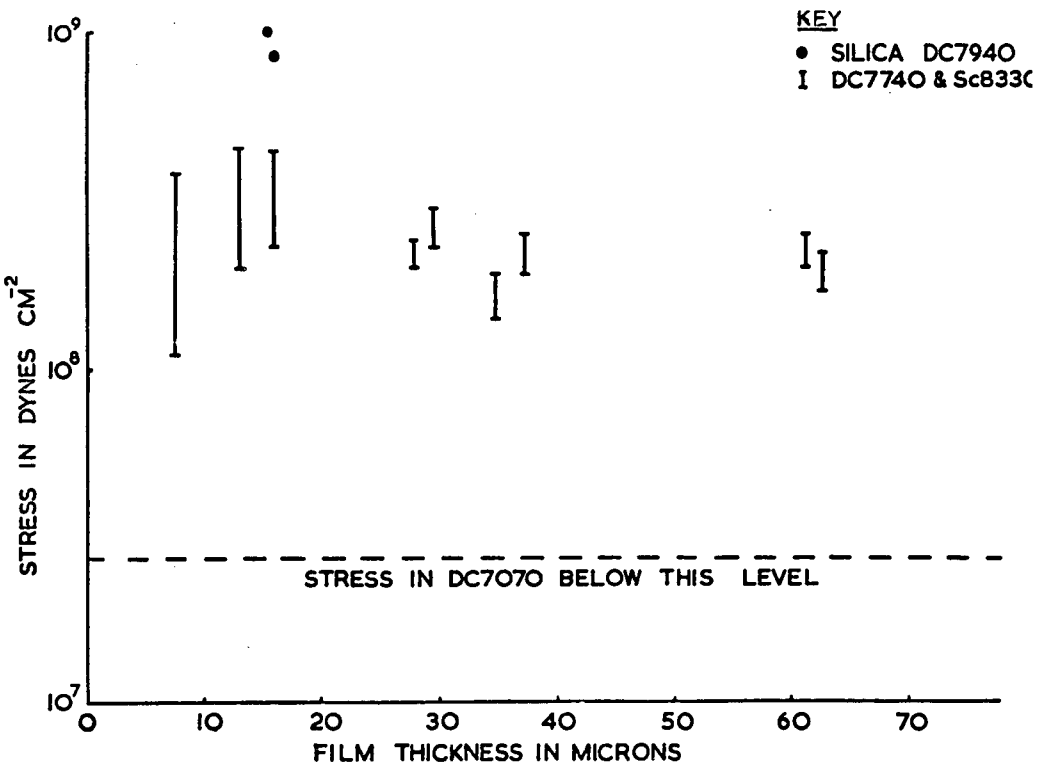

Figure 27. Stress in the Integral Cover as a Function of Film Thickness for Silica and Two Borosilicate Glasses (from Reference 28)

Thermal cycling tests of integrally covered solar cells have shown that TiO_x cell anti-reflective coating gives excellent resistance to delamination.

The optical transmission of 7070 glass layers of 100 to 150 μm thickness has been measured at 99 percent between 400 and 1200 nm, falling to 95 percent at 350 nm. These transmission properties are of material without added ingredients such as cerium oxide. The addition of such modifiers, for the purpose of improving radiation resistance, will alter transmission properties.

The irradiation of 20 μm thick films of 7070 glass (without cerium oxide) with a 1-MeV electron fluence of 10^{15} electrons/cm^2 has produced negligible change in transmission when compared with unirradiated control samples. This same fluence caused a 1 percent loss in transmission between 400 and 1200 nm for 50 μm thick specimens of the same glass. The addition of cerium oxide is known to improve the radiation resistance at the expense of some loss in unirradiated transmission. Targets of 7070 glass with cerium oxide additive have been made by sintering mixed powders. Work is proceeding to determine if this additive is beneficial, and if so, to determine the optimum content.

2.4.3.1.4 Fusion

The fusion of fine powdered glass directly onto solar cells is the subject of investigations by the General Electric Company, Space Sciences Laboratory, under contract to the Air Force Aero Propulsion Laboratory, Wright-Patterson Air Force Base (Reference 34). The objective of this program is the development of an economical, stress-free integral cover for application to large area hardened solar arrays. To date, the major effort on this program has been devoted to the formulation of glass compositions with the required fusion temperature of 500^{o}C or less. In addition, the glasses must have the chemical, mechanical, optical and radiation resistant properties required to meet the program goals. As a test of radiation resistance, annealed glass disks of the various compositions are subjected to radiation from a Sr^{90} source. Before and after transmittance measurements are compared to determine relative radiation resistance.

Work on this contract has not, as yet, progressed to the point of producing optimized integral covers on silicon solar cells.

2.4.3.2 FEP-Teflon Covers

The application of Fluorinated Ethylene Propylene (FEP) as a cover for silicon solar cells and as a method for encapsulating cells into flexible modules is reported in References 35 through 38. Two types of FEP have been investigated: FEP-A which is untreated and FEP-C which is treated to promote cementability on one or both sides. When applied to an active surface of solar cells by a direct heat-sealing technique, this film provides protection from penetrating radiation and increases the infrared emittance. FEP-A material, which is pretreated with an adhesion promotor, has demonstrated higher bond strength and improved resistance to exposure to high temperature-humidity conditions when compared to FEP-C material. FEP covered SiO coated cells have experienced delaminations of the cover when irradiated with 1-Mev electrons at a fluence of 10^{15} electrons/cm^2. FEP covered Si_3N_4 coated cells were able to withstand 10^{16} electrons/cm^2 without delamination. Limited data indicates little or no differences between the two types of FEP under electron irradiation.

FEP-C (125 μm thick) covered solar cells along with bare cells were subjected to 2 keV protons in a vacuum of 7.9×10^{-9} N/m^2 at an average dose rate of 1.3×10^{12} p/cm^2-sec. Total exposures of 1×10^{13}, 1×10^{15}, 1×10^{17}, and 2×10^{17} p/cm^2 were performed. Little effect was noted on the open-circuit voltage for the FEP-covered cells. The degradation in cell short-circuit current is shown in Figure 28. Note that the range of 2 keV protons in FEP Teflon is approximately 2.6 μm.

Measurements on FEP-C covered cells indicate that a decrease of about 3 percent on short-circuit current can be expected after exposure to 3600 equivalent sun hours under UV radiation. With FEP-A material, the reduction in short-circuit current will be about one-half this value.

The effects of long-term exposure to high humidity and temperature were evaluated by exposing 20 FEP-C covered cells to 40°C and 95 percent relative humidity. After 160 hours of exposure, some delamination on all cells was observed.

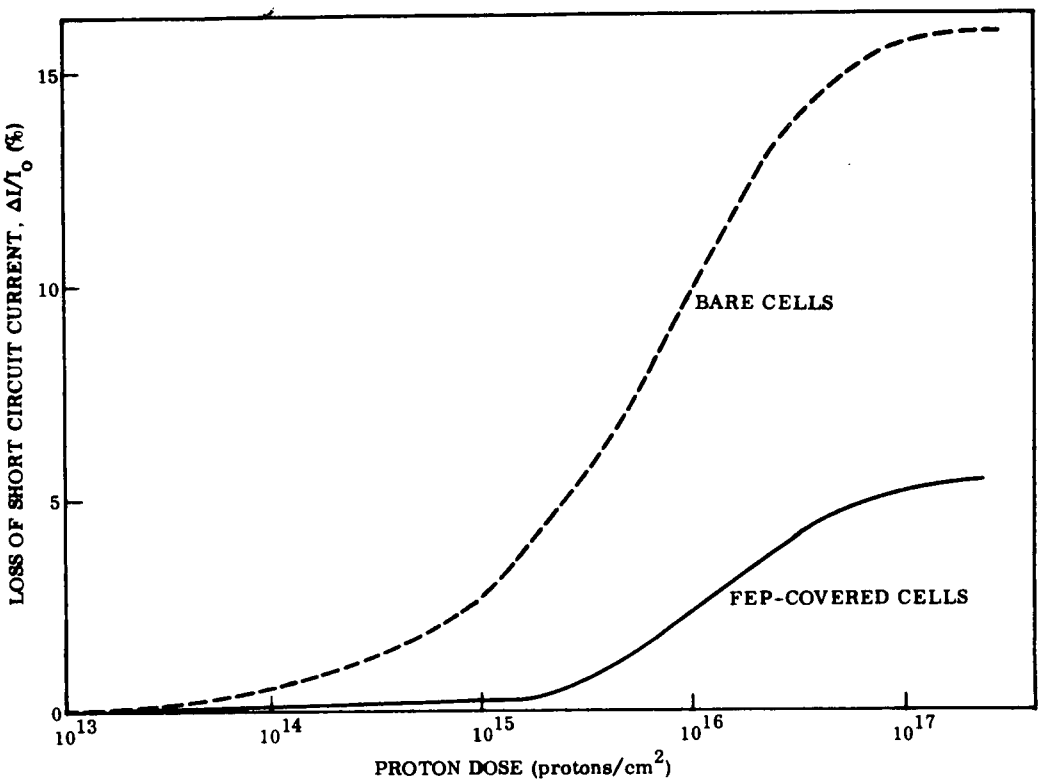

Figure 28. Effect of 2 keV Protons on Solar Cell Short-Circuit Current (from Reference 38)

Two kinds of multicell modules were constructed using the FEP cover technique. The first of these consisted of a 15 cell module (5 parallel x 3 series) which was made by first covering three 5 cell wide strings with 125 μm thick FEP-C film (see Figure 29). The substrate was fabricated by laminating a 50 μm thick copper foil to a 25 μm Kapton-H film with 25 μm FEP film used as the adhesive. The foil was then photoetched to form interconnects, soldering points for the back contacts and soldering tabs for the front contacts (see Figure 30). Next, another 25 μm layer of Kapton-H film, prepunched to expose soldering points and tabs, was laminated on top using 25 μm FEP as the adhesive. The P contact soldering points and tabs were then coated with Sn62 solder. This formed the flexible substrate with integral interconnects. The five cell strings with flux-treated back surfaces, were positioned on the substrate and the P contacts induction soldered. The N contact tabs were then bent in place and connected using solder performs and reflow solder techniques. The finished 15 cell module is shown in Figure 31. A thermal vacuum cycling test of a module of this construction resulted in the fracture of 15 of the 15 cells when the module temperature reached -140^{o}C. Subsequent examination revealed simple cell fracture in six cells without delamination. The

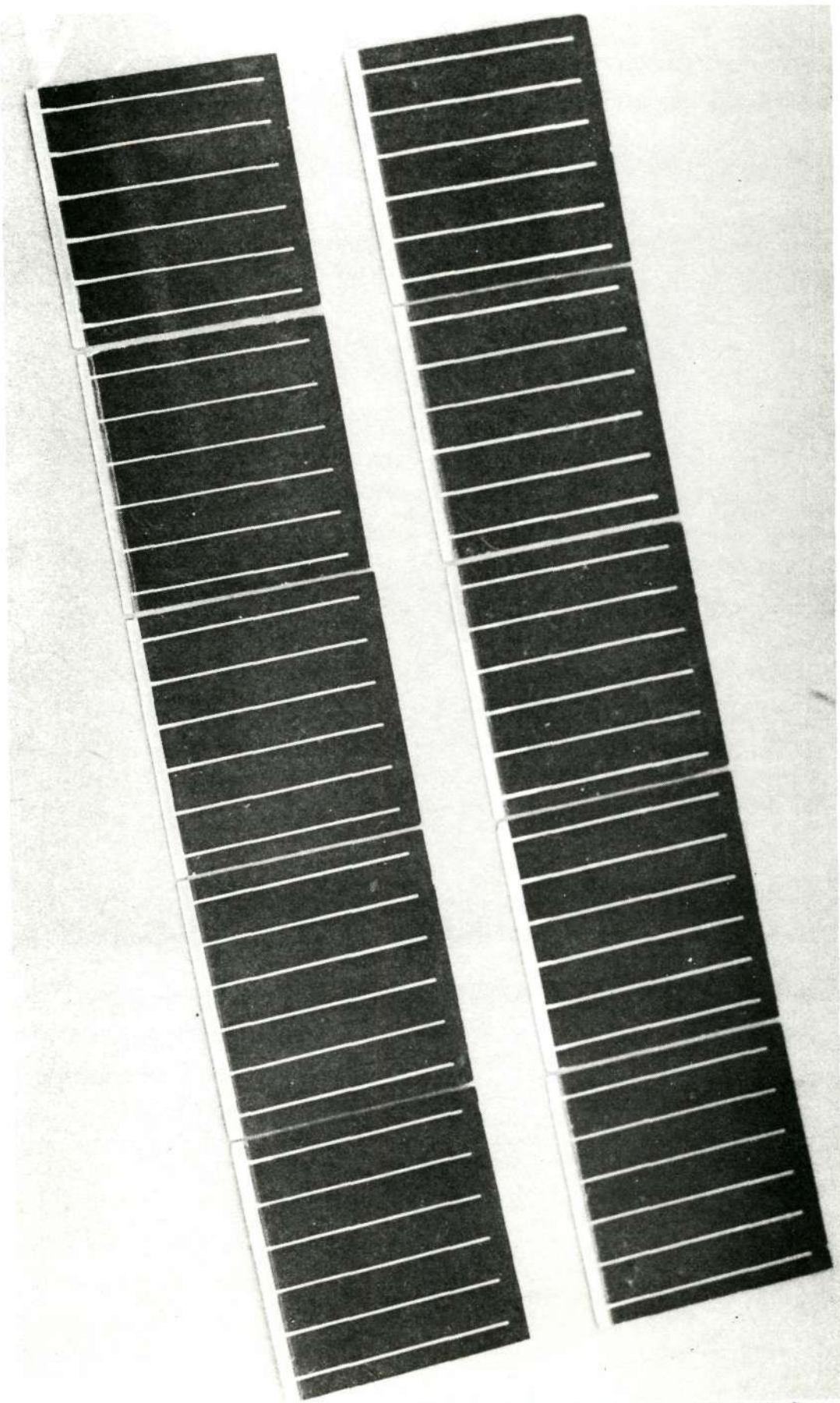

Figure 29. FEP Covered Submodules
(from Reference 38)

This page is reproduced again at the back of this report by a different reproduction method so as to furnish the best possible detail to the user.

remaining eight damaged cells have suffered a cleavage within the silicon. These failures were attributed to the mismatch of thermal expansion coefficients between the FEP on the front and the solder on the rear face of the cells.

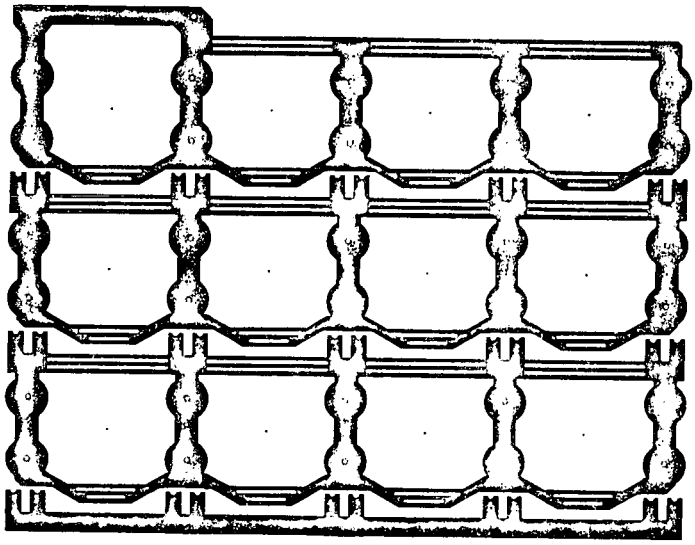

Figure 30. Circuit Interconnect Pattern
(from Reference 38)

A second configuration module was fabricated using 125 μm FEP-A as a cover and 50 μm FEP-C20 (treated on both sides) as an adhesive to bond the cells to a 25 μm Kapton-H film substrate. Thermocompression bonding of 50 μm thick silver mesh was the interconnect method used. Flexible modules prepared in this manner are unaffected by thermal shock, and thermal-vacuum cycling.

Optical properties of FEP covered cells were measured with the following results (Reference 35):

Solar absorptance (α_s) = 0.84

Total hemispherical emittance (ϵ_h) = 0.91

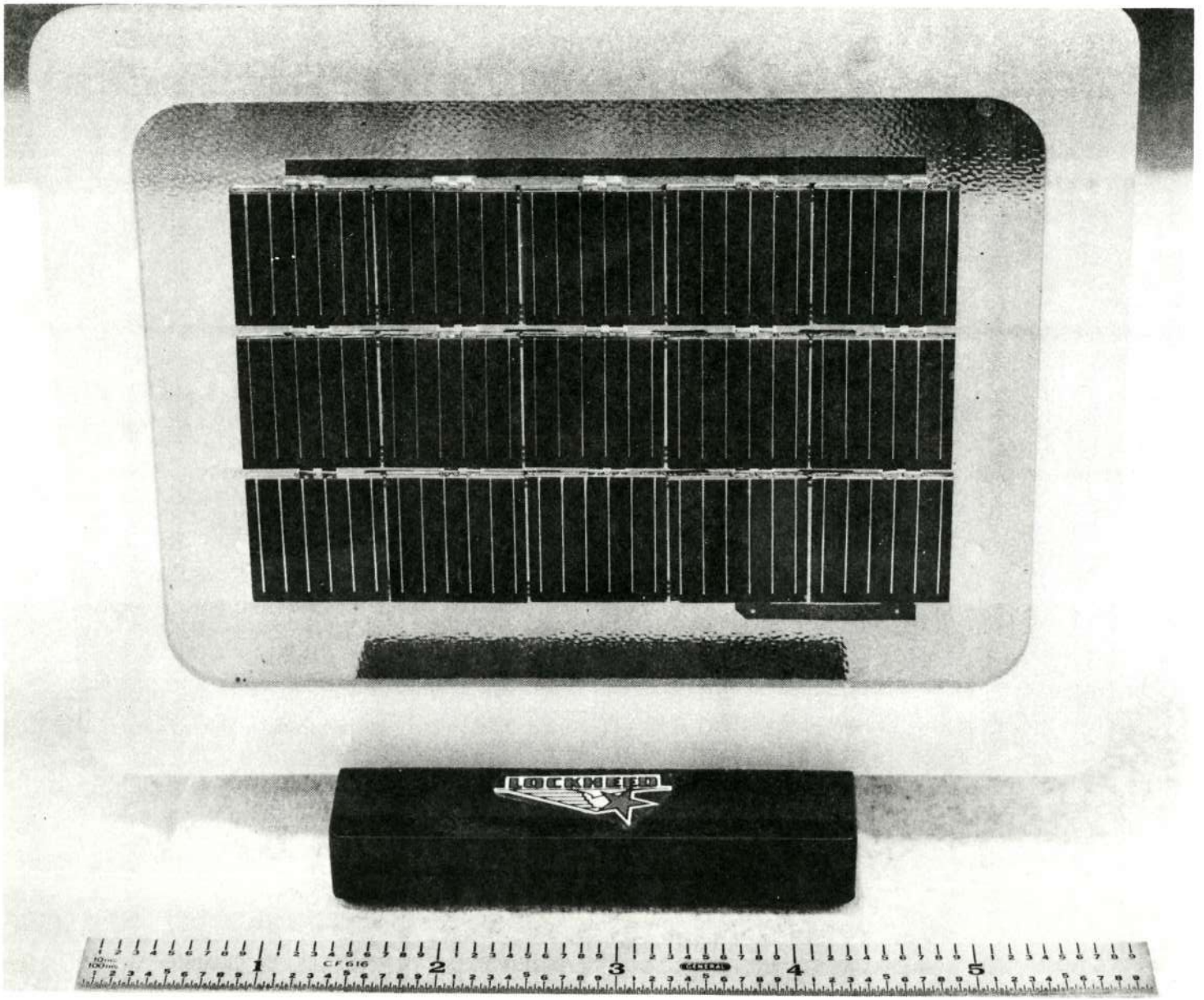

Figure 31. FEP Covered Module
(from Reference 38)

2.4.4 INTERCONNECTS AND SUBSTRATES

The use of bottom wraparound contact solar cells enables the use of a flat interconnector system which can be made integral with the supporting substrate. Two such substrate systems have been implemented in flexible solar array developments. The details of the Lockheed space station solar array substrate are shown in Figure 32. The construction of this substrate is similar to Lockheed FEP development substrate which was described in Section 2.4.3. The copper interconnection system is sandwiched between layers of Kapton-H film with FEP used as the adhesive. The solar cells are soldered to the interconnectors through holes in the upper layer of Kapton/FEP. These solder joints are the only means of attachment of the cells to the substrate. Table 10 gives a weight breakdown for the Lockheed space station substrate/interconnect system. This weight tabulation does not include the bus strip distribution system or the hinge joint reinforcement and locking bars between modules. The weight of the copper interconnectors was calculated based on a copper weight of 0.305 kg/m^2 (1 oz/ft^2) and a coverage of 33 percent of the module area which was computed from a drawing of the interconnector pattern. The resulting weight of 0.100 kg/m^2 of module area does not agree with the value published in Reference 4. In Section 3.2.9 of this reference, the weight of the copper interconnectors is given as 0.0472 kg (0.104 lb) for a module which occupies 0.966 m^2 (10.4 ft^2) for a resultant weight-to-area ratio of 0.049 kg/m^2. A copper foil of 0.152 kg/m^2 (1/2 oz/ft^2) would be required to achieve this weight for the interconnector pattern specified. The solder weight of 0.031 kg/m^2 was calculated based on a solder coverage of 9.5 percent of the module area with an average thickness of 37 μm.

The interconnect/substrate configuration used on the RAE flat-pack solar array is shown in Figure 33. This approach also consists of a cementless, soldered attachment of the solar cells to the integral substrate. The interconnectors are 25 μm thick silver-plated molybdenum rings which are soldered to the cells through punched holes in the 50 μm thick Kapton-H film substrate. The Kapton substrate is cut-out to reduce weight and to provide the solar cells with a direct radiating surface for more effective heat rejection. These cutout windows are triangular shaped in the current design. The black chromium emissive finish on the solar cell backs was found to provide insufficient protection from low energy protons. To remedy this situation, the solar cell backs were coated with a 50 μm thick layer of Midland

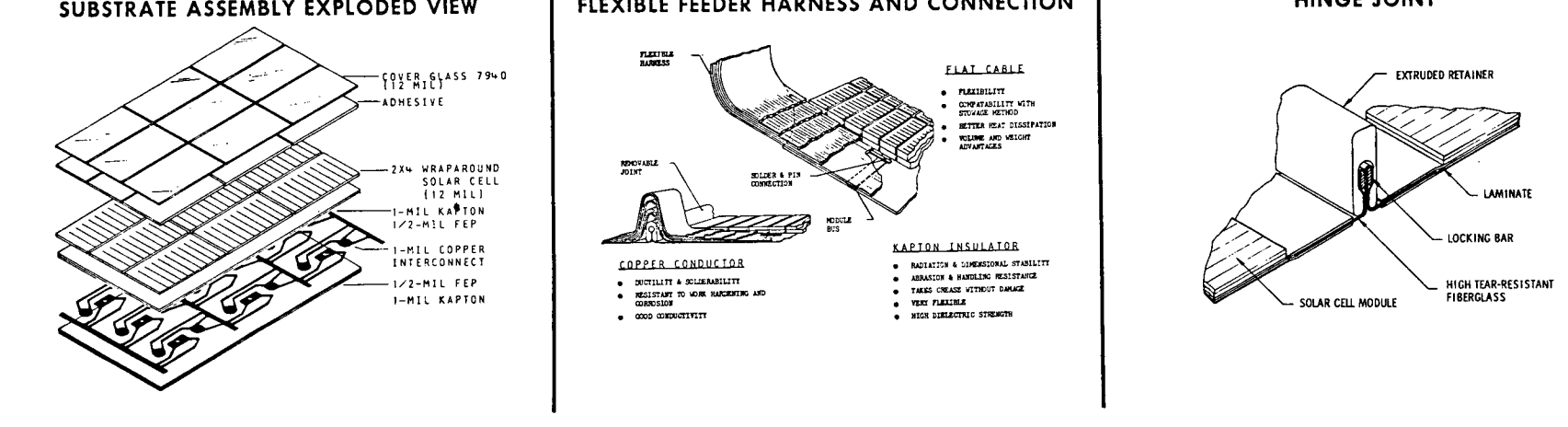

Figure 32. Details of Lockheed Space Station Solar Array Substrates (from Reference 39)

Silicones Silastoseal B adhesive. Table 11 gives the weight breakdown for the REA substrate/interconnect system.

Table 10. Weight of Lockheed Space Station Solar Array Substrate

Item	Weight (kg/m^2 of Module Area)
Kapton-H film (50 μm total thickness)	0.071
FEP-Teflon (25 μm total thickness)	0.054
Copper Interconnectors (1)	0.100
Solder	0.031
Total	0.256

(1) 0.305 kg/m^2 (1 oz/ft^2) copper which covers 33% of the module area

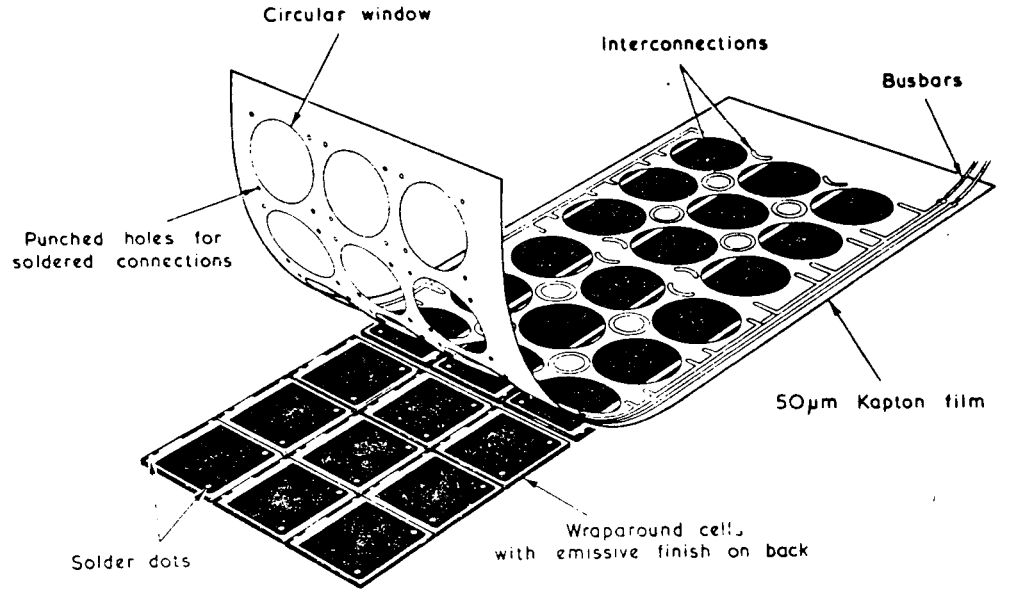

Figure 33. RAE Flat-pack Solar Array Substrate Configuration (from Reference 15)

Table 11. Weight of RAE Flat-pack Solar Array Substrate

Item	Weight (kg/m^2 of Substrate Area)
Kapton-H film (perforated, 50 μm thick) (1)	0.037
Interconnectors (Ag Plated Mo) (1)	0.022
Solder (1)	0.046
Silastoseal B Adhesive (2)	0.022
Total	0.127

(1) Based on data from Reference 15.
(2) For low energy proton protection, assumes an average thickness of 50 μm covering 50% of the back of every cell, with 2060 cells per m^2 of substrate area.

2.4.5 DEPLOYABLE BOOMS

2.4.5.1 General

An extensive summary of the deployable boom component technology as it might apply to large flexible solar arrays is contained in Section 4.1.2.2 of Reference 40. This reference lists 20 different types of deployable boom structures which have been developed. Many of these such as telescoping tubes and folding beams are obviously impractical for this application because of the large undeployed volume and relatively high weight. However, several of these boom types have shown the potentials needed for the deployable boom of a large flexible solar array. These boom categories are discussed below.

2.4.5.2 Cylindrical Booms

This category of deployable booms includes those with cross sections which are formed by one or more cylindrical shells. Stowage is generally by elastically flattening the element and reeling onto a spool or within a cassette. A typical example of this boom type is the STEM manufactured by SPAR Aerospace Products, Ltd. This boom, shown in Figure 34,

is a circular, cylindrical tube formed from a single strip of material. The edges of the deployed strip overlap as shown in the figure. Booms of this type have been fabricated of beryllium copper, stainless steel, titanium and molybdenum. A variation of this basic type, which consists of an interlocked joint between the two edges of the deployed strip and thereby provides greater torsional stiffness, has been fabricated by several organizations.

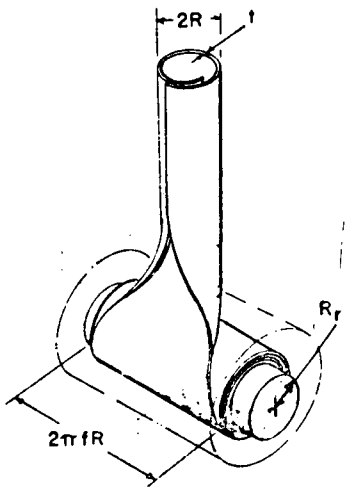

Figure 34. Schematic of STEM Boom (From Reference 41)

The BI-STEM, also manufactured by SPAR Aerospace Products, Ltd., is formed by nesting two circular, cylindrical strips as shown in Figure 35. These strips can be retracted and stowed on two separate reels, or on a single reel or cassette as shown in Figure 36. The BI-STEM has been used on the Hughes/AF roll-up solar array, the GE/JPL 30 watt/lb roll-up solar array and is planned for the CTS solar array.

The quasi-biconvex boom type shown in Figure 37 has been manufactured by Ryan Aeronautical and by ASTRO Research. The boom is a closed section made by welding two metallic strips together along the two longitudinal edges. Thus, this section has good torsional properties and it develops buckling strength similar to that exhibited by closed, circular cylindrical shells. However, stowage of the boom presents problems with buckling of the inner compressed element. Also, buckling can occur in the transition region when this region is kept small.

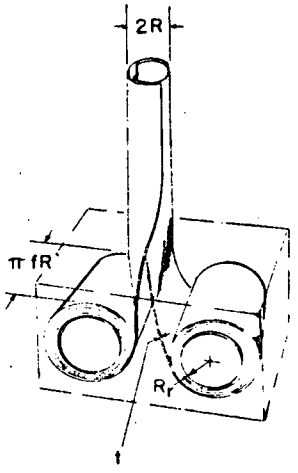

Figure 35. Schematic of BI-STEM Boom (From Reference 41)

2.4.5.3 Coilable Lattice Booms

Coilable lattice booms, of the type manufactured by ASTRO Research, consist of a lattice structure of fiberglass rods which is shear-stiffened by diagonal cables. The boom is

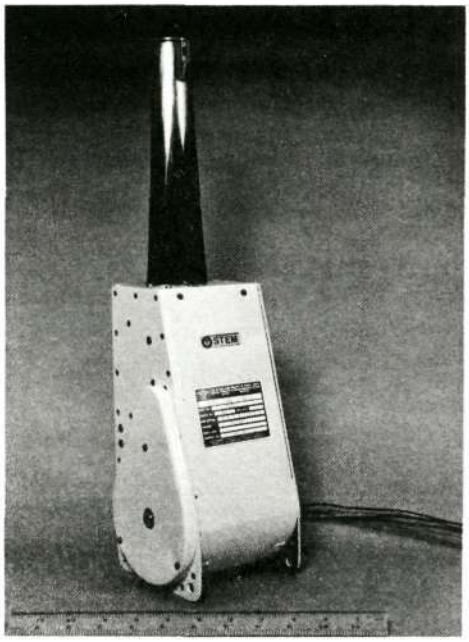

Figure 36. BI-STEM Deployable Boom and Actuator

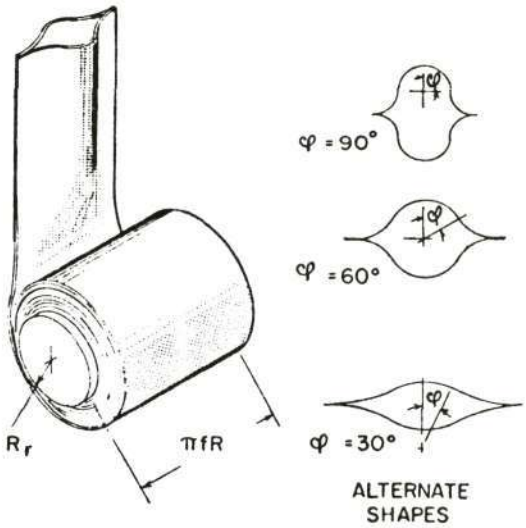

Figure 37. Schematic of Quasi-Biconvex Boom

retracted by forcibly twisting it about its axis, thereby causing the horizontal "batten" members to buckle. The continuous longerons are thus coiled to provide a compact retracted configuration. Figure 38 shows the 25.4 cm diameter by 30.5 m long lunar antenna mast which is capable of withstanding an eight degree tilt from its vertical in lunar gravity when cantilevered at its base. The primary limitation of this boom type is the fact that the longerons must remain elastic when bent in the retracted portion. Therefore, the maximum thickness allowable for the longerons depends on the mast radius and the elastic strain limit of the longeron material. Thus, the overall bending strength and stiffness of the mast is limited by the radius of the mast and by the longeron material.

2.4.5.4 Articulated Lattice Booms

If high stiffness and strength is required of a small radius Astromast, it is necessary to segment and articulate the longerons instead of elastically coiling them into the retracted position. Because there is no distortion of the longerons and battens in the stowed configuration, these members may be as large in cross section as the application requires.

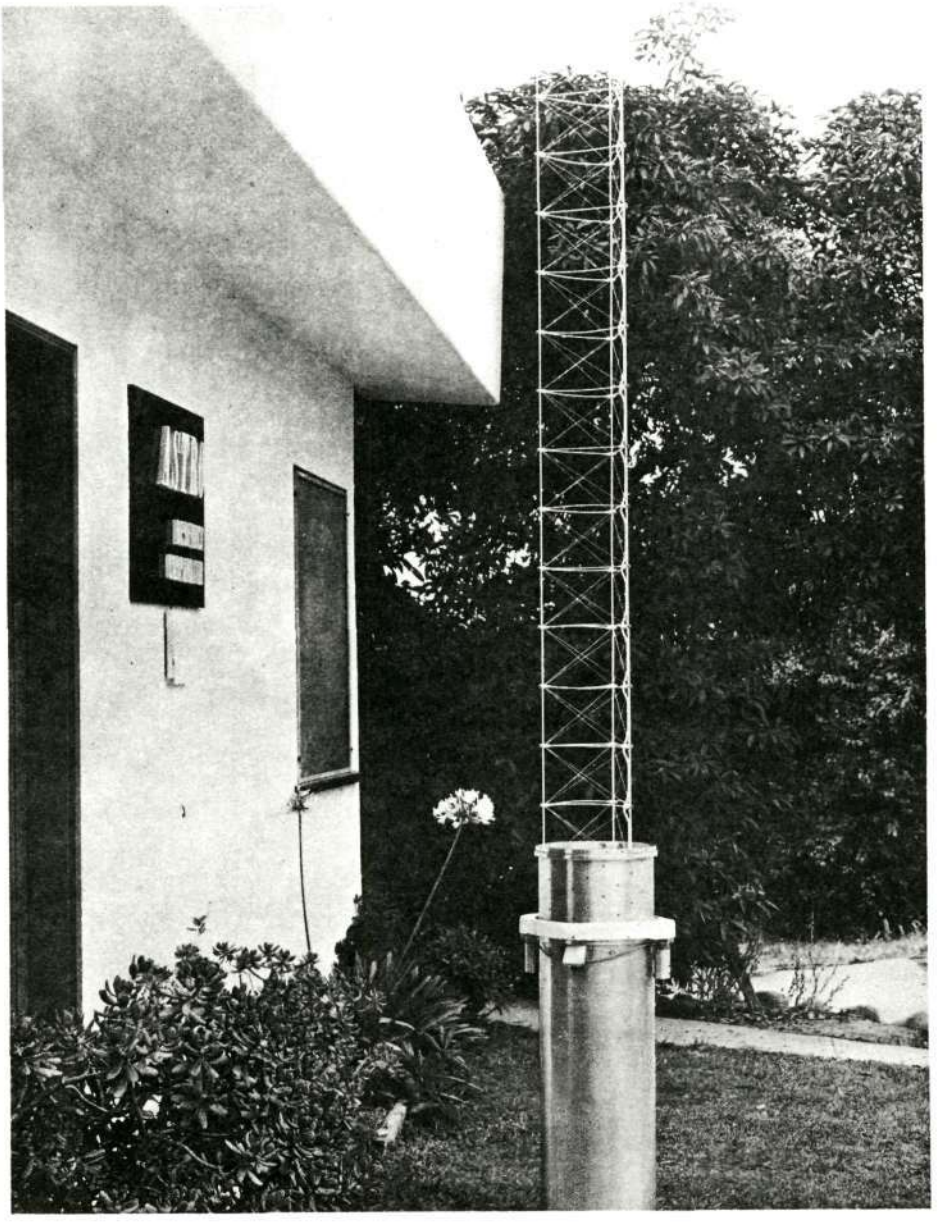

Figure 38. Astromast Coilable Lattice Boom - Lunar Antenna Mast

Figure 39 shows the articulated lattice boom which is used on the Lockheed space station solar array development program.

2.4.5.5 Comparison of Deployable Boom Types

Among the cylindrical booms, the STEM has about a 7 percent greater moment of inertia than the BI-STEM for an equal element weight. However, the deployment mechanism for a BI-STEM is considerably smaller and lighter than that required for the same diameter STEM. The result is that the overall BI-STEM system is lighter than a STEM system for an equivalent moment of inertia. The quasi-biconvex boom is even less efficient from a weight standpoint when compared to the basic STEM element. In addition, this boom configuration suffers from high stress in the weld joints when in the retracted position. Molybdenum material has the best stiffness-to-weight ratio of any of the conventional materials used.

Composite materials exhibit properties that suggest their use in this application. A boron/aluminum or graphite/aluminum composite tube with the fibers running longitudinally will have a very high bending strength-to-weight ratio. The aluminum in the composite will provide the necessary temper to maintain the tube shape. Studies of composite materials are proceeding to determine the feasibility of their use in a BI-STEM configuration. The advantages of composite materials are also applicable to lattice booms and the fabrication problems should be considerably smaller.

Figure 40 shows a comparison of these various boom configurations in terms of stiffness-to-weight ratio. This plot reveals that the lattice booms are less efficient than the deployable cylindrical tubes for the same materials and radius. The use of composite materials in lattice booms makes these booms more efficient than BI-STEMS of the same radius using conventional materials.

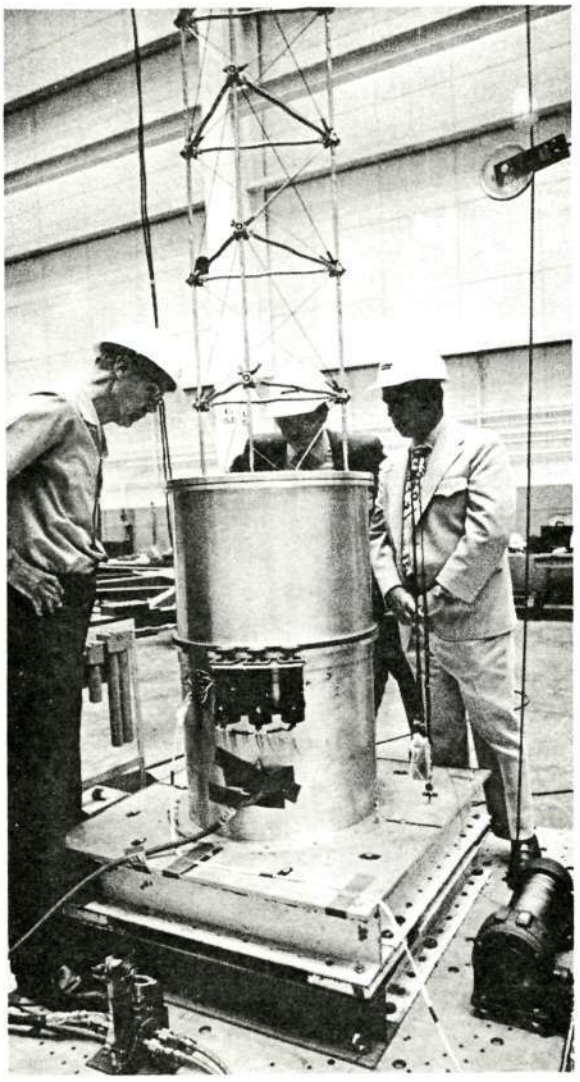

Astromast Deploying Automatically

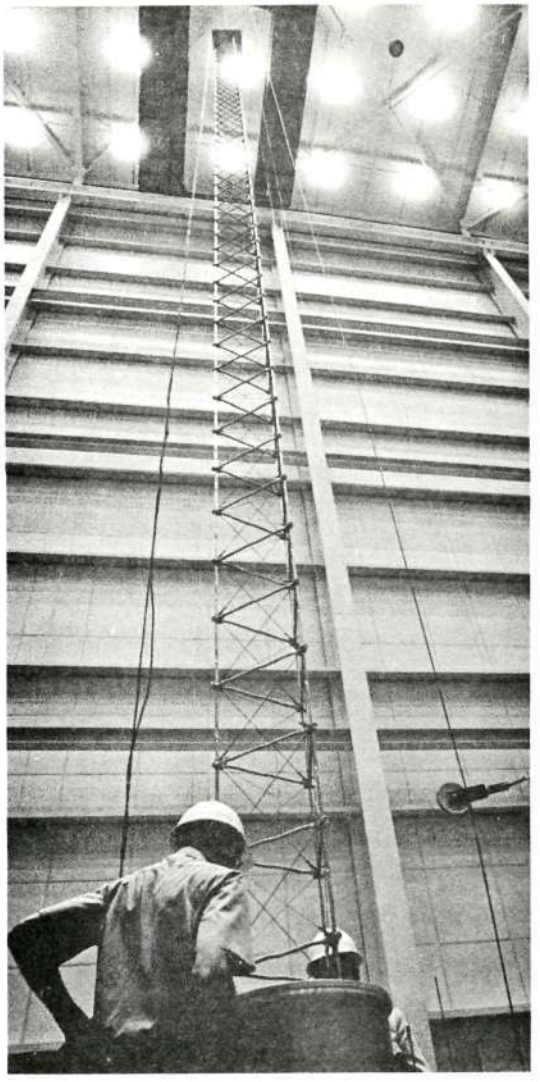

Fully Extended Mast
(84 ft long, 20 in. diam., 214 lb)

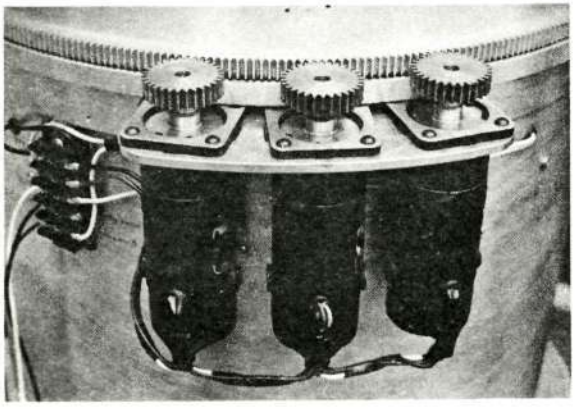

Deployment Motors

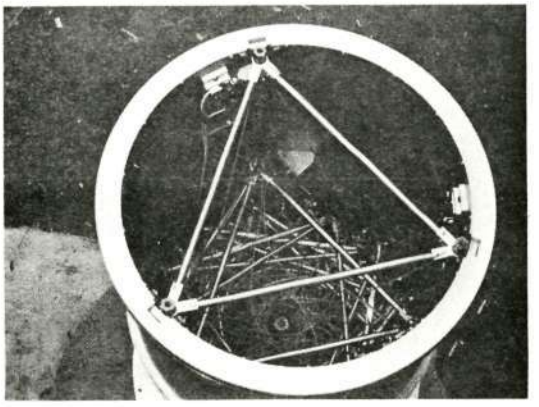

Retracted Configuration
400 lb Mast plus Canister

Figure 39. Astromast Articulated Lattice Boom for Lockheed Space Station Solar Array

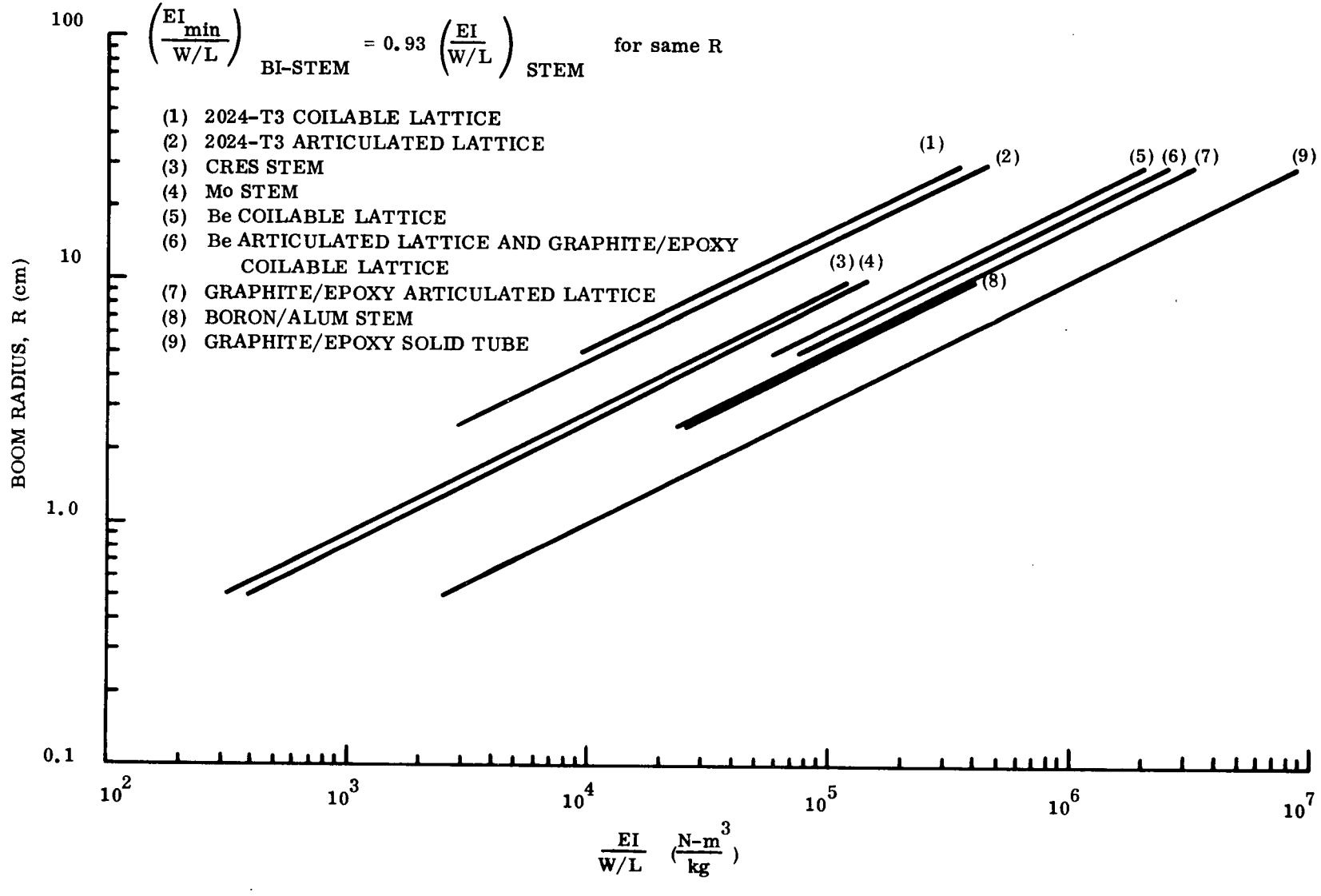

Figure 40. Comparison of Boom Stiffness-to-Weight Ratio

2.5 PARAMETRIC ANALYSIS OF THE SOLAR CELL BLANKET

2.5.1 GENERAL

The selection of the solar cell/coverglass combination is an important consideration in the feasibility of the 110 watt/kg solar array system since these components, along with the supporting substrate, represent a significant fraction of the total system weight. For example, in the 30 watt/lb roll-up solar array design, the flexible solar cell blankets constituted 56.5 percent of the total system weight. Thus, for a 110 watt/kg solar array system, it is extremely important to minimize the blanket weight consistent with the other system requirements. The beginning-of-life (BOL) solar array panel output is specified as 10,000 watts at the 1 AU intensity and equilibrium temperature. In addition, the power output under these same conditions shall not decrease by more than 20 percent over the 3-year operational life. Thus, this specification defines the allowable degradation (primarily particle radiation damage) instead of specifying a desired end-of-life (EOL) power capability with no constraint on initial power (or allowable degradation).

The objective of this trade-off analysis is to assess the impact of this allowable degradation constraint and compare this result with a design which produces a specified EOL power output with no restriction on degradation.

In order to perform these trade-offs, it is first necessary to determine the effect of the particle radiation environment on the solar cell electrical characteristics. The calculation procedure employed is based on a damage equivalent 1-MeV electron fluence method which is commonly used to relate solar cell degradation to a combined electron and proton environment. This procedure involves the determination of the damage equivalency of 1-MeV electrons for each particle type and differential energy spectra. The shielding effect of the coverglass and cell backing is accounted for in the determination of this damage equivalency.

2.5.2 SOLAR CELL RADIATION DEGRADATION

For each mission type, the particle radiation environment defined in Section 2.1 was converted into a Damage Equivalent-Normally Incident (DENI) 1-MeV electron fluence using the

calculation procedure described in Reference 42. For the interplanetary mission, the DENI 1-MeV electron fluence as a function of shield density-thickness product is shown in Figure 41 for the specified three-year mission duration.

Figure 42 shows a similar curve for the geosynchronous mission. In this case, the specified three-year mission solar flare proton energy spectra was combined with the five-year trapped electron energy spectra to yield the DENI 1-Mev electron fluence.

The DENI 1-MeV electron fluence for the manned space station mission is shown in Figure 43. The lower curve reflects the trapped particle effect over the 10-year period. The upper curve includes the solar flare proton environment from Figure 2. Also shown on Figure 43 are comparison points from the Lockheed space station solar array study. Table 12 is a reproduction of a summary table from Reference 4. The comparison data points, as indicated in Table 12, are from the column labeled 10 years, Trapped + Solar Flare, Webber and are for the 300 nm (555 km), 55 degree inclination orbit. There is very good agreement between these Lockheed data points and the upper curve of Figure 43.

The degradation of N/P silicon solar cell electrical characteristics as a function of normally incident 1-MeV electron fluence is given by the curves in Appendix B.

2.5.3 RESULTS OF TRADE STUDIES

The first part of this analysis consists of the evaluation of blanket weight for a solar array system which is sized to provide 10,000 watts of initial output at 1 AU and 55^{o}C. These initial 10,000 watt systems were investigated for various allowable maximum power degradations due to the particle radiation environment associated with each mission type. Table 13 shows the summary of this analysis for the interplanetary mission. Solar cells with two base resistivities and with nominal thicknesses of 200, 150, 125, and 100 μm were evaluated. Table 14 lists the assumed solar cell beginning-of-life (BOL) maximum power output at 1 AU, 55^{o}C.

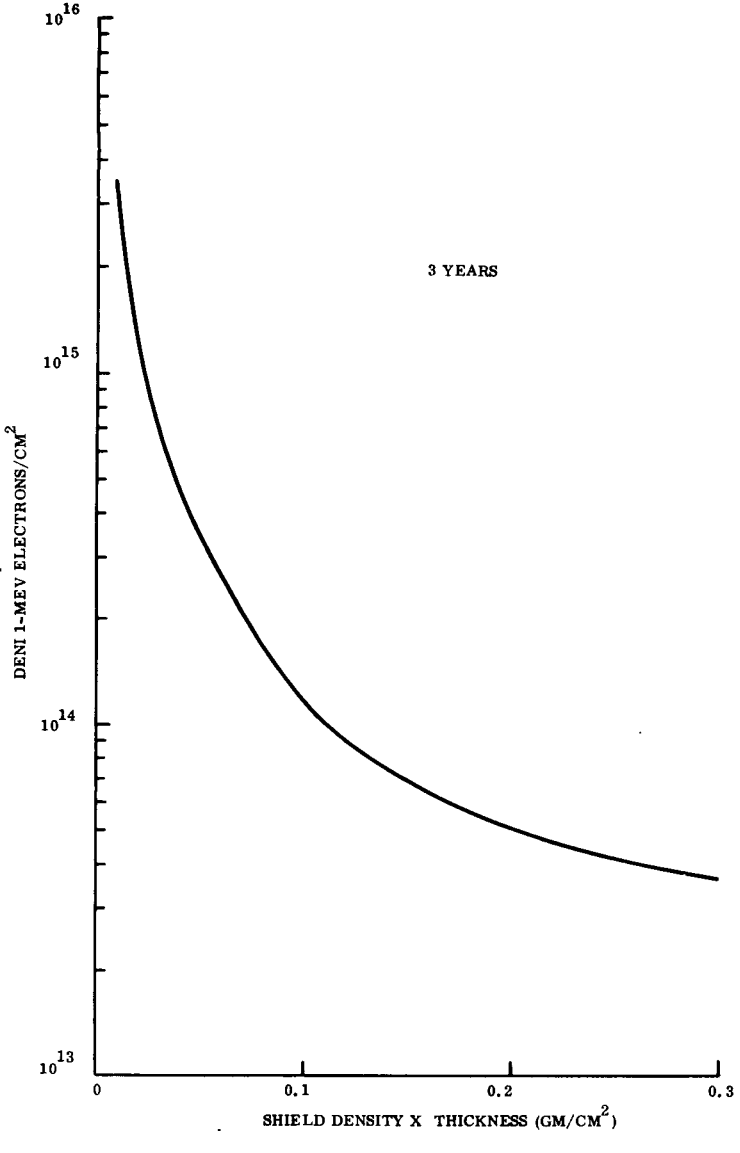

Figure 41. Damage Equivalent-Normally Incident (DENI) 1-MeV Electron Fluence with Infinite Backshielding for Interplanetary Mission

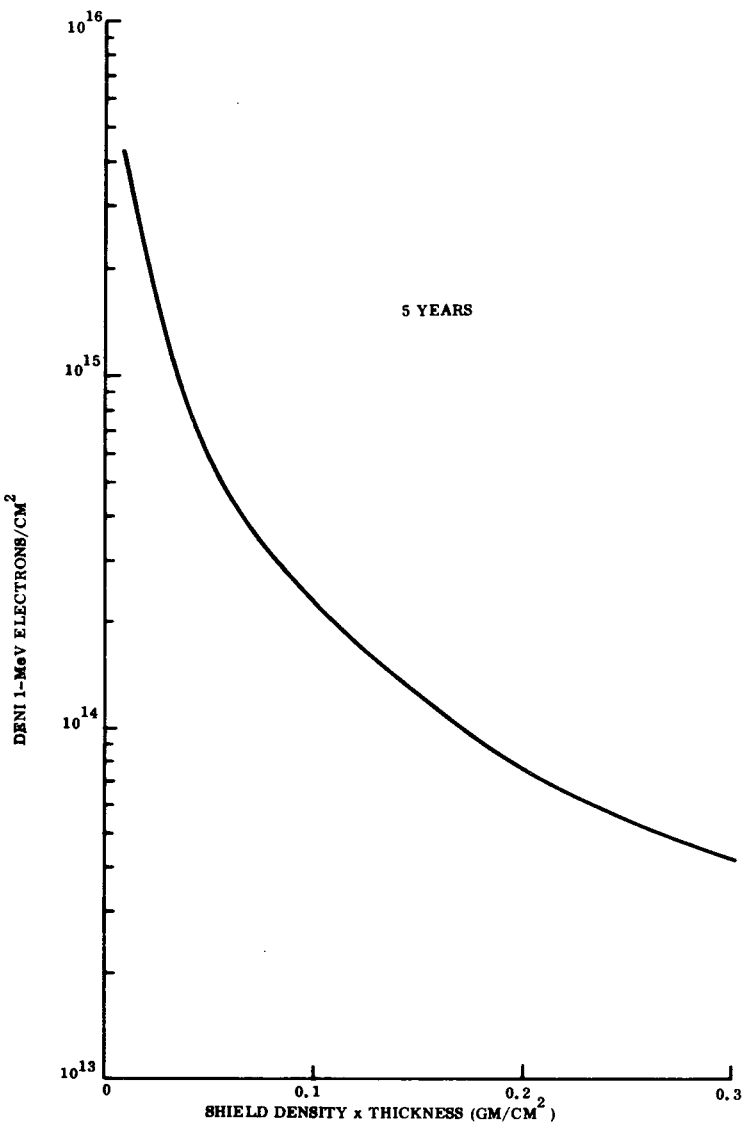

Figure 42. Damage Equivalent-Normally Incident (DENI) 1-Mev Electron Fluence with Infinite Backshielding for Geosynchronous Mission

Table 12. Equivalent 1-MeV Electron Fluences for N/P Type Silicon Solar Cells in Low Altitude Circular Orbits in the Time Period 1977 - 1990

(From Reference 4)

Mission Duration			5 years [b]			10 years			2.5 years [b]		
			Trapped Only	Trapped + Solar Flare		Trapped Only	Trapped + Solar Flare		Trapped Only	Trapped + Solar Flare	
				Bailey	Webber		Bailey	Webber		Bailey	Webber
Inclination	Altitude	Equiv. SiO_2 Shield Thick. (mils)	Φ_{eq} [a] (e/cm^2)	Φ_{eq} [a] (e/cm^2)	Φ_{eq} [a] (e/cm^2)	Φ_{eq} [a] (e/cm^2)	Φ_{eq} [a] (e/cm^2)	Φ_{eq} [a] (e/cm^2)	Φ_{eq} [a] (e/cm^2)	Φ_{eq} [a] (e/cm^2)	Φ_{eq} [a] (e/cm^2)
90	200	3	4.3	27	11	8.6	31	15	2.1	25	8.3
		6	1.9[a]	13	6.2	3.8	15	8.1	.96	12	5.2
		12[d]	.86	5.7	3.5	1.7	6.6	4.4	.43	5.3	3.1
		15.7[c]	.64	4.1	2.7	1.3	4.7	3.4	.32	3.8	2.4
	300	3	14	37	20	28	51	34	7.1	30	13
		6	6.8	18	11	14	25	18	3.4	15	7.6
		12	3.3	8.2	5.9	6.6	11	9.2	1.6	6.5	4.3
		15.7	2.4	5.9	4.5	4.8	8.3	6.9	1.2	4.7	3.3
55[e]	200	3	5.2	28	11	10	33	17	2.6	25	8.8
		6	2.6	14	6.3	5.2	17	9.4	1.3	13	5.5
		12	1.2	6.1	3.8	2.4	7.3	5	.60	5.5	3.2
		15.7	.87	4.3	3.0	1.7	5.2	3.8	.43	3.9	2.5
	300	3	18	41	24	36	59	42	9.1	32	15
		6	9.1	21	13	18	39	22	4.6	16	8.8
		12	4.4	9.3	7.0	8.8	14	11	2.2	7.1	4.8
		15.7	3.3	6.7	5.4	6.6	10	8.7	1.6	5.1	3.7
28.5	200	3	1.4	1.4	1.4	2.8	2.8	2.8	.69	.69	.69
		6	.66	.66	.66	1.3	1.3	1.3	.33	.33	.33
		12	.36	.36	.36	.72	.72	.72	.18	.18	.18
		15.7	.30	.30	.30	.30	.60	.60	.15	.15	.15
	300	3	13	13	13	25	25	25	6.3	6.3	6.3
		6	7.1	7.1	7.1	14	14	14	3.5	3.5	3.5
		12	4.0	4.0	4.0	8.1	8.1	8.1	2.0	2.0	2.0
		15.7	3.3	3.3	3.3	6.6	6.6	6.6	1.6	1.6	1.6

[a] Note that the values for Φ_{eq} are in units of 10^{13} 1 MeV electrons/cm^2.

[b] Solar Flare contribution for worst case 2.5 and 5 year mission beginning in 1977.

[c] This value is for a 12 mil cell thickness and a 3 mil equiv. thickness for the cell backing.

[d] This value is slightly greater than the actual (11.57) thickness for an 8 mil cell thickness.

[e] For this inclination orbit the solar flare contribution may be small. Values quoted are for 65° or greater inclination and are upper limits.

Table 13. Solar Cell Blanket Weight Tradeoff for Interplanetary Mission

Solar Cell Base Resistivity (ohm-cm)	Allowable Maximum Power Degradation (% of original)	Solar Cell Thickness (μm)	Solar Cell Area Required for 10,000 watts B.O.L., 55°C (m^2)	Total DENI 1-MeV Electron Fluence ($x10^{14}$ e/cm^2)	Front and Back Shield (gm/cm^2)	Blanket Weight (kg)
2	20	200	71.3	8.4	.044	105.0
		150	74.0	13.3	.032	82.7
		125	76.4	18.0	.026	71.7
		100	79.3	23.0	.022	63.6
	25	200	71.3	14.5	.030	84.4
		150	74.0	22.5	.023	69.0
		125	76.4	30.5	.018	59.2
		100	79.3	38.0	.016	53.8
	30	200	71.3	25.0	.020	69.8
		150	74.0	38.0	.016	58.4
		125	76.4	50.0	.013	51.3
		100	79.3	61.0	.011	45.7
	35	200	71.3	42.0	.014	61.0
		150	74.0	60.0	.011	50.8
		125	76.4	80.0	.009	45.1
		100	79.3	98.0	.007	39.2
10	20	200	78.6	13.0	.032	96.3
		150	84.2	22.0	.022	76.8
		125	88.3	33.5	.017	66.6
		100	93.8	48.0	.013	57.9
	25	200	78.6	24.5	.021	78.5
		150	84.2	43.0	.014	63.0
		125	88.3	64.0	.011	55.7
		100	93.8	90.0	.008	48.2
	30	200	78.6	45.0	.014	67.2
		150	84.2	83.0	.009	54.3
		125	88.3	120.0	.007	46.6
		100	93.8	160.0	.004	40.5
	35	200	78.6	83.0	.009	59.1
		150	84.2	150.	----	----
		125	88.3	220.	----	----
		100	93.8	290.	----	----

Table 14. Baseline Solar Cell Maximum Power Output

Nominal Cell Thickness (μm)	Average Cell Weight (gm/cell)	Covered Cell Maximum Power Output @ BOL, 1 AU, 55°C (Watts/Cell)	
		2 ohm-cm	10 ohm-cm
200	0.194	0.0578	0.0525
150	0.151	0.0557	0.0490
125	0.129	0.0540	0.0467
100	0.107	0.0520	0.0440

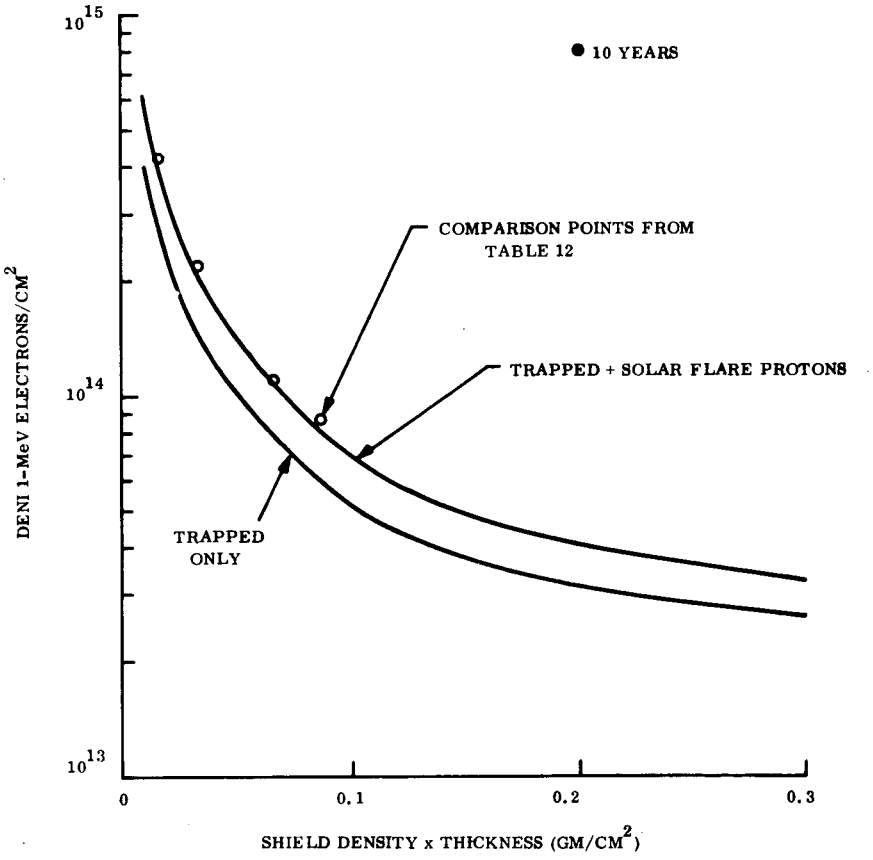

Figure 43. Damage Equivalent -Normally Incident (DENI) 1-MeV Electron Fluence with Infinite Backshielding for Manned Space Station Mission

Thus, the total solar cell area required to produce 10,000 watts at BOL is shown in Column 4 of Table 13. A 3 percent solar array fabrication loss, which accounts for cell mismatch and the series resistance of module interconnects, has been used. Bus strip distribution losses have not been included in this calculation so the 10,000 watt capability should be considered as measured at the module level. The total DENI 1-MeV electron fluence required to produce the allowable maximum power degradation was obtained from Figure B-3 and B-6 of Appendix B for 2 ohm-cm and 10 ohm-cm base resistivities, respectively. The shield factor (gm/cm^2) required to limit the DENI 1-MeV electron fluence to this value is obtained from Figure 41 and is given in Column 5 of Table 13 based on the assumption that the front and back shield factors are equal. The solar cell blanket weight is calculated as follows:

$$W_b = A_c \left[2.5 \, (W_c + W_I) + 10. \, (1 + F_p) \, W_s \right]$$

where:

W_b = Weight of solar cell blanket (kg)

W_c = Weight of solar cell (gm/cell)

W_I = Weight of interconnectors and solder = 0.033 gm/cell

A_c = Solar cell area required from Column 4 (m^2)

W_s = Front and back shield factor (gm/cm^2)

F_p = $\dfrac{\text{Solar cell blanket module area}}{\text{Solar Cell Area}} = 1.055$

This weight does not include the bus strip distribution network on the blanket and assumes that the back shield covers the complete module area of the blanket. The data contained in Table 13 is plotted in Figure 44 where the solar cell blanket weight is shown as a function of percent allowable maximum power degradation due to the particle radiation environment for the various solar cell thickness and base resistivities. In the graphical presentation of the data, blanket weights for front and back shield factors of less than 0.008 gm/cm^2 have been disallowed. This minimum shield factor, which is equivalent to a 25 μm integral coverglass or 50 μm of Kapton-H film, is considered necessary for low energy proton protection. Table 15 shows this minimum blanket weight for each cell type and thickness.

Table 15. Minimum Possible Blanket Weight for 10,000 Watts, BOL, 1 AU, 55°C

Solar Cell Base Resistivity (ohm-cm)	Nominal Cell Thickness (μm)	Cell Area Required (m^2)	*Minimum Blanket Weight-to-Area Ratio (kg/m^2)	Minimum Blanket Weight (kg)
2	200	71.3	0.732	52.2
	150	74.0	0.624	46.2
	125	76.4	0.569	43.5
	100	79.3	0.514	40.8
10	200	78.6	0.732	57.5
	150	84.2	0.624	52.5
	125	88.3	0.569	50.2
	100	93.8	0.514	48.2

*Based on a minimum front and back shield factor of 0.008 gm/cm^2

For the geosynchronous mission, the trade study results are summarized in Table 16 and plotted in Figure 45. The calculation procedure is identical to that described above for the interplanetary mission with the exception that the required front and back shield factor is obtained from Figure 42.

Table 17 summarizes the results for the manned space station mission. Note that the range of allowable maximum power degradations has been shifted to correspond to the reduced particle radiation environment for this mission. The required front and back shield factor is obtained from Figure 43. The results are plotted in Figure 46.

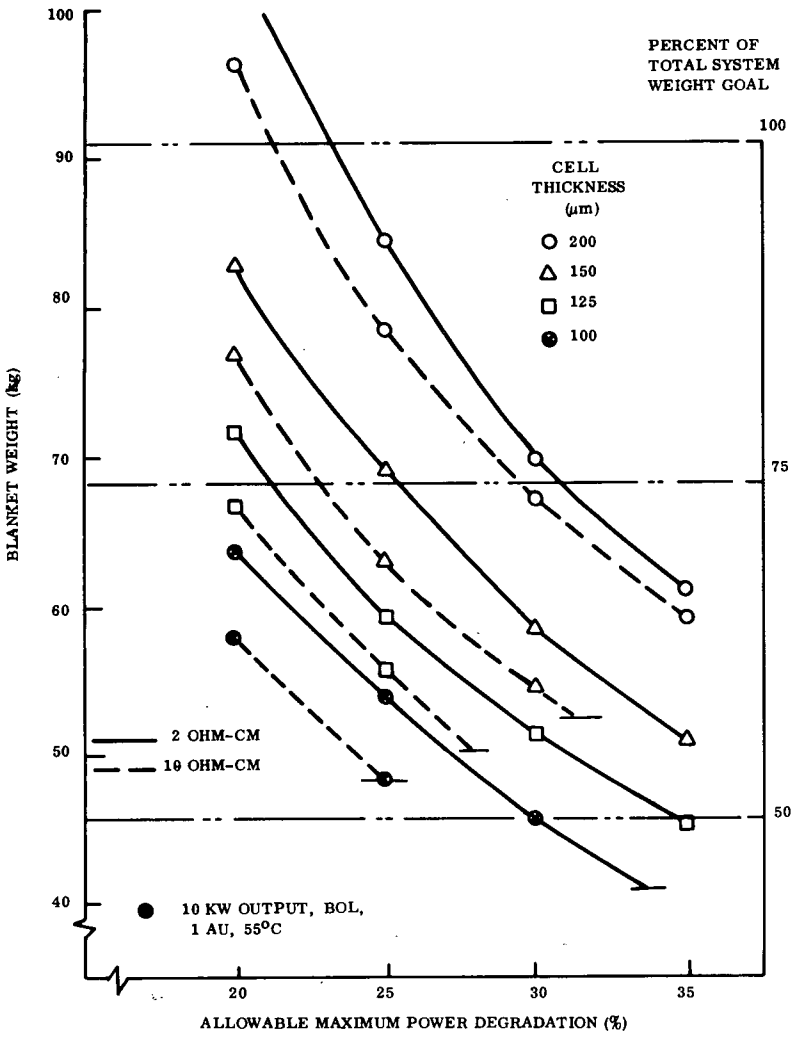

Figure 44. Solar Cell Blanket Weight for Interplanetary Mission (10 kW, BOL Output)

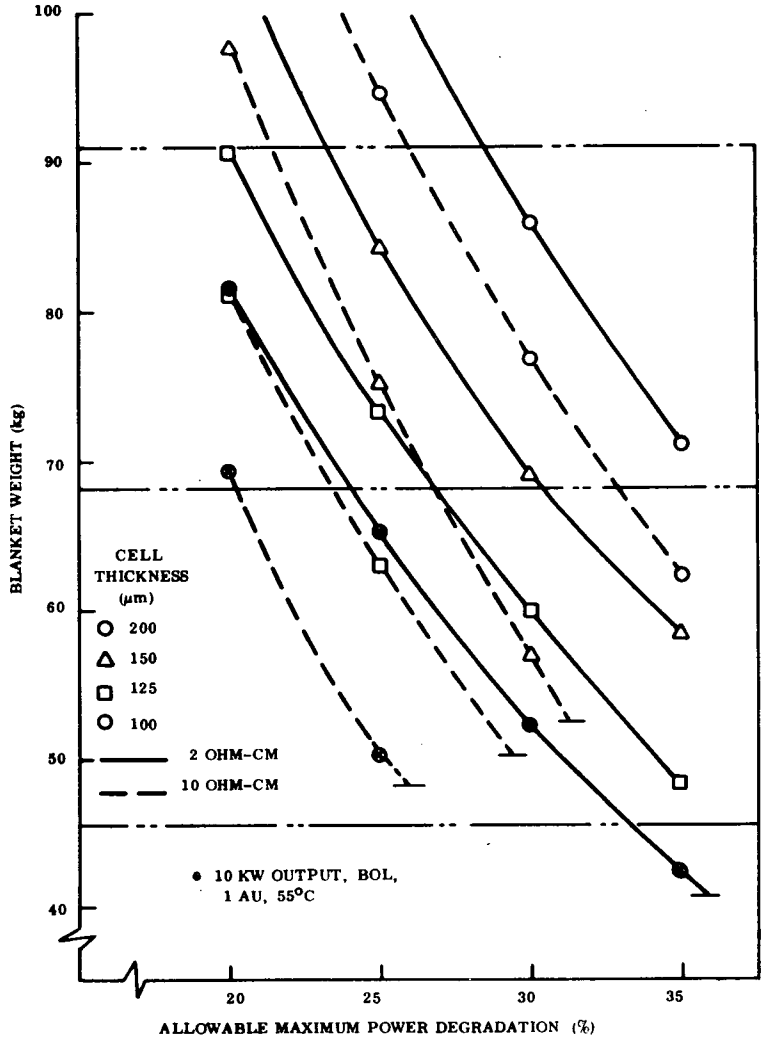

Figure 45. Solar Cell Blanket Weight for Geosynchronous Mission (10 kW, BOL Output)

Table 16. Solar Cell Blanket Weight Tradeoff for Geosynchronous Mission

Solar Cell Base Resistivity (ohm-cm)	Allowable Maximum Power Degradation (% of original)	Solar Cell Thickness (μm)	Solar Cell Area Required for 10,000 watts B.O.L., 55°C (m^2)	Total DENI 1-MeV Electron Fluence ($x10^{14}$ e/cm^2)	Front and Back Shield (gm/cm^2)	Blanket Weight (kg)
2	20	200	71.3	8.4	.064	134.3
		150	74.0	13.3	.046	104.0
		125	76.4	18.0	.038	90.6
		100	79.3	23.0	.033	81.5
	25	200	71.3	14.5	.044	105.0
		150	74.0	22.5	.033	84.2
		125	76.4	30.5	.027	73.3
		100	79.3	38.0	.023	65.3
	30	200	71.3	25.0	.031	85.9
		150	74.0	38.0	.023	69.0
		125	76.4	50.0	.0185	60.0
		100	79.3	61.0	.015	52.2
	35	200	71.3	42.0	.021	71.2
		150	74.0	60.0	.016	58.4
		125	76.4	80.0	.011	48.2
		100	79.3	98.0	.009	42.4
10	20	200	78.6	13.0	.047	120.5
		150	84.2	22.0	.034	97.6
		125	88.3	33.5	.025	81.1
		100	93.8	48.0	.019	69.4
	25	200	78.6	24.5	.031	94.7
		150	84.2	43.0	.021	75.1
		125	88.3	64.0	.015	63.0
		100	93.8	90.0	.009	50.2
	30	200	78.6	45.0	.020	76.9
		150	84.2	83.0	.0105	56.9
		125	88.3	120.0	.007	48.5
		100	93.8	160.0	.005	42.5
	35	200	78.6	83.0	.011	62.4
		150	84.2	150.0	----	----
		125	88.3	220.0	----	----
		100	93.8	290.0	----	----

Table 17. Solar Cell Blanket Weight Tradeoff for Manned Space Station Mission

Solar Cell Base Resistivity (ohm-cm)	Allowable Maximum Power Degradation (% of original)	Solar Cell Thickness (μm)	Solar Cell Area Required for 10,000 watts B.O.L., 55°C (m^2)	Total DENI 1-MeV Electron Fluence ($x10^{14}$ e/cm^2)	Front and Back Shield (gm/cm^2)	Blanket Weight (kg)
2	5	200	71.3	0.9	.168	286.6
		150	74.0	1.8	.077	151.1
		125	76.4	2.2	.065	133.0
		100	79.3	2.8	.051	110.9
	10	200	71.3	2.3	.062	131.3
		150	74.0	4.0	.034	85.8
		125	76.4	5.4	.024	68.6
		100	79.3	6.9	.020	60.3
	15	200	71.3	4.6	.030	84.4
		150	74.0	7.7	.017	59.9
		125	76.4	10.5	.012	49.8
		100	79.3	13.1	.009	42.4
	20	200	71.3	8.4	.016	64.0
		150	74.0	13.5	.009	47.7
		125	76.4	18.0	.006	40.3
		100	79.3	23.0	----	----
10	5	200	78.6	1.35	.103	211.0
		150	84.2	2.25	.063	147.8
		125	88.3	3.7	.037	102.9
		100	93.8	6.0	.022	75.2
	10	200	78.6	3.3	.042	112.5
		150	84.2	5.3	.026	83.7
		125	88.3	8.6	.016	64.8
		100	93.8	13.0	.009	50.2
	15	200	78.6	6.8	.020	76.9
		150	84.2	11.0	.011	57.8
		125	88.3	17.5	.006	46.6
		100	93.8	26.0	.003	38.6
	20	200	78.6	13.0	.009	59.1
		150	84.2	22.0	.005	47.4
		125	88.3	33.0	----	----
		100	93.8	48.0	----	----

The second part of this analysis consisted of an evaluation of the blanket weight for a specified end-of-life (EOL) power output capability with no restriction on the BOL power output (or allowable maximum power degradation). The results of this analysis are shown in Figures 47, 48, and 49 for the interplanetary, geosynchronous and manned space station missions, respectively. In each of these figures, the blanket weight, solar cell area, and fraction of original maximum power remaining are plotted as a function of front and back shield factor. The EOL power output is assumed to be 7,500 watts for all missions.

2.5.4 DISCUSSION OF RESULTS

If the initial solar array output power of 10,000 watts is coupled with an allowable maximum power degradation over the mission duration, the results of the first part of this study aree as summarized in Figures 50 and 51, for 100μm and 125μm thick cells, respectively. These curves were generated from the data presented in Figures 44, 45 and 46. For the interplanetary mission (see Figure 50), the minimum blanket weight is obtained with 10 ohm-cm cells as the allowable maximum power degradation is increased from 20 percent to 25 percent. At a blanket weight of 48.2 kg, the front and back shields have reached the maximum allowable shield factor of 0.008 gm/cm^2. At this point, it is not possible to reduce the blanket weight until the 2 ohm-cm base resistivity curve is reached. As the allowable maximum power degradation is increased further, the blanket weight can be decreased until the minimum weight for these 2 ohm-cm cells is reached at 40.8 kg. This is the absolute minimum blanket weight possible without considering cells thinner than 100 μm.

The curve for the geosynchronous mission (see Figure 50) is basically the same as for the interplanetary mission except that the permissible maximum power degradation for a given blanket weight must be increased slightly because of the more severe particle radiation environment in the geosynchronous mission. For example, with the 100 μm thick, 10 ohm-cm cell, a 26 percent allowable maximum power degradation is required for a 48.2 kg blanket weight. This is approximately one percentage point greater than required for the interplanetary mission. Expressed in different terms for an allowable maximum power degradation of 25 percent, the geosynchronous mission blanket weight would be approximately 2 kg heavier than required for the interplanetary mission using 100 μm thick, 10 ohm-cm cells. For the manned

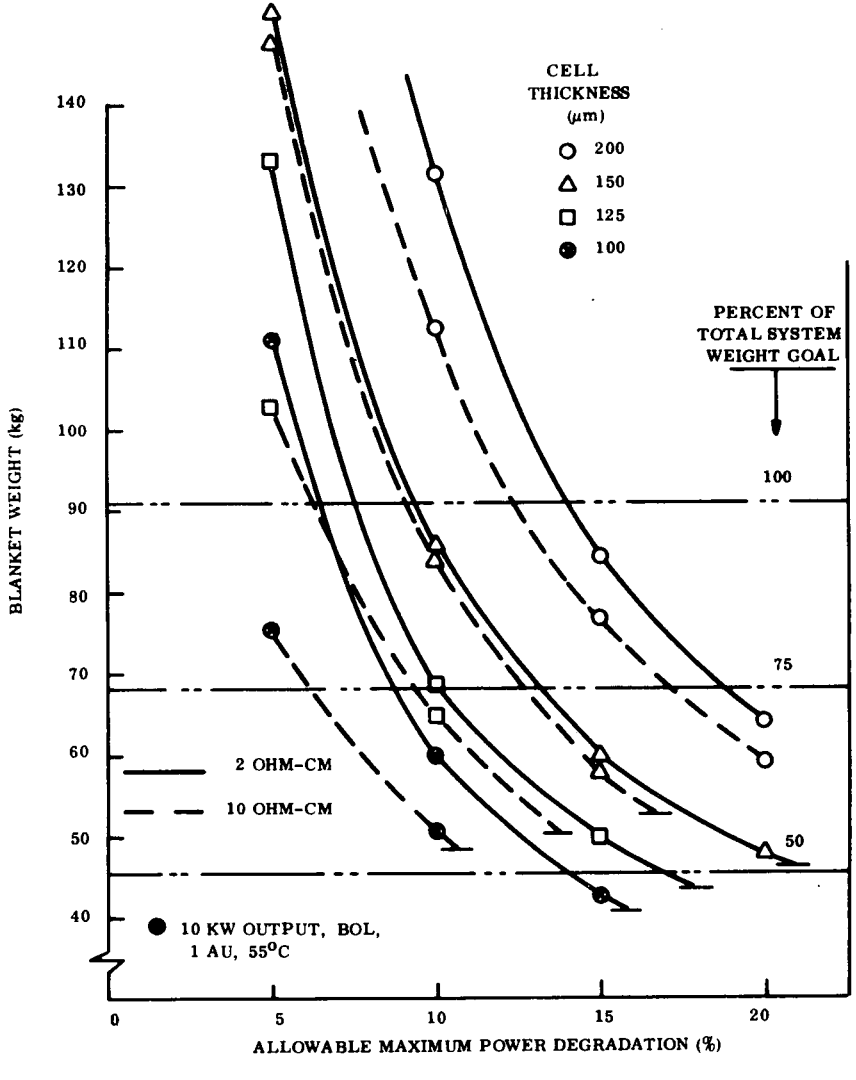

Figure 46. Solar Cell Blanket Weight for Manned Space Station Mission (10 kW, BOL Output)

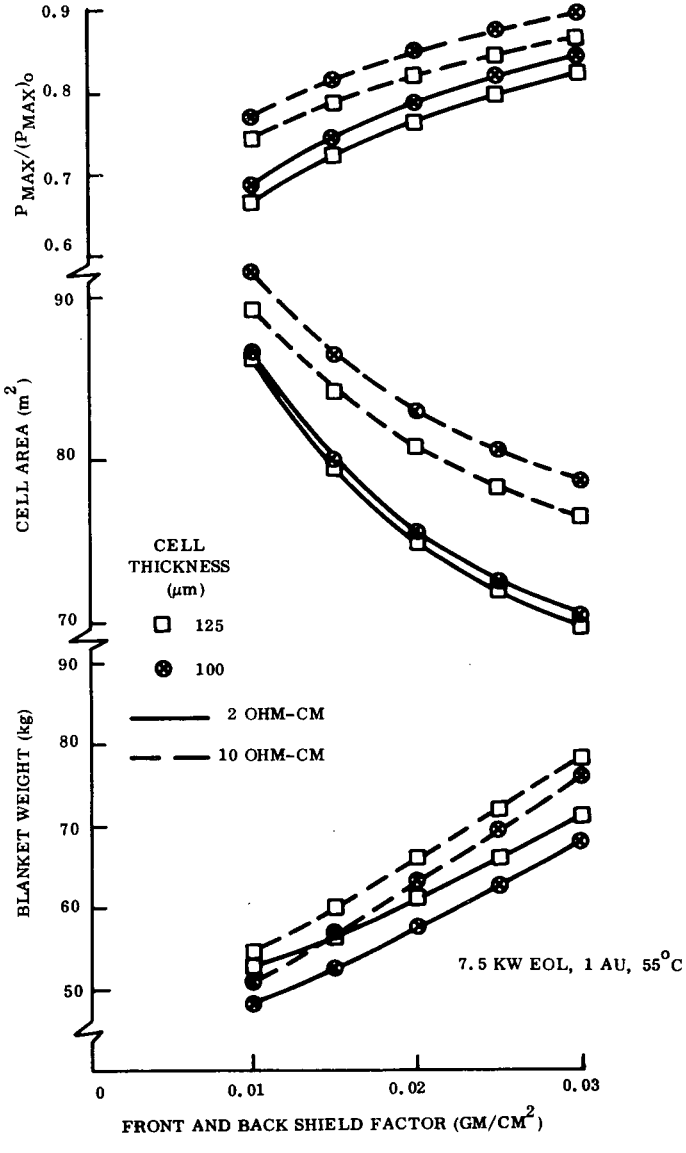

Figure 47. Solar Cell Blanket Trade-off for Interplanetary Mission (7.5 kW, EOL Output)

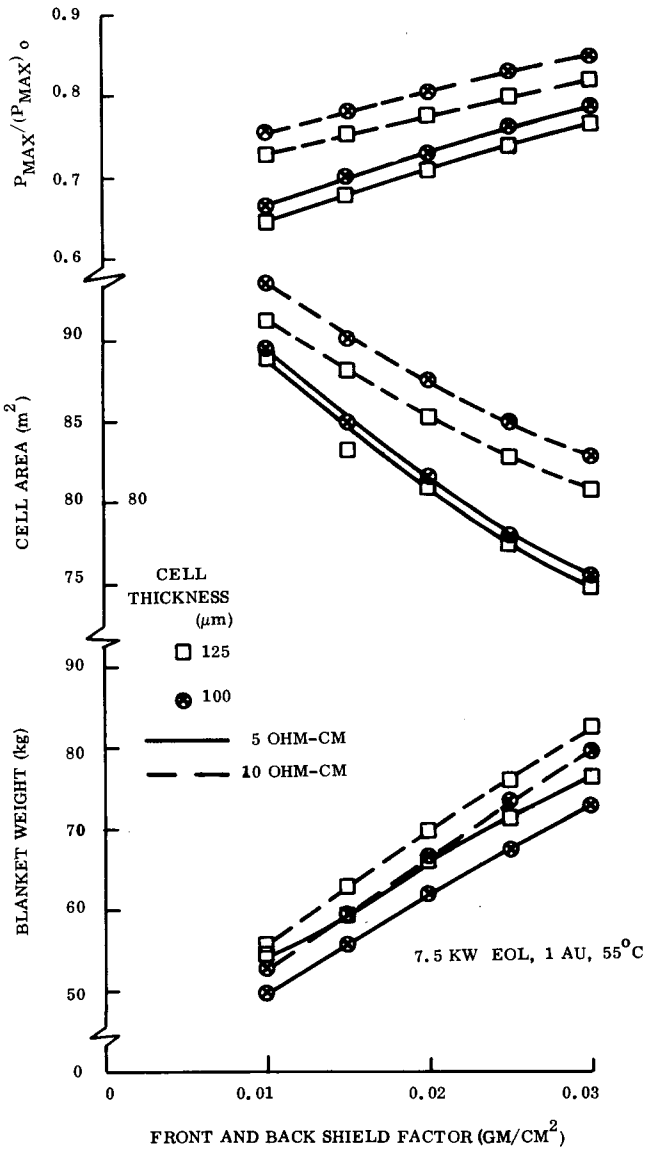

Figure 48. Solar Cell Blanket Trade-off for Geosynchronous Mission (7.5 kW, EOL Output)

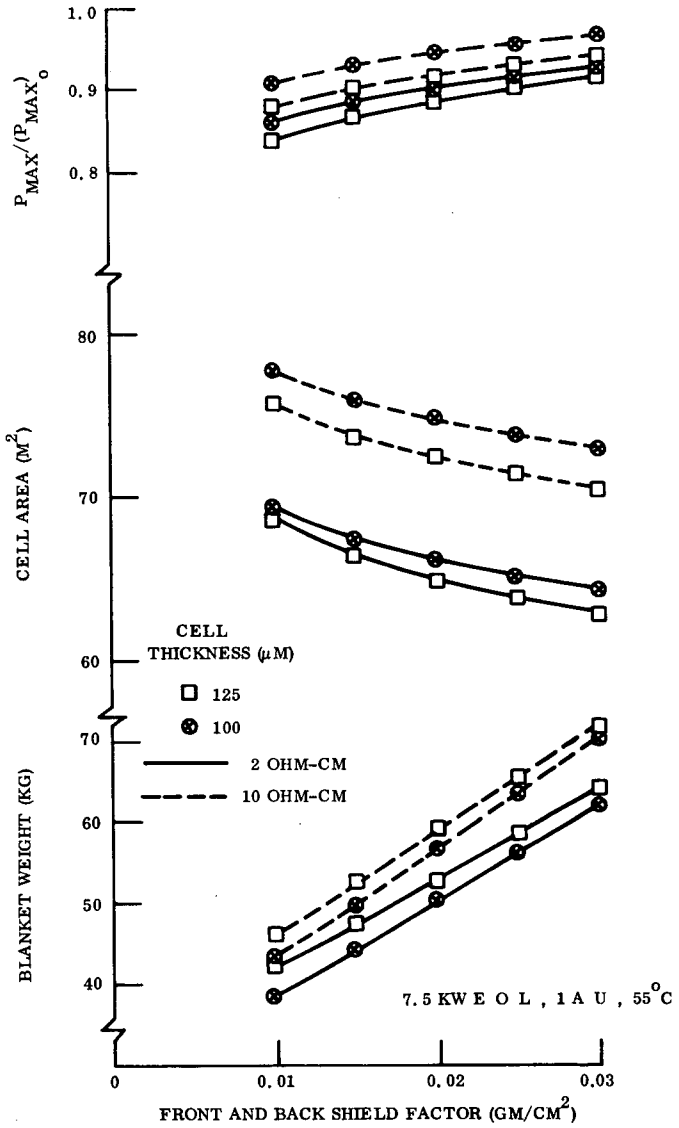

Figure 49. Solar Blanket Trade-off for Manned Space Station Mission (7.5 kW, EOL Output)

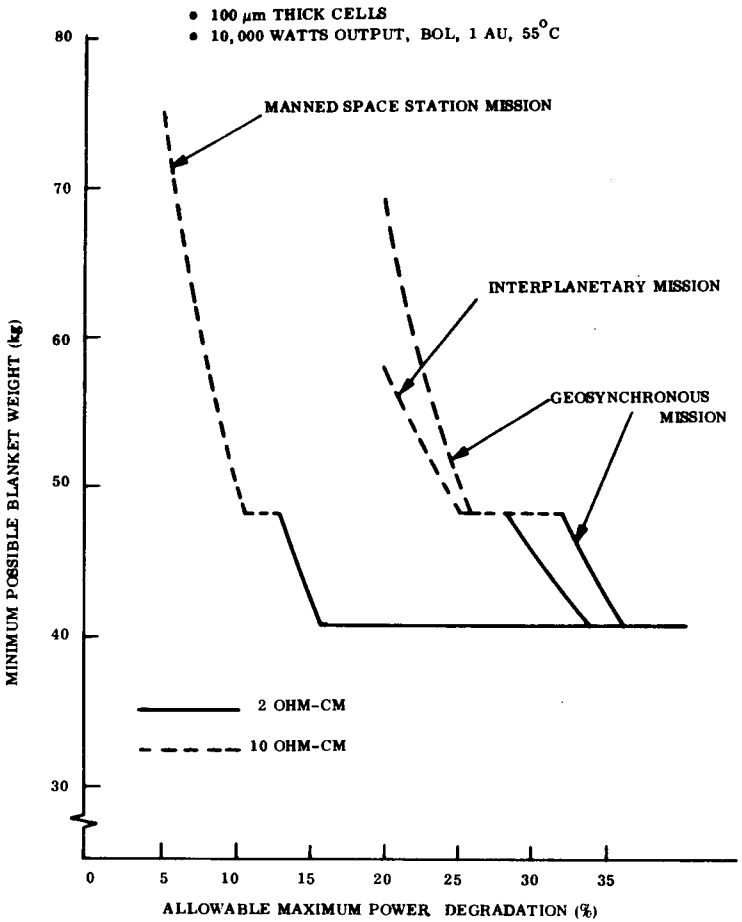

Figure 50. Minimum Possible Blanket Weight for 100 μm Thick Cells

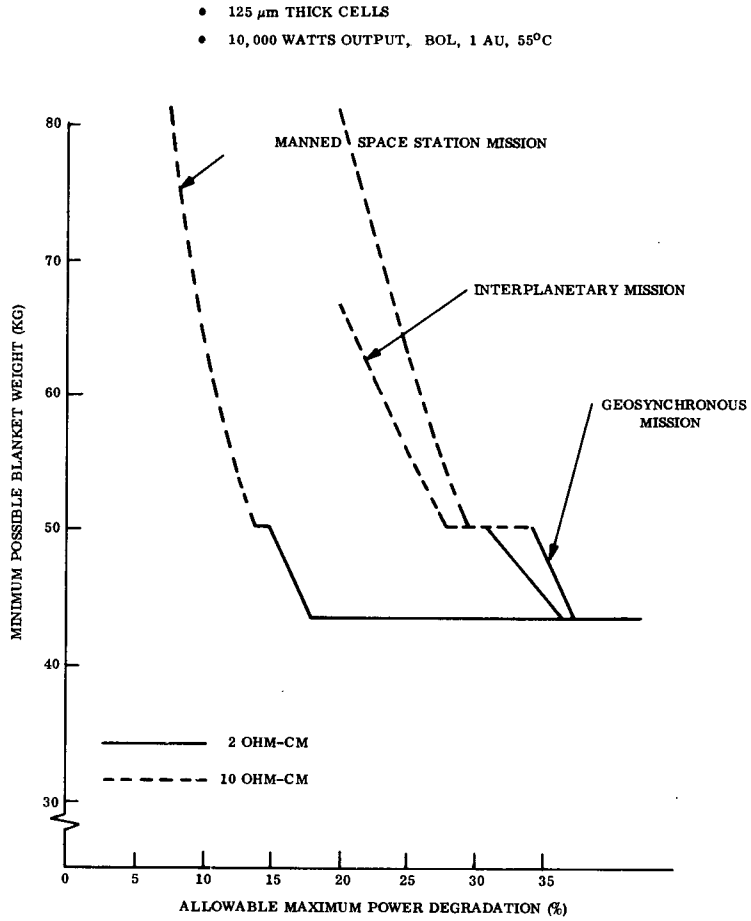

Figure 51. Minimum Possible Blanket Weight for 125 μm Thick Cells

space station mission, the lowest possible blanket weight of 40.8 kg can be achieved with 100 μm thick, 2 ohm cells if the allowable maximum power degradation is specified as 16 percent or greater.

Figure 51 shows a similar set of curves for 125 μm thick cells. Cell thicknesses greater than 125 μm are not presented here because it is unlikely that the system power-to-weight goal can be realized with cells which are thicker than 125 μm, regardless of the allowable maximum power degradation.

The second part of the trade study, which evaluated the blanket weight for a specified EOL power capability, yielded the results shown in Figures 47, 48 and 49. These curves show that the minimum blanket weight is achieved with 100 μm thick, 2 ohm-cm cells. For the interplanetary and geosynchronous missions, the difference between 2 ohm-cm and 10 ohm-cm base resistivities is not great for lightly shielded, low weight blanket constructions.

Thus, the trade-off between base resistivities should be made based on other factors which depend on overall power subsystem requirements including load power demand profile. For some missions it may be desirable to limit the maximum power degradation to some upper limit. For a dissipative type shunt voltage regulator and a constant average load power demand, increased maximum power degradation results in the need for greater power dissipation capability at the beginning-of-life. On the other hand, if the load can use the integrated energy available over the life of the mission, then the selection of the lower base resistivity will give the highest integrated solar array output for a specified end-of-life power capability.

For the manned space station mission, the choice is more clearly directed toward 2 ohm-cm base resistivity.

2.6 PARAMETIC ANALYSIS OF BUS STRIP WEIGHT

2.6.1 GENERAL

The weight of the bus strip network required to distribute the solar cell module current from the generation site on the blanket to the inboard end of the blanket is a significant factor which must be considered in the 110 watt/kg solar array feasibility study. The power dissipation in the bus strip distribution system must be compensated for by increased generating capability if a specified power output is to be delivered at the interface of the solar array with the remainder of the power subsystem. The use of low resistance conductors, with the associated weight penalty, will reduce the distribution power losses thereby reducing the extra generating capability required to supply these losses. On the other hand, higher resistance, lower weight conductors will increase the distribution power losses thereby increasing the extra generating capability required to supply these losses. Thus, an optimum power loss and associated bus strip weight should exist for a given set of design conditions.

The purpose of this analysis is to define this optimum bus strip power loss and associated bus strip weight required for solar array configurations which meet the requirements for this feasibility study and have the potential for meeting the 110 watt/kg power-to-weight ratio goal.

2.6.2 METHOD OF ANALYSIS

The method of analysis follows the mathematical procedures described by J. Roger in Reference 43. A similar analysis, with specific application to the 30 watt/lb roll-up array, is discussed in Reference 44. For this analysis, it is assumed that the circuits are arranged on the two solar cell blankets as shown in Figure 52. All circuits (n per solar cell blanket, or 2n for the total solar array panel) are identical and each supplies the full voltage, V, to the bus. Each circuit is assumed to have separate positive and negative bus strips which run down to the base of the blanket. All bus strip conductors are sized to have the same voltage drop, ΔV. The power at the terminals of each blanket are given by:

$$n(V - \Delta V)\, i = (V - \Delta V)\, I$$

where $I = ni$ is the total current from one blanket.

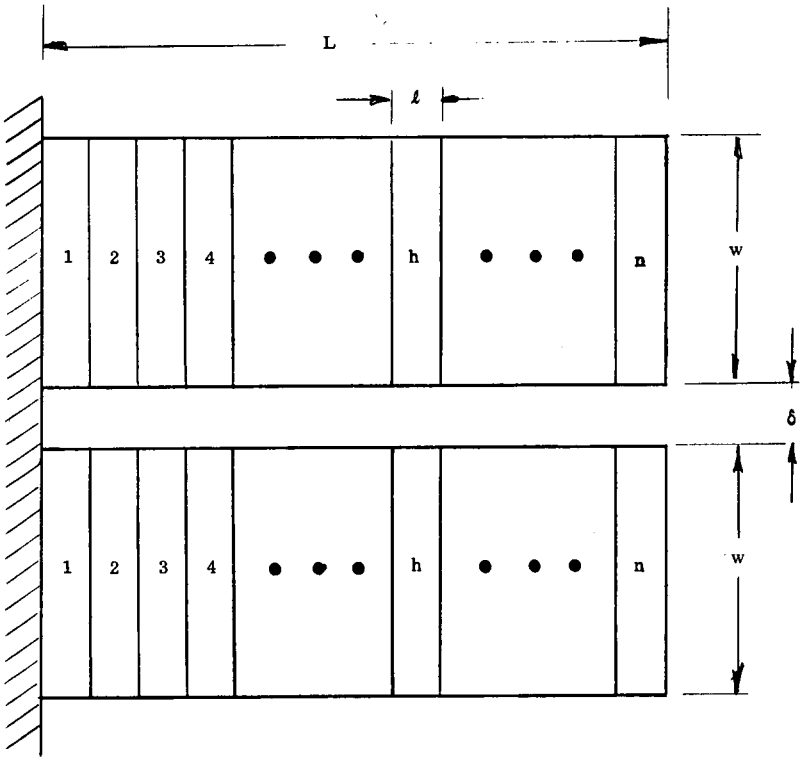

Figure 52. Schematic of Solar Cell Blanket Circuit Configuration

Based on the derivation in Reference 43, the total bus strip weight for the solar array panel (both solar cell blankets) is given by:

$$W_b = \frac{4\rho d \bar{w} \ell^2}{3\alpha V^2} n (n+1)(2n+1) \qquad [1]$$

where: ρ = resistivity of the bus strip conductors [ohm-m]

d = density of the bus strip conductor material including allowance for the insulation [kg/m^3]

V = circuit operating voltage measured at the circuit terminals [volts]

$\bar{w}$ = nominal power output from one circuit [watts]

ℓ = dimension of one circuit along the length of the blanket [m]

α = fraction of circuit voltage (or power) loss in bus strips

$$= \frac{\Delta V}{V} = \frac{\Delta P}{P}.$$

The total weight of the solar array panel is given by:

$$W_t = Sf_s + W_b \qquad [2]$$

where

S = total solar array panel area $[m^2]$

$= 2Lw$

f_s = system weight-to-area ratio including the weight of solar cell blankets, deployment and stowage mechanisms and structures $[kg/m^2]$.

By defining

$$m = \frac{2\rho \overline{dw}\,\ell}{3V_w^2}(n+1)(2n+1) \qquad [3]$$

Equation [1] becomes

$$W_b = \frac{mS}{\alpha}$$

The figure of merit of the solar array panel, in terms of power delivered to the interface per unit weight is:

$$p = \frac{(1-\alpha)P}{Sf_s + \frac{mS}{\alpha}} = \frac{\alpha(1-\alpha)s}{\alpha f_s + m} \qquad [4]$$

where s = system power-to-area ratio with the power measured at the circuit level $[watt/m^2]$

The optimum value of α, defined as α_o, is obtained by setting the derivative of equation [4], with respect to α, equal to zero. Thus, this optimum value of α is given by:

$$\alpha_o = \frac{m}{f_s}\left[\sqrt{1+\frac{f_s}{m}} - 1\right] \qquad [5]$$

At this optimum value of voltage drop, we can write:

$$m_o = \frac{\alpha_o^2 f_s}{1 - 2\alpha_o}$$

$$W_{bo} = \frac{\alpha_o S f_s}{1 - 2\alpha_o} \qquad [6]$$

$$p_o = \frac{P(1 - 2\alpha_o)}{S f_s}$$

2.6.3 RESULTS OF ANALYSIS

The general analysis approach described above was utilized to study the bus strip weight associated with a solar array panel which produces 10,000 watts with a power-to-weight ratio of at least 110 watt/kg. For this preliminary analysis, the two solar cell blankets per panel will be mounted with 100 μm thick, 10 ohm-cm bottom wrap-around contact solar cells. The total blanket weight (not including distribution bus strips) is 48.2 kg based on the analysis in Section 2.5. The required area of solar cells is 93.8 m^2. Assuming a packing factor of 1.055, the total blanket module area is equal to 99.0 m^2. The aspect ratio of the blanket, R_b, defined as L/w, has a significant effect on the bus strip weight and will be used as a parameter in this analysis.

The bus strip conductors were assumed to be copper with a resistivity, ρ, equal to 1.724×10^{-8} ohm-m at 20^oC. With a temperature coefficient of resistance at 20^oC of 0.00393, the resistivity of the copper at 55^oC is 1.960×10^{-8} ohm-m. The bus strips are composed of copper foil conductors with Kapton-H film insulating layers. The equivalent density of this composite was derived based on the assumption that the copper strip and the Kapton insulator are the same width and the thickness of the copper is 1.5 times the thickness of the insulator. With those assumptions, the equivalent density, d, is given by:

$$d = d_{cu} + 2/3\, d_k$$

$$= 8940 + 2/3\,(1420) = 9900 \text{ kg/m}^3$$

where

d_{cu} = density of copper = 8940 kg/m^3

d_k = density of Kapton-H film = 1420 kg/m^3

The system weight-to-area ratio, f_s, is assumed to be approximately given by:

$$f_s = \frac{10,000}{110\ (99.0)} = 0.92 \text{ kg/m}^2$$

By substitution of appropriate values into equation [3], the parameter m is represented by:

$$m = \frac{2\ (1.960 \times 10^{-8})\ (9900)\ (5,000)\ L\ (n+1)\ (2n+1)}{3V^2wn^2}$$

If the value of m is substituted into equation [5], the optimum value of power loss, α_o, is as plotted in Figure 53 as a function of circuit voltage, V. Four different values of blanket aspect ratio, as well as three values of n have been plotted to show the affect of these variables. Figure 54 shows the total bus strip weight (W_{bo} from equation [6]) at the optimum power loss as a function of the circuit voltage, V. The number of circuits per blanket, n, has been selected as 10 for this presentation, but the same four blanket aspect ratios are plotted.

In Table 18, the constituents of the total blanket weight are summarized based on the previous analysis. Column 3 is the optimum power loss from Figure 53 for a value of n = 10. Column 4 is the solar cell area required to produce 10,000 watts output at beginning-of-life, 1 AU and 55^{o}C. This output is measured at the interface and includes the power losses in the bus strip distribution network. The blanket weight in Column 5 is based on the use of 100 μm thick, 10 ohm-cm bottom wraparound contact cells with a minimum front and back shielding of 0.008 gm/cm^2. The bus strip weight in Column 6 is from Figure 54 with a proportionate increase to reflect the increased solar cell blanket area necessary to make up for the power loss in the bus strips. The total blanket weight from Column 7 is plotted in Figure 55 as a function of blanket aspect ratio, L/w.

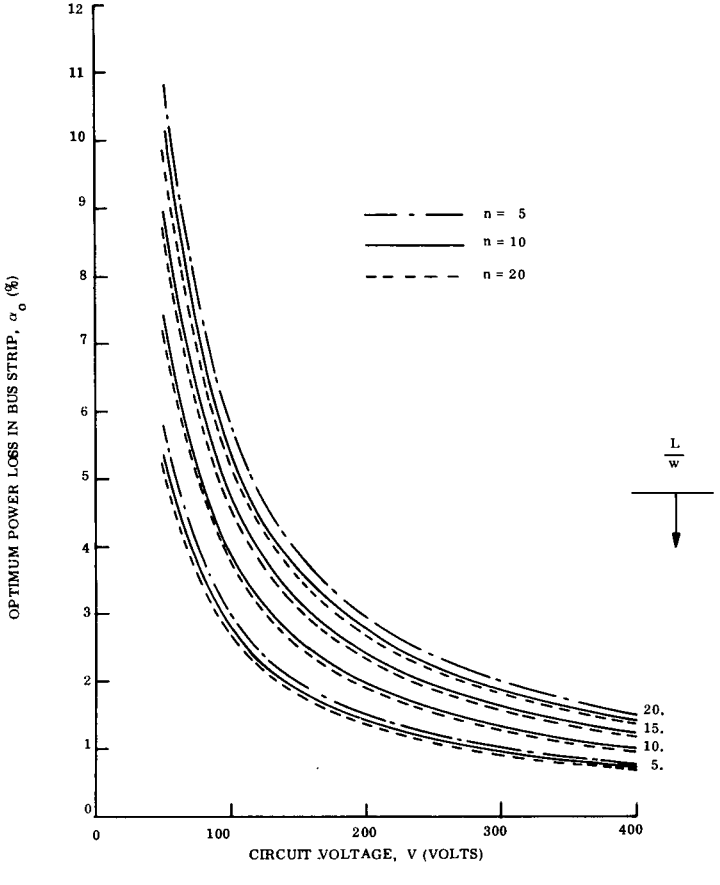

Figure 53. Optimum Bus Strip Power Loss vs Voltage

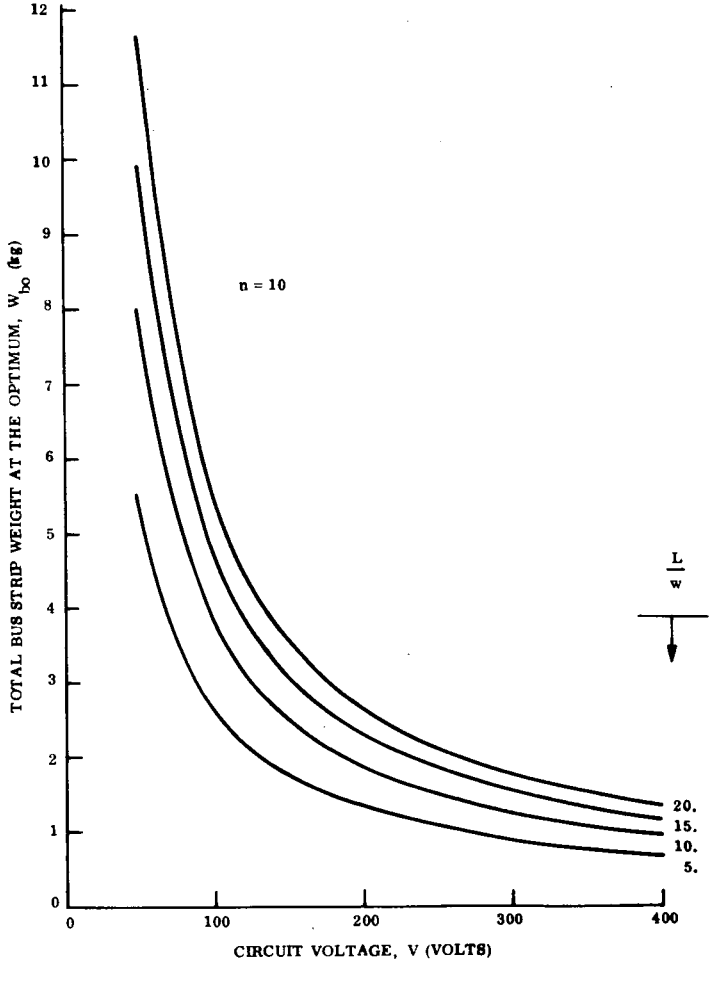

Figure 54. Total Bus Strip Weight at the Optimum vs Voltage

Table 18. Summary of Blanket Weight vs Aspect Ratio Trade Study

V (volts)	$\frac{L}{w}$	α_o	Cell Area Required for 10,000 watts at Interface (m^2)	Blanket Weight Less Bus Strips (kg)	Bus Strip Weight (kg)	Total Blanket Weight (kg)
100	5	0.02770	96.47	49.59	2.75	52.34
	10	0.03871	97.58	50.16	3.97	54.13
	15	0.04698	98.42	50.59	4.95	55.54
	20	0.05384	99.14	50.96	5.81	56.77
200	5	0.01405	95.14	48.90	1.34	50.24
	10	0.01975	95.69	49.18	1.91	51.09
	15	0.02408	96.11	49.40	2.36	51.76
	20	0.02770	96.47	49.59	2.75	52.34
300	5	0.00941	94.69	48.67	0.88	49.55
	10	0.01325	95.06	48.86	1.26	50.12
	15	0.01618	95.34	49.00	1.54	50.54
	20	0.01864	95.58	49.13	1.79	50.92
400	5	0.00707	94.47	48.56	0.65	49.21
	10	0.00997	94.74	48.70	0.94	49.64
	15	0.01219	94.96	48.81	1.15	49.96
	20	0.01405	95.14	48.90	1.34	50.24

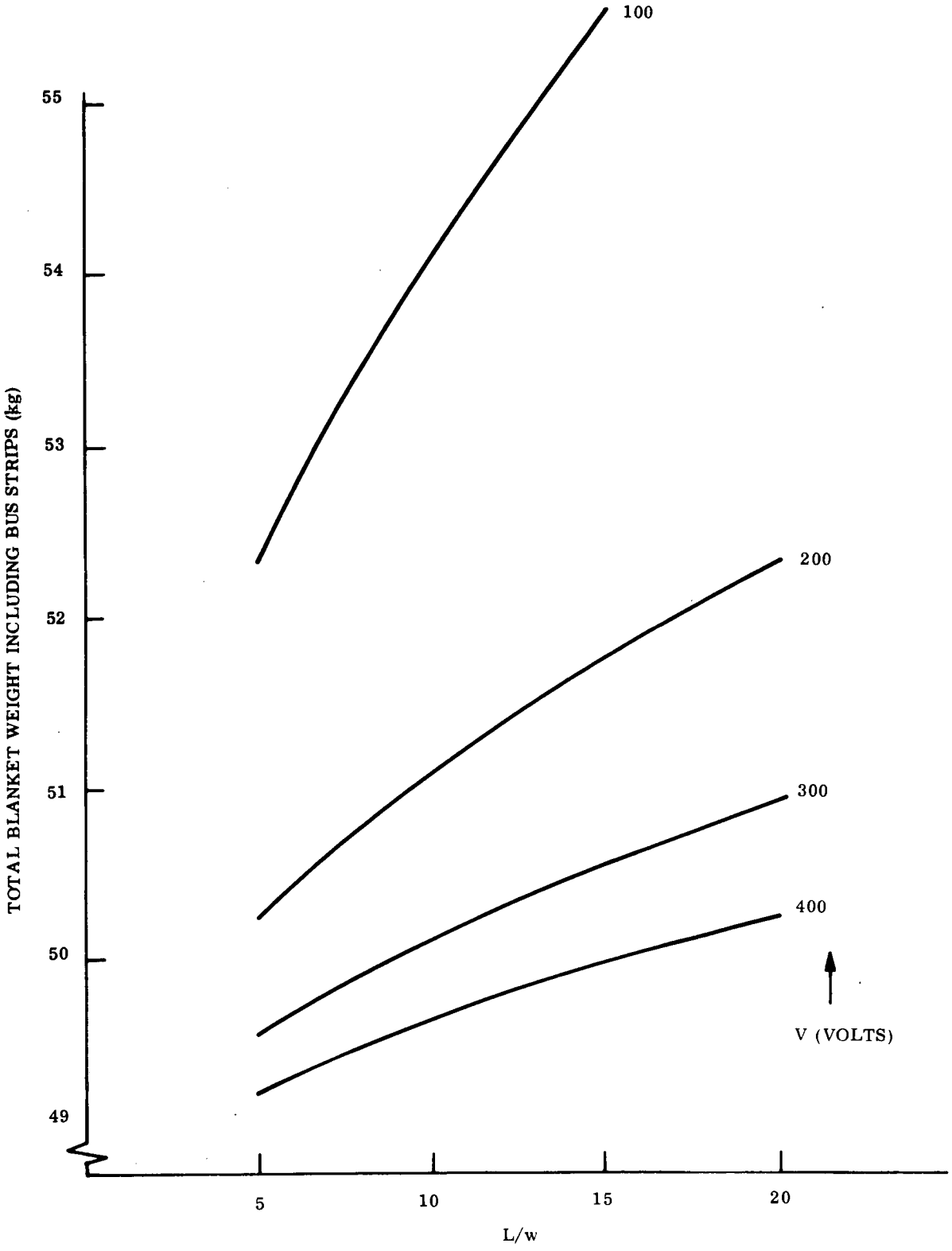

Figure 55. Total Blanket Weight vs Blanket Aspect Ratio

2.7 ATTITUDE CONTROL INTERACTION CONSIDERATIONS

2.7.1 INTRODUCTION

Interaction between the vehicle attitude system and large lightweight solar arrays is a factor in the evaluation and selection of these arrays for space missions. Since the intent of this study is to generate design concepts applicable to future missions it is essential that the performance characteristics of the concepts be acceptable to system designers. The approach to be used in the study is to develop design requirements or guidelines that will provide this performance.

There are no design criteria that both eliminate interaction considerations and allow a large lightweight array for the missions of interest. However, the problem is considered solvable for specific missions and designs with the solution involving the participation of several spacecraft design and analysis disciplines. For example the attitude control of a Solar Electric Multimission Spacecraft (SEMMS) with large solar arrays has been investigated by JPL (see Reference 45) with the conclusion that attitude control of a vehicle with a large flexible solar array can be accomplished for interplanetary missions. Though not as well documented, attitude control specialists have similar opinions with respect to the other two missions included in this study.

This discussion first lists the design guidelines currently being used by this study with a discussion of the interaction problem following.

2.7.2 DESIGN GUIDELINES

The most important requirement with respect to integrating a large lightweight solar array into a spacecraft with an active attitude control system is to have the capability of adequately modeling the array dynamic characteristics. This allows the design of the attitude control equipment to proceed on a rational basis, and assuming adequate modeling of the other system elements. The capability to adequately model the array for system dynamics analysis implies that the structural dynamics are understood well enough to analyze the effects of other forcing functions such as propulsion devices on the array system.

The capability to model the solar array does not provide the design constraint needed for the study. The structural rigidity or stiffness constraint adopted for the study is that the solar panel shall have sufficient rigidity so that its lowest natural frequency of vibration is equal to or greater than 0.04 Hz. As discussed in the following section this value has been used on several lightweight array studies in the past and is an acceptable value for at least the interplanetary and synchronous earth orbit missions.

2.7.3 DISCUSSION

The structural rigidity design requirements used in previous development programs for large lightweight solar arrays were surveyed as one step in generating a rational design requirement for this study. Results are summarized in Table 19. Except for one system, structural rigidity is specified by constraining the natural frequencies of the solar array system. This is as expected since one of the basic attitude control interaction considerations is whether or not there are structural resonances within the bandwidth of the attitude control system. In most systems this is the first problem that is encountered as the structural frequency is reduced. However, other considerations such as the vehicle accelerations can be constraining as is evidently the case for the Flexible Rolled-Up Solar Array (FRUSA).

The relation between the fundamental frequency, an acceleration environment, and the maximum panel deflection for any configuration can be approximated by considering the panel as a single-degree-of-freedom spring mass system. Results are given in Figure 56. At the selected lowest natural frequency of 0.04 Hz the static deflection with a 0.1 g force is about 25 meters, an unrealistically large deflection for the size system being considered. Thus, the FRUSA stiffness requirement implies a higher frequency than the value selected for this study.

The preferred approach in control system design is to have all structural resonance outside the bandwidth of the control system. This is the approach used in the CTS program (see Table 19) where the "rule of thumb" of a decade of separation was used.

Table 19. Structural Rigidity Design Requirements for Large Lightweight Solar Array Programs

Program	Design Requirement	Data Source	Comments
30 Watt per Pound Roll-up Solar Array	First natural frequency equal to or greater than 0.04 Hz	Ref. 11	
Large Area Solar Array (20 Watt per Pound)	First natural frequency equal to or greater than 0.04 Hz	Ref. 17	
Space Station Solar Array Technology Program	Fundamental frequency to be less than 0.1 Hz	Ref. 4	Artificial "g" conditions provides most severe structural requirement
Space Station Solar Array Design Study	No fundamental frequencies in the range of 0.1 Hz to 2 Hz	Ref. 46	Design study in support of NAR Space Station Study
Flexible Rolled-Up Solar Array (FRUSA)	0.1 g acceleration environment	Ref. 12	
Communications Technology Satellite (CTS) Lightweight Solar Array	Fundamental frequency to be greater than 0.1 Hz	Ref. 47	Natural frequency is 10 times the bandwidth of the attitude control subsystem

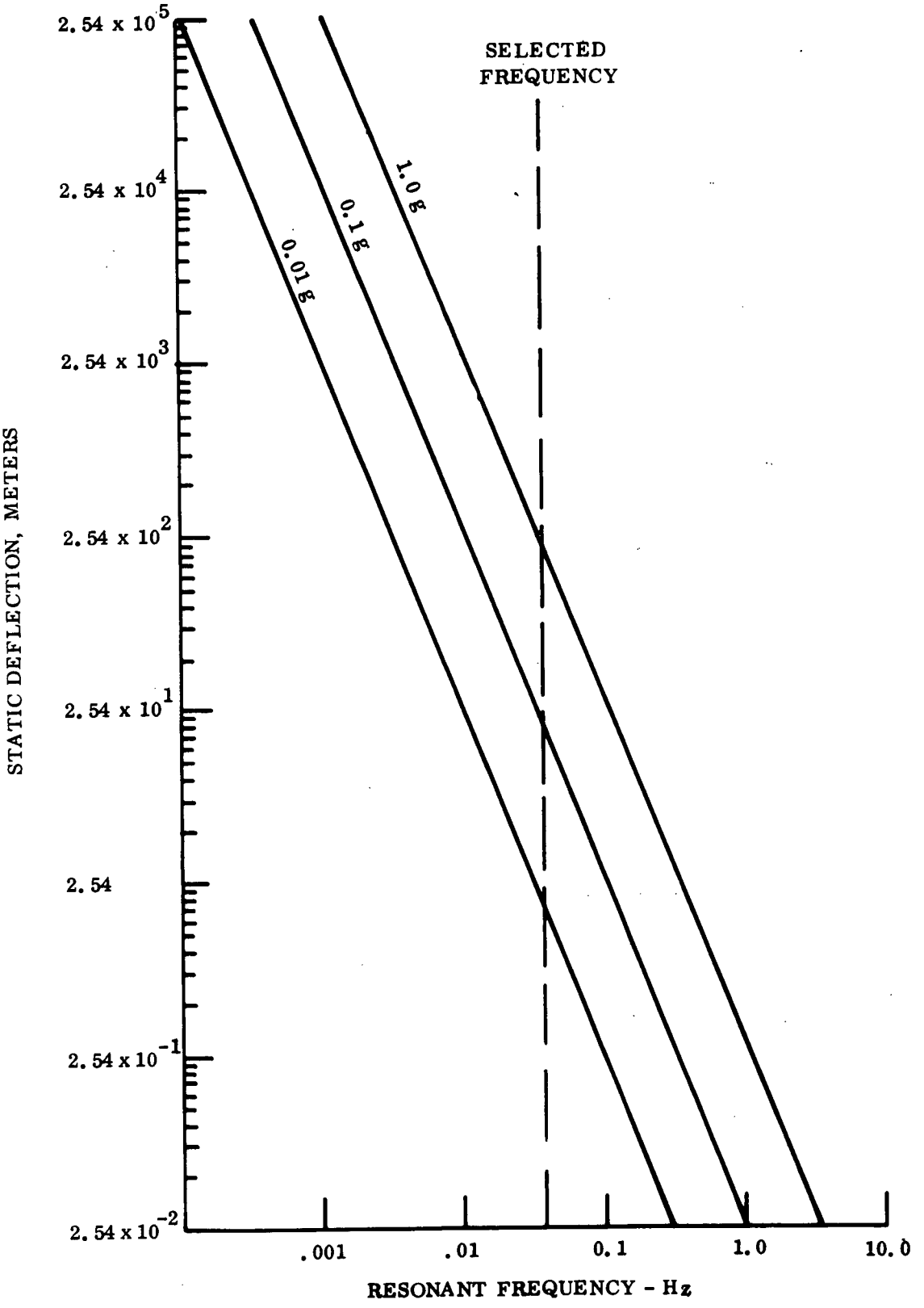

Figure 56. Static Deflection vs Frequency

Control system bandwidths for synchronous earth orbits and interplanetary missions are typically in the range of 0.0016 to 0.016 Hz while manned space stations using control moment gyros could have bandwidths of 0.16 to 1.6 Hz. This wide range of bandwidths does not converge on a value for lowest natural frequency that is typical for all missions. The value of 0.04 Hz was selected as a baseline because it is within the range of interest and because of its use in previous studies. Thus the results of this study are directly comparable with previous studies since the structural stiffness requirement is the same. Parametric studies will be carried out to show the effect of this requirement on weight.

Although a minimum frequency requirement for the general mission categories can be established, integration studies have been carried out for the 0.04 Hz value. Reference 45 concludes that natural frequencies below 0.04 Hz can be accommodated on the SEMMS vehicle designs and unpublished studies at General Electric indicated that 0.04 Hz solar panels could be accommodated on the ATS F and G vehicle with acceptable attitude control performance.

The design of a spacecraft for a particular mission will involve dynamics analysis of the system and it is unlikely that any design requirement adopted in this study will satisfy all mission requirements. It is also likely that at some future date the control system bandwidth will include some of the array natural frequencies. The technique of keeping the frequencies outside the control bandwidth essentially decouples the system and interaction does not occur. There are a number of control system techniques that can be used to maintain stability and control system performance when this is the case. Though they increase the complexity of the control system this may be preferable to the increased weight that results from the simple approach of stiffening the structure to increase its frequency. Reference 48 lists artificially stiffening the structure through the use of special, inner control loops, utilization of a low pass filter within the control amplifier, artificially lowering the bandwidth of the control through use of a special actuator lag which inhibits sign reversal of the control at a rate higher than that needed to follow control commands, or through the use of notch filters. This list should be considered typical rather than all inclusive since the technology of control systems and associated equipment such as on-board computers allows many and varied approaches to the attitude control of a spacecraft.

SECTION 3

CONCLUSIONS

At this point in the study, it is possible to draw some preliminary conclusions based on the work performed to date. The review of existing lightweight solar array system concepts (see Section 2.2) leads to a number of conclusions regarding the application of these concepts to the formulation of a 110 watt/kg solar array concept. These conclusions are listed below along with the associated rationale:

1. "Rigid" folding panel design concepts can be eliminated from further consideration in the 110 watt/kg feasibility study. This conclusion is based on the weight of the Boeing folding panel design. This array is approximately the size required for the 10,000 watt, 110 watt/kg array and has a structural weight-to-area ratio of 1.486 kg/m^2. Based on this structural weight, the power-to-weight ratio would be approximately 70 watts/kg if it is assumed that the blanket weight is zero. The addition of a blanket weighing 0.53* kg/m^2 will reduce the power-to-weight ratio to about 52 watts/kg which is far from the goal of 110 watts/kg. The use of a multiple panel EOS Hollowcore approach offers no potential for improvement of this power-to-weight ratio.

2. A single boom deployment system is lighter than a similar system with two booms. A comparison of the GE roll-up with the Hughes roll-up shows a significant difference in the weight per unit area associated with the deployment related structure. Part of this difference can be attributed to the difference in size and deployed natural frequency. In order to provide a valid comparison between these two concepts, the GE roll-up was scaled down in area and up in deployed frequency using the techniques described by Coyner and Ross in Reference 49. The width of 2.52 m was held constant, and the cell area was reduced to 13.8 m^2 with the lowest deployed natural frequency increased to 0.25 Hz. Under these conditions, a BI-STEM boom stiffness of 1200 $N\text{-}m^2$ (2.9×10^3 $lb\text{-}ft^2$) is required with an associated deployed structure weight of 5.4 kg including the boom, actuator and leading edge member. The resulting deployment equipment weight-to-area ratio of 0.391 kg/m^2 is still considerably less than the 0.632 kg/m^2 for the Hughes roll-up.

3. A flat-pack packaging concept offers weight advantages when compared to roll-up stowage. This conclusion is subtantiated by comparing the large RAE flat-pack design with either the GE or Hughes roll-up.

*Based on the use of 100μm thick, 10 ohm-cm cells with 0.008 gm/cm^2 of front and back shielding with a 200 volt array bus and a blanket aspect ratio of 10 (see Section 2.6).

4. Improvements in the structural concept of these existing designs is required to meet the 110 watt/kg goal. With a blanket power-to-area ratio of 104.5 watt/m^2 of cell area, it is necessary to have a total weight-to-area ratio of 0.95 kg/m^2 in order to achieve an overall power-to-weight ratio of 110 watt/kg. With a blanket weight of 0.53 kg/m^2, the remaining 0.42 kg/m^2 is available for deployment and stowage structure. With the present concepts, the best available structure weights are 0.258 kg/m^2 for deployment with the GE roll-up and 0.299 kg/m^2 for the RAE flat-pack stowage system. Thus, improvements in both the deployment and stowage weights are necessary to achieve the 110 watt/kg goal.

The review of the existing component technology base (see Section 2.4) leads to the following conclusions:

1. Nominal solar cell thicknesses of 125 or 100 μm appear feasible from an overall weight and electrical performance standpoint. Cell thicknesses of greater than 125 μm result in too large a portion of the total allowable system weight being used for the solar cell blankets. This is a manner of judgement based on the distribution of weight in existing lightweight flexible solar array system. Cell thicknesses of less than 100 μm have only been produced in very small quantities and there is a complete lack of published performance data for thinner cells. The 125 μm thick, 10 ohm-cm, bottom wraparound contact cell manufactured by Ferranti, Ltd., is the best currently available in terms of power-to-weight ratio and has been used as the basis for cell performance predictions. This cell has a power-to-weight ratio of 360 watt/kg at 55°C. By comparison, the cell used on the 30 watt/lb roll-up solar array program had a power-to-weight ratio of 270 watt/kg at 55°C.

2. Pertaining to solar cell covers, a review of existing technology leads to the conclusion that integral glass covers of Corning 7070 glass (with or without ceria stabilization) which are deposited by the Ion Physic's HVIBS process or by the ERA's RF sputtering process offer the best approach for performing this function. The low instrinsic stress associated with this glass make it an attractive choice for deposition in thicknesses of 25 to 50 μm on 100 to 125 μm thick solar cells. More work with cells of this thickness would be required to verify this point. Both of these deposition processes are reported to have produced integral covers with consistently excellent optical and physical properties. It is expected that some amount of ceria doping of the 7070 glass will be required, but this determination will require additional work to optimize the level for a particular particle radiation environment. Both of these processes are capable of depositing some glass on the cell edges to provide a desirable protection against low energy protons.

   At the present time, the FEP-Teflon cover does not appear to offer the same degree of environmental stability as the integral glass approaches described above. Further development may reverse this conclusion.

3. For the solar cell blanket substrate, Kapton-H film appears to offer the best solution, but there appears to be little reason to cut-out sections of the substrate, thereby exposing the rear side of the solar cells. This approach was taken on the RAE flat-pack solar array with the result that it was later necessary to cover the rear surfaces of each solar cell with 50 μm thick layer of Midland Silicones Silastoseal B adhesive to provide the necessary low energy proton protection. With a cementless attachment of the solar cells to the substrate, there may be some advantage to these cut-outs as far as reducing cell operating temperature. A detailed thermal analysis of the solar cell blanket should be performed to determine the effect of a potential cut-out pattern on the average solar cell temperature.

   The use of a Kapton/FEP/Interconnect/FEP/Kapton sandwich construction for the substrate is not the most weight effective approach. The direct deposition of the interconnector metal pattern on the Kapton substrate should be investigated.

   Solder constitutes a significant fraction of the total substrate weight. The elimination of this item by a welded connection between the solar cells and interconnectors will make an obvious improvement in the overall system power-to-weight ratio.

4. The application of composite materials, such as boron/aluminum and graphite/aluminum, to the fabrication of deployable boom structures shows promise from a theoretical standpoint. Further study should be undertaken to evaluate the practical feasibility of this application.

The parametric analysis of the solar cell blanket portion of the system (see Section 2.5) yielded certain conclusions which are listed below:

1. The allowable 20 percent maximum power degradation over the mission lifetime imposes shielding requirements which result in a total blanket weight which is too high in relationship to the total system power-to-weight goal.

2. The use of a minimum shielding of 0.008 gm/cm^2, which is considered sufficient to prevent low energy proton damage, results in reasonable blanket weights for 100 or 125 μm thick solar cells. Under this minimum shielding condition and with 100 μm thick, 10 ohm-cm cells, the calculated degradation due to the particle radiation environment is 25, 26, and 11 percent for the interplanetary, geosynchronous and manned space station missions, respectively. For the same thickness cells of 2 ohm-cm base resistivity and with the same minimum shielding, these radiation degradations would be increased to 34, 36, and 16 percent, respectively. The use of a 125 μm nominal cell thickness will increase these degradation values slightly due to the increased radiation damage for the same equivalent 1-MeV electron fluence.

3. The specification of beginning-of-life power along with a maximum allowable power degradation over the mission lifetime leads to the conclusion that 10 ohm-cm resistivity results in the minimum weight blanket for both the interplanetary and geosynchronous missions, while 2 ohm-cm base resistivity is the best choice for the manned space station mission. For example, with a 20 percent allowable particle radiation damage, the blanket weights are as shown in Table 20. Note that, for the manned space station mission application, the degradation will be less than 20 percent since the shielding has been maintained at a minimum of 0.008 gm/cm^2 to provide adequate low energy proton protection.

   If the end-of-life power requirement were specified with no restrictions on beginning-of-life output, the selection of 2 ohm-cm base resistivity is indicated for the interplanetary and geosynchronous misssions, but the difference is not great for lightly shielded ultra-thin cells.

4. The selection of solar cell base resistivity has no real affect on the design details of the solar array system. For preliminary sizing purposes, the performance characteristics of 10 ohm-cm cells will be used for the interplanetary and geosynchronous missions. These arrays will be sized to produce approximately 10,000 watts of deliverable power at the interface at the beginning-of-life and will be lightly shielded, front and back, to provide protection against low energy proton damage. For the manned space station mission, the use of 2 ohm-cm cells on the same basic solar array configuration will provide increased power generation capability to counter balance the increased operating temperature.

Table 20. Solar Cell Blanket Weight Required for 20 Percent Maximum Degradation for Each Mission Type

Nominal Cell Thickness (μm)	Base Resistivity (ohm-cm)	Blanket Weight (kg)		
		Interplanetary	Geosynchronous	Manned Space Station
100	2	63.6	81.5	40.8
	10	57.9	69.4	48.2
125	2	71.7	90.6	43.5
	10	66.6	81.1	50.2

The parametric analysis of the bus strip distribution network (see Section 2.6) revealed the importance of voltage in determining the weight associated with this portion of the system. It is advantageous to select a circuit voltage which is as high as practical. A circuit voltage of less than 100 volts is obviously impractical if the goal is to design a solar array to meet a 110 watt/kg power-to-weight ratio goal. In general, the solar array voltage is predetermined by the power subsystem interface requirements and is beyond the control of the solar array designer. Present day limits on power transistor reverse breakdown voltage would restrict the solar array operating voltage to about 200 volts.

During the course of this study, the solar array operating voltage will be treated as a variable with a range from 100 to 400 volts.

SECTION 4

RECOMMENDATIONS

No specific recommendations are made at this early point in the study.

SECTION 5

NEW TECHNOLOGY

No items of new technology have been reported during this period.

SECTION 6

REFERENCES

1. Weidner, D. K., "Natural Environment Criteria for the NASA Space Station Program (Second Edition)," NASA TMX-53865, August 20, 1970.

2. Vette, J. I., et. al., "Models of the Trapped Radiation Environment, Volume III: Electrons at Synchronous Altitudes," NASA SP-3024.

3. "ATS Power Subsystem Radiation Effects Study, Phase I/Final Report," HAC Report No. SSD80089R, February 1968.

4. "Second Topical Report - Design and Analysis - Space Station Solar Array Technology Evaluation Program," LMSC Report No. A995719, November 1971.

5. "Space Station - A Guide for Experimenters," North American Rockwell - Space Division Document No. SD70-534, October 1970.

6. King, J. H., "Models of the Trapped Radiation Environment, Volume IV: Low Energy Protons," NASA SP-3024.

7. Lavine and Vette, "Models of the Trapped Radiation Environment, Volume V: Inner Belt Protons," NASA SP-3024.

8. Lavine and Vette, "Models of the Trapped Radiation Environment, Volume VI: High Energy Protons," NASA SP-3024.

9. Vette, Lucero, and Wright, "Models of the Trapped Radiation Environment, Volume II: Inner and Outer Zone Electrons," NASA SP-3024.

10. Andrews, J., "Space Radiation Estimates: NASA Space Base," GE Internal Document No. PIR-SB-8014, October 19, 1970.

11. "Final Report - Roll-up Subsolar Array, Volume I - Program Summary," GE-SSO Report No. 70SD4286, February 1971.

12. Wolff, G., "Oriented Flexible Rolled-up Solar Array," AIAA Paper No. 70-738 presented at the 3rd Communication Satellite Systems Conference, April 1970.

13. Wolff, G., "The Flexible Roll-up Solar Array Flight Experiment," paper presented at the 9th Photovoltaic Specialists Conference, May 1972.

14. Treble, F. C., "Status Report on RAE Advanced Solar Array Development," paper presented at the 9th Photovoltaics Specialists Conference, May 1972.

15. Treble, F. C., "Progress in Advanced Solar Array Development," paper presented at the 8th Photovoltaics Specialists Conference, August 1970.

16. Franklin, C. A. and Davison, E. H., "A High-Power Communications Technology Satellite for the 12 and 14 GHz Bands," AIAA Paper No. 72-580 presented at the 4th Communications Satellite Systems Conference, April 1972.

17. "Final Report - Phase II, Large Area Solar Array," Boeing Report No. D2-113355-7, October 1968.

18. Carlson, J. A., "Development of Lightweight Solar Panels," NASA CR-66832.

19. Private communication with R. Lohnes, SPAR Aerospace Products, Ltd., July 18, 1972.

20. Scheel, H. W., "Low Cost Solar Electric Testbed for Ion Thruster Systems," AIAA Paper No. 72-466 presented at the 9th Electric Propulsion Conference, Bethesda, Maryland, April 1972.

21. Woodall, J. M. and Hovel, H. J., "High Efficiency Ga_{1-X} Al_XAs-Ga As Solar Cells."

22. Ralph, E. L., et al., "Development of an Integrated Lightweight Flexible Silicon Solar Cell Array," Final Report under JPL Contract 952560.

23. Webb, H., "The Design and Practical Aspects of Maximum Efficiency Silicon Solar Cells for Satellite Applications," paper presented at the 9th Photovoltaic Specialists Conference, May 1972.

24. Crabb, R. L., And Atzec, A., "Environmental Study of European Silicon Solar Cells with Improved Antireflection Coatings," paper presented at the 8th Photovoltaic Specialists Conference, August 1970.

25. Ferranti Catalog entitled, "Satellite Power Sources - Silicon Solar Cells," ESB 581271, December 1971.

26. Private communication with Ira S. Gewant, Ferranti Electric, Inc., June 6, 1972.

27. Ralph, E. L., "Performance of Very Thin Silicon Solar Cells," paper presented at the 6th Photovoltaic Specialists Conference, March 1967.

28. Brackley, G., "Integral Covers for Silicon Solar Cells," paper presented at the 9th Photovoltaic Specialists Conference, May 1972.

29. Stella, P., and Somberg, H., "Integrally Covered Silicon Solar Cells," paper presented at the 9th Photovoltaic Specialists Conference, May 1972.

30. Kirkpatrick, A. R., et al., "Low Stress Integral Cover Slips," paper presented at the 8th Photovoltaic Specialists Conference, August 1970.

31. Fairbanks, J. W., "Evaluation of Integral Covers on Silicon Solar Cells," paper presented at the 1969 Intersociety Energy Conversion Engineering Conference.

32. Kirkpatrick, A. R., et al., "Solar Cell Cover Glass Development," Final Report on Contract NAS 5-10236, March 1971.

33. Ralph, E. L., Somberg, H., and Payne, P., "Manufacturing Methods for Protecting Silicon Solar Cells with Integral Coverslips," Interim Technical Report 504-0(3), Heliotek, Division of Textron, Inc., March 1971.

34. Stress Free Solar Cell Cover Research," Quarterly Status Report No. 3, Contract No. F33615-71-C-1656, January 1972.

35. Broder, J. D., et al., "Recent Results of FEP Solar Cell Cover Development," paper presented at the 9th Photovoltaic Specialists Conference, May 1972.

36. Forestieri, A. F., and Broder, J. D., "Improvements in Silicon Solar Cell Cover Glass Assembly and Packaging using FEP Teflon," paper presented at the 8th Photovoltaic Specialists Conference, August 1970, also released as NASA TM X-52875.

37. Forestieri, A. F., et al., "FEP Covers for Silicon Solar Cells," paper presented at the 1971 Intersociety Energy Conversion Engineering Conference.

38. Greenberg, S. A., McCargo, M., and Palmer, W. L., "Investigation of FEP Teflon as a Cover for Silicon Solar Cells," NASA CR-72970, August 1971.

39. "Final Review - Space Station Solar Array Technology Program," March 30, 1972.

40. "First Topical Report - Evaluation of Space Station Solar Array Technology and Recommended Advanced Development Programs," LMSC Report No. A981486, December 1970.

41. Crawford, R. F., "Strength and Efficiency of Deployable Booms for Space Applications," AIAA Paper No. 71-396.

42. Rasmussen, R., "Calculation of 1 MeV Electron Flux and Irradiation Degradation of Solar Cell I-V Curves by Computer," paper presented at the 6th Photovoltaic Specialists Conference, 1967.

43. Roger, J., "Optimal Bus Bars for Rectangular Solar Arrays," paper presented at the 9th Photovoltaic Specialists Conference, May 1972.

44. "Final Report - Feasibility Study, 30 Watts Per Pound Roll-up Solar Array," NASA-CR-96230, 21 June 1968.

45. "Solar Electric Multimission Spacecraft (SEMMS), Phase A Final Report, Technical Summary," Report No. 617-2, 30 July 1971, Jet Propulsion Laboratory, Pasadena, California.

46. Shepard, N. F., Jr., Ferguson, R. C., Jr., Roach, R. E., Jr., Matteo, D. N., "Final Summary Report - Solar Array," Report EL-405, March 16, 1970. General Electric Company, Philadelphia, Pa.

47. Private communication with Canadian Department of Communications Personnel.

48. "NASA Space Vehicle Design Criteria (Guidance and Control) Effects of Structural Control Systems," NASA SP-8016, April 1969.

49. Coyner, J. V., Jr. and Ross, R. G., Jr., "Parametric Study of the Performance Characteristics and Weight Variations of Large Area Roll-up Solar Arrays," JPL Technical Report 32-1502, December 15, 1970.

50. Martin, J. H., Statler, R. L., and Ralph, E. L., "Radiation Damage to Thin Silicon Solar Cells," paper presented at the 1967 IECEC.

APPENDIX A

JPL SPECIFICATION ES506080B

LIGHTWEIGHT SOLAR PANEL SUBSYSTEM, 110 WATTS PER KILOGRAM, DETAIL SPECIFICATION FOR

6-5

EQUIPMENT SPECIFICATION

CODE IDENT NO. 23835

SPEC NO. ES506080 REV. B

ISSUE DATE 17 September 1971

SUPERSEDING ES506080 A

DATED 4 August 1971

LIGHTWEIGHT SOLAR PANEL SUBSYSTEM
110 WATTS PER KILOGRAM
DETAIL SPECIFICATION FOR

Walter A. Hasbach 14 Sept 71
ENGINEER W. A. Hasbach DATE
Section 342 Cognizant Engineer

John V. Goldsmith 14 Sept 71
APPROVED BY J. V. Goldsmith DATE
Section 342 Group Supervisor

WRITTEN and G Inouye 9/17/71
RELEASED BY G. Inouye DATE
Section 356 Design Section
Group Supervisor

Richard G Rose 16 Sept 71
APPROVED BY Dr. R. G. Rose DATE
Section 358 Structures and Dynamics

JET PROPULSION LABORATORY
CALIFORNIA INSTITUTE OF TECHNOLOGY
PASADENA, CALIFORNIA

CHANGE INCORPORATION LOG

CHG LTR	WRITER		AUTHORITY	PAGES AFFECTED	DATE	ENG APPROVAL	
	INITIAL	SECTION				INITIAL	SECTION
A	GI	356			8/4/71	WAH	342
B	GI	356				WAH	342

1. SCOPE

1.1 This specification covers the requirements for the design of a 10 kilowatt solar panel having a power-to-weight ratio greater than 110 watts per kilogram.

2. APPLICABLE DOCUMENT

2.1 The following document of the issue shown forms a part of this specification to the extent specified herein:

STANDARD

Military

MIL-HDBK 5	Metallic Materials and Elements for Flight Vehicle Structures

3. REQUIREMENTS

3.1 Conflicting requirements. In case of conflict between the requirements of this specification and the documents referenced herein, the requirements of this specification shall govern.

3.1.1 Deviations from standard practices. Any deviations from generally accepted standard practices will be approved by the Jet Propulsion Laboratory (JPL), after it has been demonstrated by analysis or test that the deviations will not degrade the overall probability of attaining the objectives of this effort. The burden of proof in such circumstances shall rest upon the contractor and not upon JPL.

3.2 Performance requirements. The solar panel shall be designed so that the following performance requirements can be met.

3.2.1 General. In the stowed configuration, the solar panel shall be supported in a manner that will prevent damage to the solar panel under shock

and vibration loads. Upon command and in proper sequence, the release and deployment mechanism shall extend and lock the solar panel into the deployed position at a rate to be defined by the contractor.

3.2.2 Power requirement. Following launch, the deployed solar panel shall be capable of supplying 10 kilowatts of electrical power at the spacecraft interface at a solar intensity of 140 mw/cm^2 and at the predicted solar array temperature at this intensity.

3.2.3 Lifetime. The solar panel shall be designed to perform over a period of 3 years with no greater than a 20 percent loss of power and with no failures which would prevent the panel from performing successfully in both mechanical and electrical modes.

3.2.4 Solar panel operating temperature. The thermal characteristics of the deployed panel shall be adjusted so that the celled area maintains an operating temperature between 50 and 70 °C at a solar intensity of 140 mw/cm^2.

3.2.5 Solar panel weight. The weight of the solar panel, including the release and deployment mechanisms but not including the solar panel gimbaling mechanisms, shall be so that the solar panel specific power exceeds 110 watts per kilogram at a solar intensity of 140 mw/cm^2.

3.2.6 Packaging volume envelope. The volume and shape of the stowed solar panel, including the release and deployment mechanisms, shall be determined by the contractor in order to maximize the solar panels adaptability to various spacecraft configurations. In these design considerations, a 2000-pound spacecraft containing two 10-kilowatt solar panels and a Titan-Centaur launch vehicle shall be assumed. The following requirements shall also be included:

a. Launch vehicle shroud volume restrictions.
b. Spacecraft structural interface requirements.
c. Solar panel deployment complexity (reliability).
d. Solar panel gimbaling (Sun tracking) requirements.

3.2.7 Structural interfaces. The solar panel to spacecraft attachment points shall be considered to provide the most efficient interface capable of performing the mission. Consideration shall be given to the ease with which the deployed solar panel can be gimbaled (tilted or rotated) with respect to the spacecraft as required by the Sun tracking requirements. Consideration shall also be given to the requirements imposed on the spacecraft structure by the solar panel. A solar panel, requiring an extremely rigid support or negligible relative motion between widely spaced support points, would be undesirable because meeting these requirements would result in increased spacecraft weight.

3.2.8 Structural rigidity. In the deployed configuration, the solar panel shall have sufficient rigidity so that its lowest natural frequency of vibration is equal to or greater than 0.04 Hz.

3.2.9 Mass center location. The solar panel shall be designed to minimize displacement of the vehicle mass center and center of solar pressure caused by thermal gradients and solar panel temperatures.

3.2.10 Flatness. In the deployed configuration, the solar panel celled area shall lie in a predetermined plane with a maximum angular deviation of ±10 degrees between any portion of the celled area and the plane. This tolerance shall include deflections from the thermal gradients arising from the operation at any heliocentric distance from 0.5 to 5.0 AU, but shall not include deflections due to dyanmic load inputs.

3.2.11 Inspection. Release, deployment, and locking mechanisms, not necessarily the assembled solar panel, shall be designed so that, with suitable equipment, their operating functions can be inspected in a one-g Earth field environment.

3.2.12 Reliability. The solar panel design shall incorporate design practices that maximize the probability that the solar panel will operate successfully in both mechanical and electrical modes.

3.3 Environmental requirements. The following environmental requirements shall be considered in the design of the solar panel.

3.3.1 Ground handling. The solar panel's structural, mechanical, and electrical performance shall not be degraded because of ground handling during manufacturing, testing, and transportation operations.

3.3.2 Launch environment. The following environmental constraints, representing the launch environment of the solar panel in the stowed configuration, shall be considered in the solar panel design.

3.3.2.1 Sinusoidal vibration. The sinusoidal vibration input levels at frequencies between 5 and 2000 Hz shall be as specified on Figure 1. These levels are specified at the interface between the solar panel assembly and the spacecraft in each of three axes. For configurations with widely spaced support points, these input levels shall be simultaneously applied at each support point, but the worst case phase relationship shall be assumed for motion perpendicular to the line joining the supports.

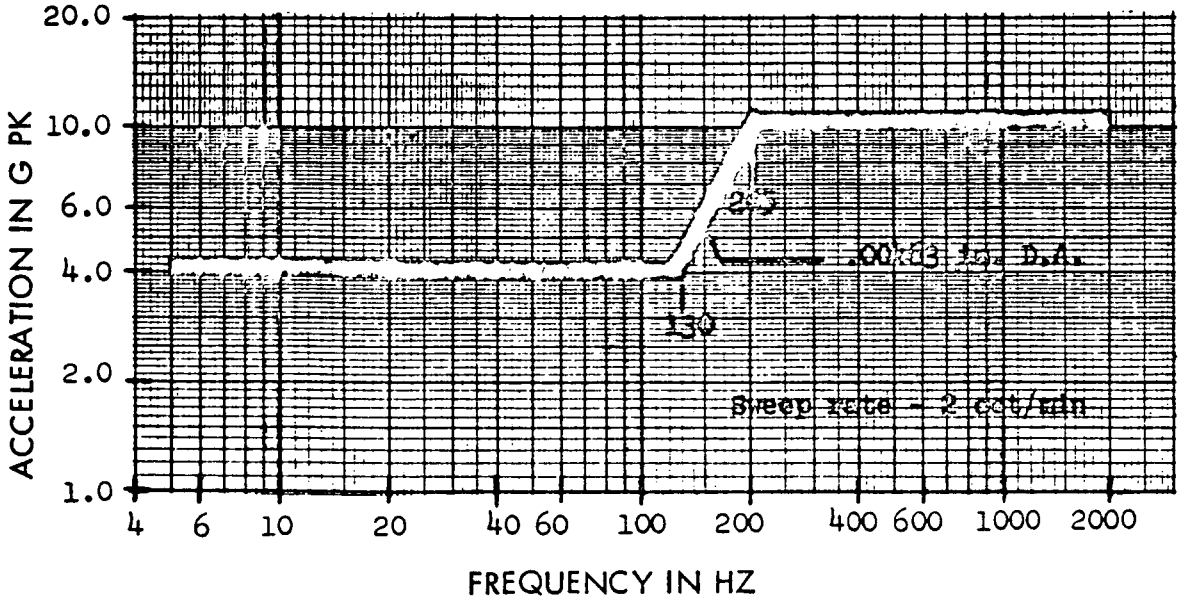

Figure 1. Sinusoidal Vibration Test Requirements

3.3.2.2 Acoustic. The launch acoustics environment shall be 60 seconds of random incidence, reverberant sound field, having the third-octave band sound pressure levels defined in Table I. The overall sound pressure level for the spectrum given in Table I shall be approximately 150 db reference to 0.0002 dyne/cm^2; however, the spectral levels within each one-third octave band defines the basic requirements.

Table I. Acoustic Test Levels

1/3 Octave Band Center Frequency (Hz)	Sound Pressure Level in 1/3 Octave Bands (db ref 2 x 10^{-4} dynes/cm^2)
80	132.5
100	136.0
125	138.0
160	140.0
200	142.0
250	142.5
315	143.0
400	142.5
500	141.5
630	140.0
800	138.0
1000	136.0
1250	135.0
1600	133.0
2000	132.0
2500	130.0
3150	128.5
4000	127.0
5000	125.5
6300	124.0
8000	122.5
10,000	120.0

3.3.2.3 Shock. The mechanical shock environment shall be the shock pulse shown on Figure 2 and shall be applicable to each of the three mutually perpendicular axes defined in 3.3.2.1.

3.3.2.4 Static acceleration. The static acceleration environments shall be 9 g's at the approximate center of mass of the solar panel in the stowed configuration. This environment shall be considered equal for each of three mutually perpendicular axes.

3.3.2.5 Launch pressure profile. The solar panel temperature shall be initially at 27 ±6 °C and at atmospheric pressure. The pressure shall be continuously reduced, and the rate of change of pressure shall obtain a maximum of 116 ±8 torr/second, beginning from a rate of less than 16 torr/second and returning to a rate of less than 16 torr/second in a period of less than 10 seconds, and a minimum pressure level of 20 percent of the atmospheric pressure in less than 65 seconds.

3.3.2.6 Aerodynamic heating. The aerodynamic heating rate of the solar panel's external surface during boost in the stowed configuration shall be considered as +30 °C/minute for a period of 200 seconds. Initial temperature shall be taken to be 27 ±6 °C.

3.3.3 Space flight environment. The following space flight environmental constraints shall be considered in the solar panel design. These environments are applicable for both the stowed and the deployed configurations.

3.3.3.1 Steady state thermal/vacuum environment. The steady state thermal vacuum environment shall cover the range from -130 to +140 °C and a pressure of 10^{-5} torr or less.

3.3.3.2 Thermal shock environment. The thermal shock temperature extremes shall be considered to be -190 and +140 °C and a pressure of 10^{-5} torr or less. The temperature time rates of change during thermal shock shall be at the natural cooling rate of the solar panel in a simulated passage through planetary shadow, and the natural heating rate of the solar panel in a normal solar

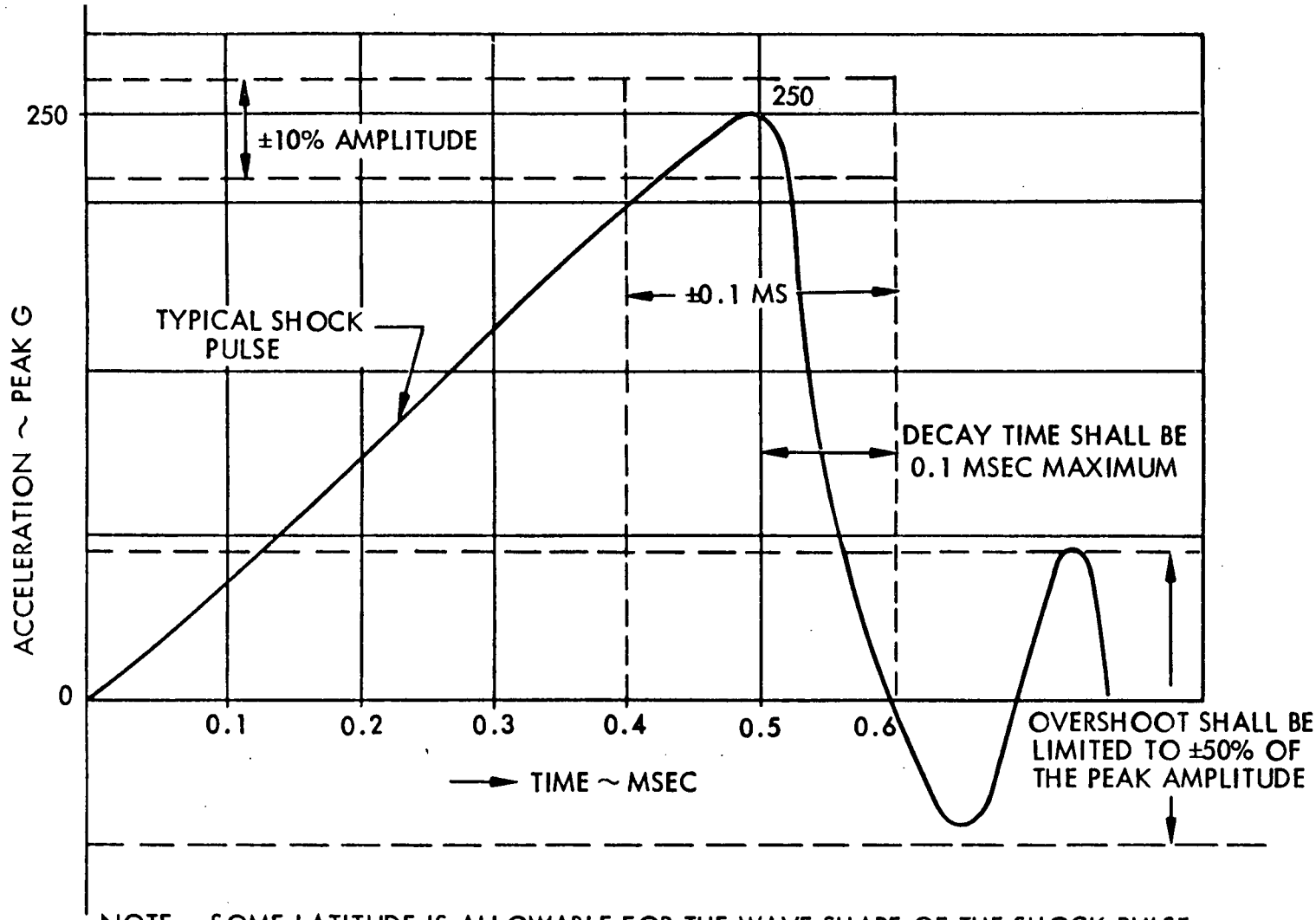

NOTE: SOME LATITUDE IS ALLOWABLE FOR THE WAVE SHAPE OF THE SHOCK PULSE. HOWEVER, IT IS DESIRABLE THAT THE SHAPE CONFORM TO THAT OF A TERMINAL PEAK SAWTOOTH AS NEAR AS PRACTICAL.

Figure 2. Shock Pulse

flux of intensity corresponding to a steady state temperature of 140 °C on the solar panel. The total thermal shock environment shall consist of 1000 complete cooling and heating cycles.

3.3.3.3 Solar flare proton radiation environment. The proton fluency for the 3 year mission shall be defined in Table II.

Table II. Mission Proton Fluency

Proton Energy (Mev)	Total Fluency (Particles/cm^2)
1	2.0×10^{12}
10	4.0×10^{10}
30	9.0×10^{9}
100	1.0×10^{9}

3.3.3.4 Pyrotechnic shock environment. The solar panel assembly shall be capable of withstanding shock environments induced by the firing of any pyrotechnics of the assembly that may be required for the operation of the assembly.

3.4 Materials, parts, and processes. Materials, parts and processes used in the design of the solar panel shall conform to the requirements specified herein. Any materials, parts, and processes that are not so covered shall be subject to the approval of the JPL cognizant engineer. In every case, the contractor's selection shall assure the highest uniform quality of the solar panel.

3.4.1 Material selection criteria. The influence of the following environments and those specified in 3.3 on the design properties of the structural, electrical, thermal control, and lubricant materials in the solar panel shall be considered:

a. Storage at 95 percent relative humidity at 55 °C for 50 hours.
b. 150 thermal cycles between -120 and +60 °C at 10^{-7} torr with a rate of change that permits temperature stabilization dwell at the extreme temperatures.
c. 10,000 thermal cycles between -195 and +140 °C at 10^{-7} torr with a 90 minute cycle, and a temperature stabilization (< 2 °C/hr) dwell at the extreme temperature.
d. 1000 thermal shocks of less than 30 °C/minute.

3.4.1.1 Flight environment materials. The materials shall be capable of enduring all space environments without releasing any significant condensing gases which would decrease the solar cell efficiency, or could potentially lead to electrical shorts or degradation to the spacecraft systems operation.

3.4.2 Radiation resistance. The dosage and energy levels of the particulate radiation encountered during a mission shall not produce a significant effect on the metallic structural elements. Polymeric materials shall be either shielded or selected to resist a radiation dosage of 10^7 rads without decreasing the critical design properties below the design allowables.

3.4.3 Exposed structural adhesives. When used to bond transparent or partially transparent structural components, the influence of particulate radiation of 10^7 rads, and ultraviolet radiation equal to 3650 days of solar radiation at the rate of 2.002 calories/cm^2/minute, on the adhesive shall be considered.

3.4.4 Solar cell adhesives. A requirement for two separate adhesives can exist in the solar cell area. One requirement shall be for an adhesive used to attach the solar cells to the structure; and the second shall be to bond the solar cell cover glasses to the cells. The adhesive for bonding the cover glasses

to the solar cells shall be transparent to electromagnetic radiation in the wavelengths from 0.4 to 1.0 micron, and shall be resistant to ultraviolet and particulate radiation. The adhesives shall have the following properties:

a. High thermal conductivity.
b. Low outgassing in the vacuum environment.
c. A modulus of elasticity compatible with the thermal motion of the cells and structure.
d. Repairability during the fabrication phase.

3.4.5 Thermal control coatings. Degradation of the coatings by the ultraviolet and particulate radiation of the flight environment shall be considered.

3.4.6 Bearings and lubricants. In the event bearings and lubricants are required in the solar panel design, the bearing materials shall resist the thermal excursions and particulate radiation of the flight environment. Lubricants shall not degrade: i.e., lose lubricity under flight conditions up to 3650 days, or release any condensing gases, which may potentially cause degradation to the spacecraft system. Possible occurrence of cold welding at hard vacuum shall be evaluated.

3.4.7 Part producibility. Configuration and size of parts shall be compatible with normal tooling practices. Very thin foil gage parts shall be capable of being fabricated with reasonable assurance that damage will not occur; and that the part can be handled without damage when reasonable precautions are taken.

3.4.8 Solar cell adhesive thickness tolerance. Solar panel and solar cell installation normally shall require the extensive use of bonding materials. The thickness and area of application of these materials, if used, shall be accurately controlled. The designs and processes shall include control requirements and tolerances that can be maintained in the fabrication shops.

3.4.9 Solar cell tolerances. The control of solar cell processing through the fabrication shops shall be dependent upon the comparison of initial testing and grading to subsequent cell testing during the fabrication sequence. The tolerances set by the design shall be adequate to allow a high yield of good assemblies.

3.4.10 Solar cell connections. The heat required in joining solar cells by soldering can cause degradation in cell performance. The solar cell electrical connecting technique shall be comparable with solar cell interconnection methods and shall exhibit accurate temperature control for minimum power loss.

3.4.11 Solar cell installation. The installation of solar cell assemblies on to substrate panels, and the assembly of structural components parts shall be accomplished with protective coverings on the operator's hands; or the handling shall be done with suitable mechanical devices. The configuration of these assemblies shall be designed so that the required work can be accomplished while complying with all handling restrictions.

3.4.12 Configuration of the solar panel. The configuration of the solar panel shall be designed so that positioning and holding of components and subassemblies can be accomplished to provide support during solar panel assembly.

3.4.13 Repair and replacement. Fabrication personnel shall be able to repair or replace any components of the solar panel at any time during the fabrication or ground handling sequence. The extent of repairability shall be determined by the ease of access to the damaged part without damage to adjacent parts when the repair is made.

3.5 Mechanical design criteria. The following criteria shall govern the mechanical design of the solar panel.

3.5.1 Strength and deflection requirements. All structures, with minimum material and geometric properties, shall have adequate strength and

rigidity to accomplish all requirements. In the fulfillment of the strength and deflection requirements, the worst possible combination of simultaneously applied loads and environmental conditions shall be used to determine limit loads and design loads. Particular attention shall be given to the following.

3.5.1.1 Dynamic loads. During the loads analysis, consideration shall be given to loads induced by the solar panel's elastic and rigid-body response to dynamic excitation.

3.5.1.2 Quasi-static loads. All quasi-static loads shall be considered, including launch vehicle thrust and flight maneuver loads.

3.5.1.3 Fatigue considerations. Fatigue shall be considered in the design of structural elements by the avoidance of deleterious residual stresses and stress concentrations in conformity with good design practice. Special attention shall be given to elements subjected to repeated load cycles at high stress levels. Material selection shall consider fatigue characteristics in relation to the design requirements of the structural element.

3.5.1.4 Thermal considerations. Consideration shall be given to deterioration of material properties and to stresses and deformation caused by temperature effects, both prolonged and transient.

3.5.2 Limit load. The limit load shall be considered the maximum load a structural element is expected to experience during its required functional lifetime, including fabrication, handling, and ground testing. No structural element with minimum material and geometric properties shall yield at limit loads or impair the required functions of the solar panel.

3.5.3 Design load. The design load shall be considered the limit load multiplied by the safety factor. No structural element with minimum material and geometric properties shall exceed the ultimate stress, failure by instability, or rupture at design load.

3.5.4 Material properties. The allowable material properties shall be selected to satisfy the environmental conditions that affect material properties. Metallic materials shall be in accordance with MIL-HDBK 5.

3.5.5 Safety factors. The following safety factors shall be used:

a. Structures: 1.25.
b. Structural joints, fittings, and brittle material: 1.44.

3.5.6 Structural qualification test levels. The environmental levels defined in 3.3 shall be considered as the qualification test levels.

3.5.7 Structural design. Simplicity of the analyses and tests shall be considered in the structural design. All structural components shall be amenable to either analytical or experimental demonstration of adequacy.

3.5.8 Structural nonlinearities. Nonlinear structural characteristics shall be kept to a minimum; however, two types of nonlinearities that are of prime importance are as follows and should be given consideration:

a. Nonlinearities in energy dissipation mechanisms.
b. Mechanical backlash.

3.5.8.1 Energy dissipating mechanisms. Where possible, all energy dissipating mechanisms used shall have linear force-velocity relationships over a wide range of frequencies, loads, and temperatures.

3.5.8.2 Mechanical backlash. Particular effort shall be made to avoid any mechanical backlash in all structural connections.

3.5.9 Separation joint preload. Attachment of any component to another shall provide for sufficient axial preload so that no physical separation will occur during any ultimate load conditions.

3.5.10 Design flexibility. The solar panel shall be designed so that additional data and advances of technology may be incorporated at later dates.

3.5.11 Thermal gradients. The solar panel shall be designed to minimize thermal gradients in the plane of the solar panel.

3.5.12 Mechanical integrity. The solar panel shall be designed to prevent the release of loose parts or gases that could damage or impair the function of the solar panel or other spacecraft subsystems.

3.5.13 Margins of safety. Margins of safety are defined with respect to the limit load or the design load as:

$$MS = \frac{* \quad (\quad ** \quad)}{\text{limit load (design load)}} - 1$$

*Load corresponding to yield stress of a structure with minimum geometric and material properties with consideration of environmental effects on material properties.

**Load corresponding to ultimate stress, instability, or rupture of a structure with minimum geometric and material properties with consideration of environmental effects on material properties.

3.6 Electrical design criteria. The following criteria shall govern the electrical design of the solar panel.

3.6.1 Solar cell efficiency. The contractor shall establish the power output based on the photovoltaic characteristics of the proposed solar cell and the predicted operating temperature of the solar panel. This design effort shall include the power losses incurred during fabrication, assembly, cabling, and solar panel/spacecraft interfacing considerations.

3.6.2 Electrical insulation. The electrical insulation between the solar cells and the solar panel structure shall provide a maximum dielectric breakdown strength in air, at standard temperatures and pressure conditions,

greater than three times the open circuit voltage of the solar panel. Leakage resistance under the test conditions shall be greater than 10^9 ohms per square centimeter of cell area.

3.6.3 Repairability. The solar cell modules shall be constructed, and materials shall be selected so that any defective cell can be replaced in a fabrication repair area without damage to adjacent cells, electrical insulation, or mounting substrate.

3.6.4 Compatibility of materials. The solar cell stack shall be designed to use only materials that are compatible thermally, mechanically, and electrically with each other, with the space environment, and interface requirements of the solar cells substrate.

3.6.5 Interconnections. The solar cells shall be interconnected both in parallel and in series by a metallic conductor. This conductor shall be designed to minimize both thermal and flexural stresses on the solar cell interconnection. The resistance of the interconnection, plus solder, shall not exceed 2 percent of the total series resistance of the solar cells. The joint shall have a strength equal to, or greater than the strength of the bond between the semiconductor material and the ohmic contacts. The joining materials shall exhibit stable physical and electrical characteristics in both space and terrestrial environments.

3.6.6 Magnetic field. Solar cell wiring, interconnecting and structural techniques shall be designed to minimize the magnetic field produced by the flow of current in the solar panel.

3.6.7 Electrical conductors. The size and configuration of electrical conductors shall be determined by the following considerations:

a. Minimum possible weight.
b. Minimum resistivity.
c. Minimum magnetic field.
d. Mechanical strength to endure design loads.

e. Exterior finish to be resistant to natural and induced environments.
f. Process adaptability.
g. Redundancy.
h. Thermal coefficient of expansion.
i. Thermal shock (minimum of 30 °C/minute) on the cells.
j. Repairability.
k. Conductor flexibility.

3.6.8 Conductor insulation. Conductor insulating materials shall be selected on the basis of the following considerations:

a. Mechanical strength.
b. Flexibility.
c. Dielectric characteristics.
d. Ease of forming or fabricating.
e. Flight environment considerations.
f. Minimum weight.

3.6.9 Electrical terminals. Terminals shall be used to facilitate maintenance, repair, and replacement of electrical components. The following requirements for terminals shall be met:

a. Voltage drop across any terminal shall not exceed 25 millivolts at rated load.
b. The terminals shall withstand 50 cycles of manual mating and unmating without replacement of parts.
c. The terminals shall be accessible for ease of wiring installation and for factory or field checkout.
d. Ther terminals shall be rigidly attached to primary or secondary structure.
e. The terminals shall have minimum possible weight.
f. Exterior finish of the terminals shall be resistant to both natural and induced environments.

3.6.10 Installation. The installation of wires, terminals, electrical connectors, and busses shall conform to the following requirements:

a. Busses and other wiring shall be installed in order to minimize magnetic fields.
b. Installation shall withstand the rigors of normal handling and transportation as well as launch and operational maneuvers.
c. Installation shall be designed to facilitate service and repair activities.

3.6.11 Electrical checkout. Test terminals shall be provided on the solar panel to permit ground testing and checkout prior to launch, in a one-g Earth field, with suitable ground support equipment (GSE).

3.7 Workmanship. Workmanship of the solar panel model shall be of such quality that the model shall be free from any defects that would affect its performance or appearance.

4. QUALITY ASSURANCE PROVISIONS

4.1 Contractor inspection. The contractor shall perform all necessary Quality Assurance control and inspection to assure that compliance with the requirements of this specification have been fulfilled.

4.2 Rejection and resubmittal. Units that do not meet all the test requirements of this specification shall be rejected. Before resubmittal, complete particulars concerning the previous rejection and the action taken to correct the defects shall be furnished.

5. PREPARATION FOR DELIVERY

5.1 Packaging, packing and shipping. The point of inspection, acceptance, and the delivery of all deliverable supplies specified herein shall be made at Jet Propulsion Laboratory, 4800 Oak Grove Drive, Pasadena, California. All deliverable supplies shall be packaged, packed, boxed, or crated in a manner that will assure safe delivery and shall be shipped prepaid to JPL.

6. NOTES

None.

APPENDIX B

SOLAR CELL RADIATION DAMAGE

VS

1-MeV ELECTRON FLUENCE

SOLAR CELL RADIATION DAMAGE
VS
1-MeV ELECTRON FLUENCE

The following figures show the degradation in solar cell short-circuit current, open-circuit voltage, and maximum power as a function of 1-MeV electron fluence. Two nominal solar cell base resistivities are shown: Figures B-1, B-2 and B-3 for 2 ohm-cm and Figures B-4, B-5 and B-6 for 10 ohm-cm.

Cell thicknesses from 300 to 86 μm are shown for the 2 ohm-cm resistivity, while thicknesses from 305 to 94 μm are shown for the 10 ohm-cm resistivity. All these curves are based on data obtained from Reference 50.

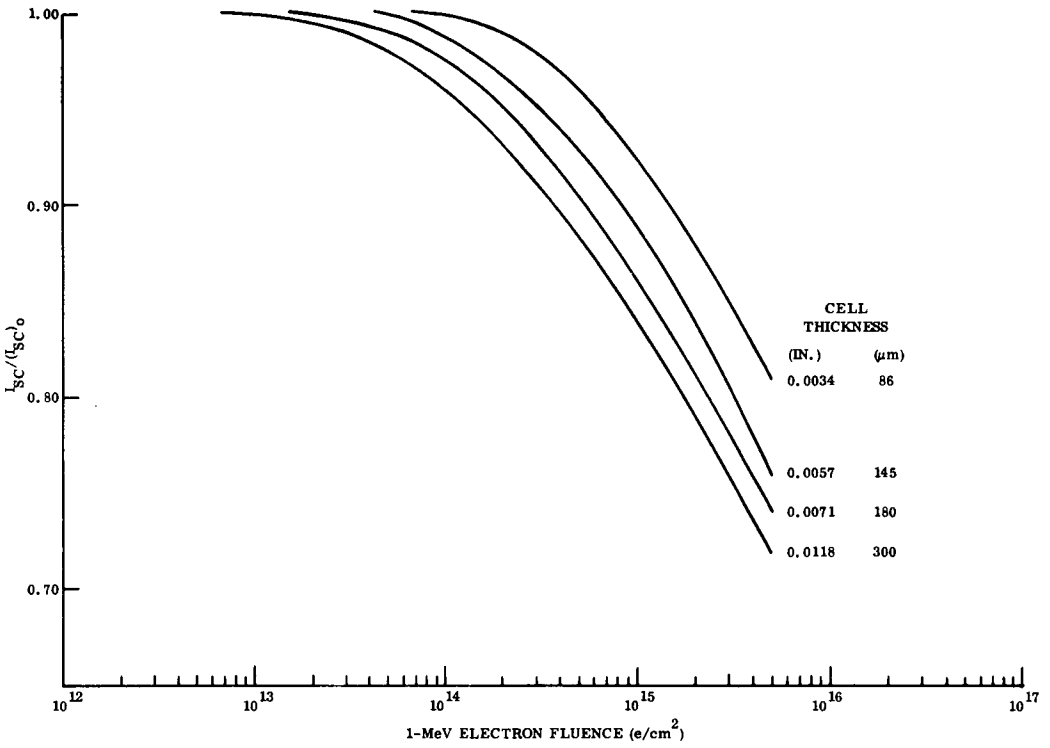

Figure B-1. Short-Circuit Current Degradation for 2 ohm-cm N/P Silicon Solar Cells (from Reference 50)

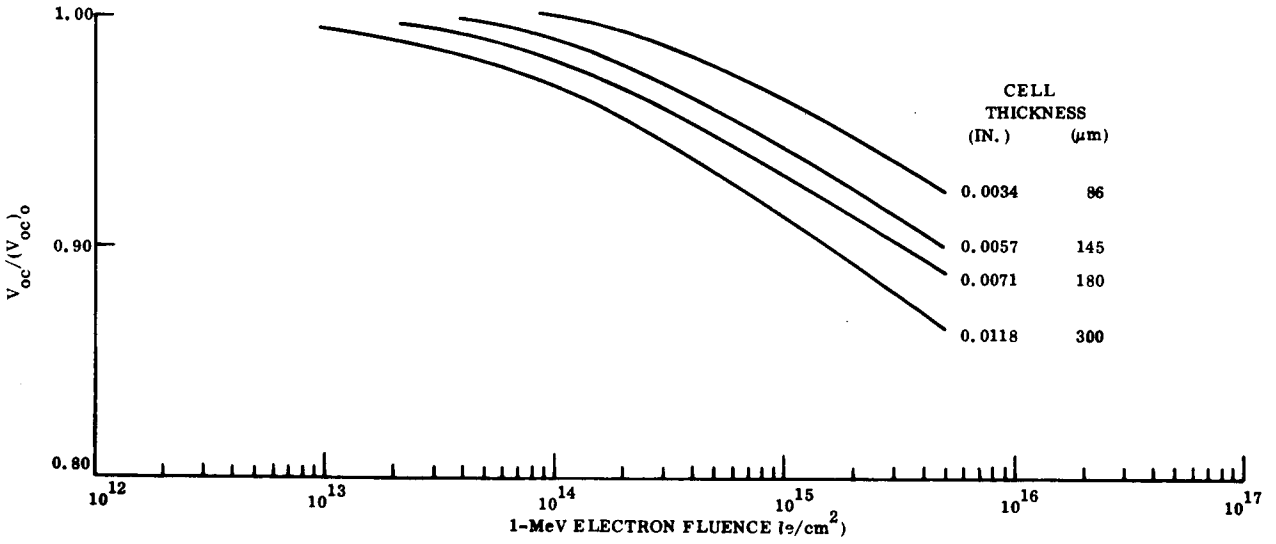

Figure B-2. Open-Circuit Voltage Degradation for 2 ohm-cm N/P Silicon Solar Cells (from Reference 50)

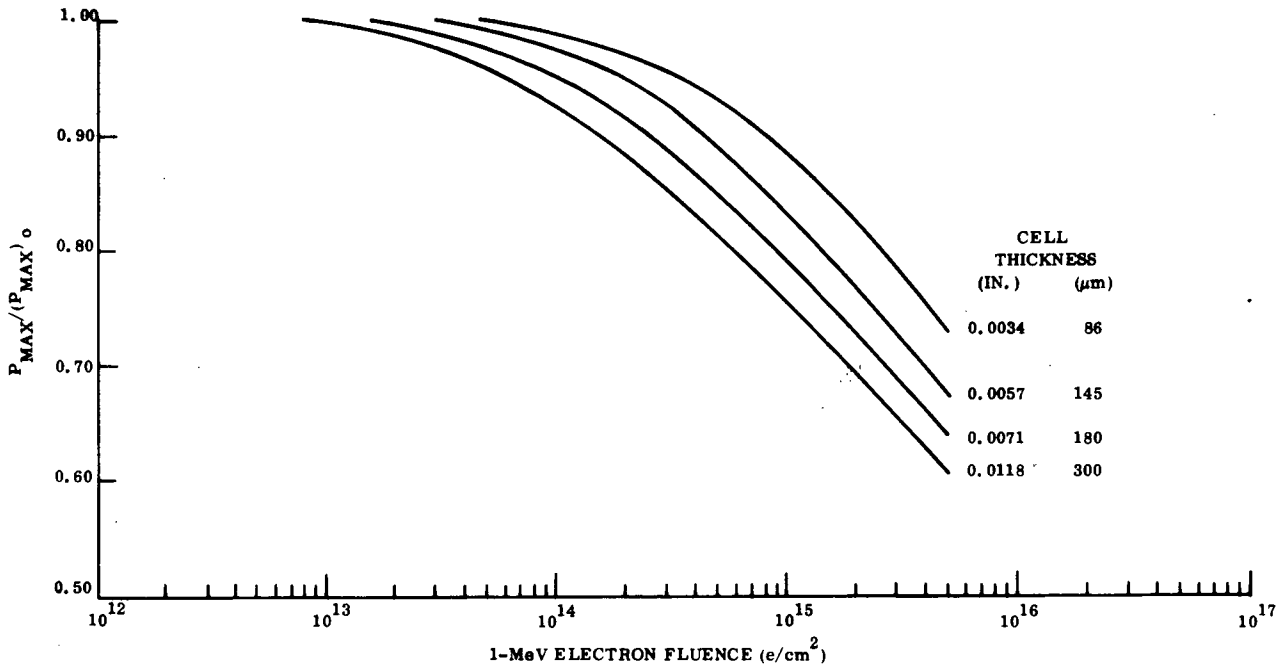

Figure B-3. Maximum Power Degradation for 2 ohm-cm N/P Silicon Solar Cells (from Reference 50)

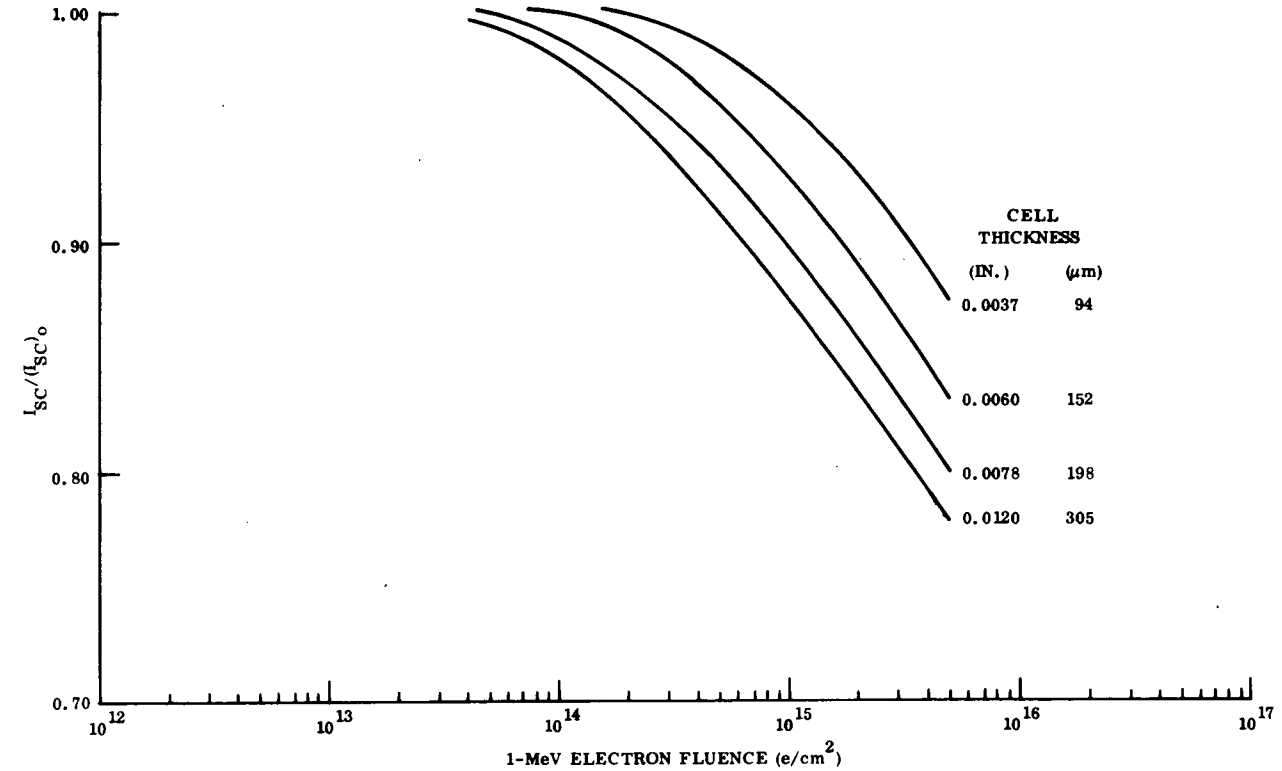

Figure B-4. Short-Circuit Current Degradation for 10 ohm-cm N/P Silicon Solar Cells (from Reference 50)

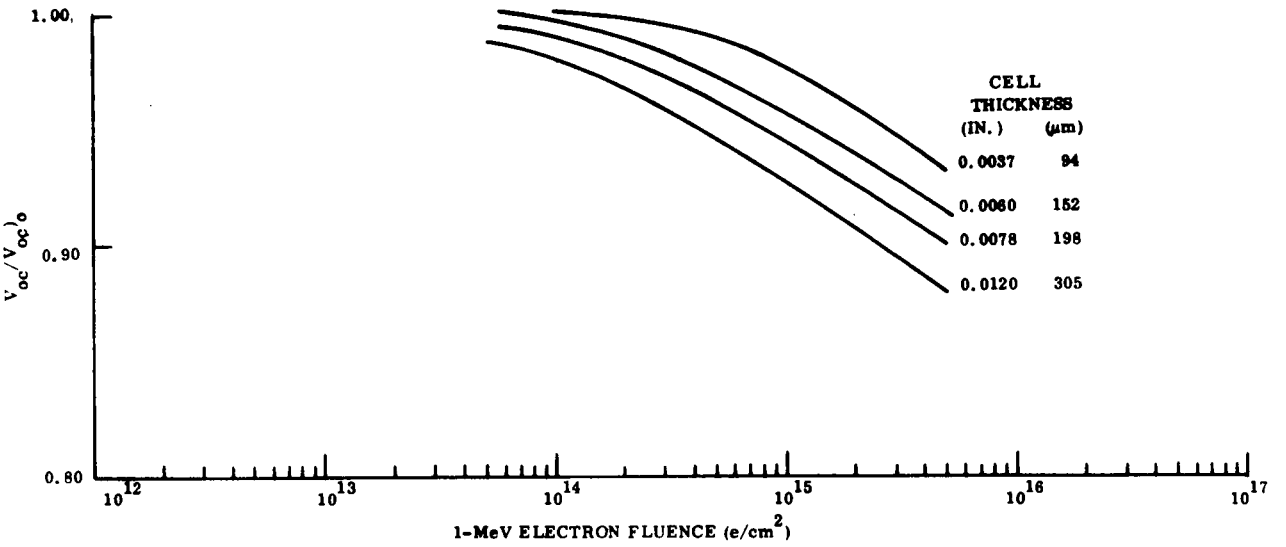

Figure B-5. Open-Circuit Voltage Degradation for 10 ohm-cm N/P Silicon Solar Cells (from Reference 50)

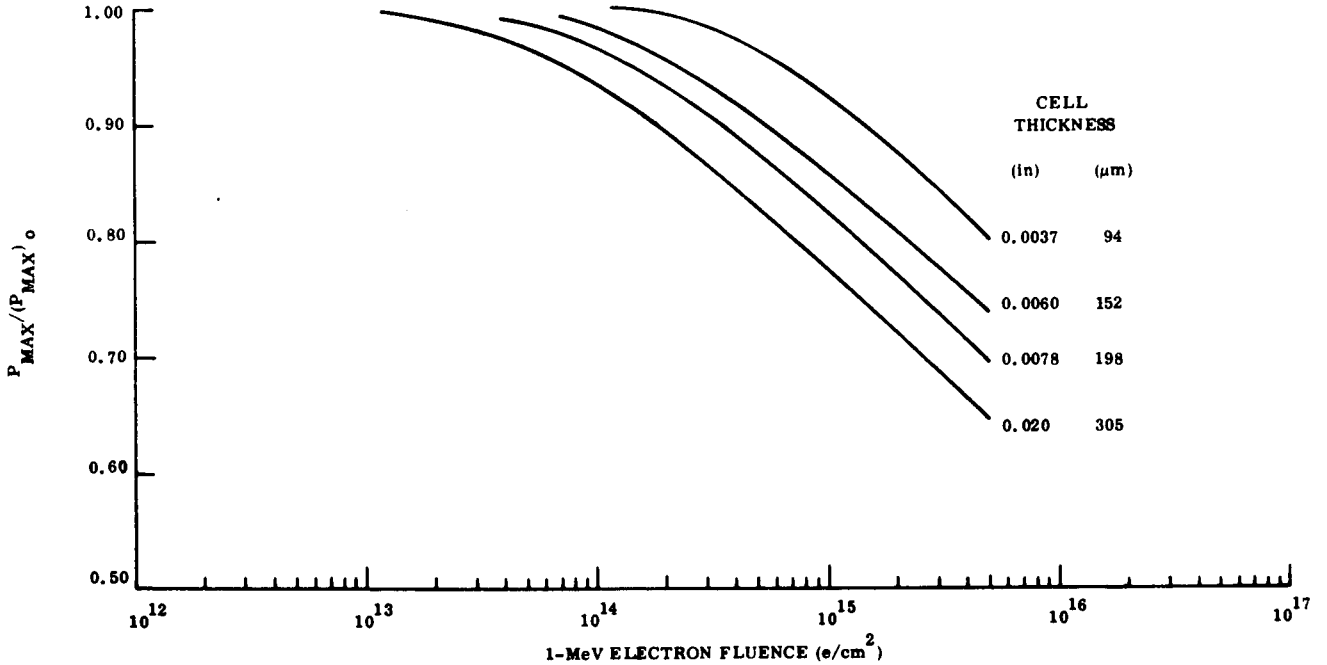

Figure B-6. Maximum Power Degradation for 10 ohm-cm N/P Silicon Solar Cells (from Reference 50)